Interfacial Enzymology: The Secreted Phospholipase A_2-Paradigm

Otto G. Berg

Evolutionary Biology Center, Uppsala University, Uppsala, Sweden

Michael H. Gelb

Departments of Chemistry and Biochemistry, University of Washington, Seattle, Washington 98195

Ming-Daw Tsai

Department of Chemistry, Ohio State University, Columbus, Ohio 43210

Mahendra Kumar Jain*

Department of Chemistry and Biochemistry, University of Delaware, Newark, Delaware 19716

Received March 12, 2001

Contents

10.1021/cr990139w CCC: $36.00
Published on Web 09/12/2001

If Shakespeare had Hamlet say "I think, therefore I am", would that prove to us that Hamlet exists?

Robert Nozick

Politics is for the present. But an equation is for eternity.

Albert Einstein

I. Introduction

Tissue and cellular *milieux* have microscopically fragmented aqueous compartments separated by vesiculated membranes. Roughly one-half of the protein in cells is estimated to be membrane associated. Many of the membrane enzymes are operationally interfacial enzymes that access the substrate directly from the lipid−water interface.[1−6] On the other hand, the noninterfacial membrane-associated enzymes,[7,8] which for brevity we call matrix enzymes, access their substrate directly from the aqueous phase. In the functional sense the matrix enzymes are like the classical soluble enzymes that also access the substrate from the aqueous phase. The observed kinetics of soluble enzymes may be influenced if the enzyme or substrate is in partitioning equilibrium

* To whom correspondence should be addressed.

Otto G. Berg received his M.S. degree in Engineering Physics in 1971 at the Royal Institute of Technology in Stockholm, Sweden. This is also where, in 1977, he received his Ph.D. degree in Theoretical Physics under the direction of Clas Blomberg. His graduate work focused on mathematical modeling of the kinetics and thermodynamics of diffusion-limited reactions. This line of work was continued and extended for four years with Peter H. von Hippel at the University of Oregon. In 1986 he moved to the Department of Molecular Biology at the Biomedical Center in Uppsala, where he was appointed Associate Professor in 1989. Since 2000 he has been at the Department of Molecular Evolution at the Evolutionary Biology Centre in Uppsala. Major research interests in include the kinetic and stochastic modeling of intracellular processes, the evolution of DNA sequence, and the activity of interfacial enzymes.

Michael H. Gelb received his B.S. degree in Chemistry and Biochemistry in 1979 at the University of California at Davis and his Ph.D. degree in Biochemistry in 1982 at Yale University. His undergraduate studies with D. C. Harris focused on iron transport by transferrin, and his doctoral studies with S. G. Sligar were on the mechanisms of action of cytochrome P450. He spent two years as an American Cancer Society Postdoctoral Fellow in R. H. Abeles' Laboratory at Brandeis University studying protease inhibitors and joined the University of Washington as a faculty member in 1985. Major research interests are interfacial enzymology of phospholipases, protein prenylation, structure-based design of ant-parasitic drugs, and multiplex clinical enzymology.

Ming-Daw Tsai received his B.S. degree in Chemistry from National Taiwan University in 1972. After two years of military service, he attended Purdue University and received his Ph.D. degree with Heinz G. Floss in 1978. He stayed on as a postdoctoral fellow for one year and as a Visiting Assistant Professor for another year. He did a brief postdoctoral stay with Eric Oldfield at the University of Illinois and became Assistant Professor of Chemistry at Rutgers University (Newark) in 1980. He moved to Ohio State University in 1981, where he is now Professor in both the Chemistry and Biochemistry departments. He was an Alfred P. Sloan Fellow (1983–1985) and Camille and Henry Dreyfus Teacher–Scholar (1985–1990), received a Distinguished Scholar Award from Ohio State University in 1992, and has been an elected Fellow of the American Association for the Advancement of Science since 1992. His research interest has been in the interface between chemistry and biology, and he has served as Director of the Chemistry/Biology Interface Training Program and Director of the Campus Chemical Instrument Center at Ohio State University since 1995. He is a member of the Board of Consulting Editors for *Bioorganic and Medicinal Chemistry* as well as *Bioorganic and Medicinal Chemistry Letters*. His current research projects include the structure–function relationship of DNA polymerases, phospholipases, kinases, tumor suppressor proteins, and forkhead-associate (FHA) domains.

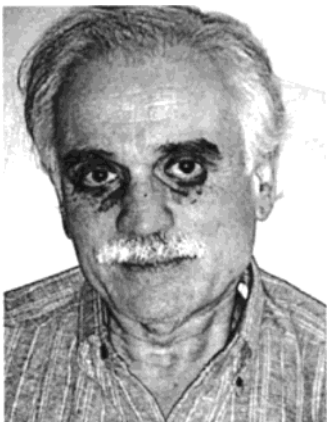

Mahendra Kumar Jain was born (1938) and was raised in India. After completing his M.Sc. degree in 1959 (Vikram University, India) and teaching for six years in India, he received his Ph.D. degree in 1967 with David Lavie (Weizman Institute, Israel) in Natural Product Chemistry. He started work on the relationship of phospholipases with interfaces as a postdoctoral associate (1967–73) with Eugene Cordes (Indiana University). He joined the University of Delaware faculty in 1973, and since 1981 he has been Professor of Chemistry and Biochemistry. He spent sabbatical leaves with G. H. DeHaas at Utrecht (1979–80), Hans Eibl at Gottingen (1986–87), and K. Eswaran and S. Vishweshwara at Bangalore (1993–94). His work for the last three decades has focused on interfacial enzymology with excursions in related areas including the phase changes in bilayers, natural products, protein-meditated selective exchange of phospholipids, and mechanism of action of cationic peptide antimicrobials.

with extraneous interface. In addition, the interface may also have an allosteric effect on the intrinsic catalytic parameters of matrix enzymes as well as on interfacial enzymes.

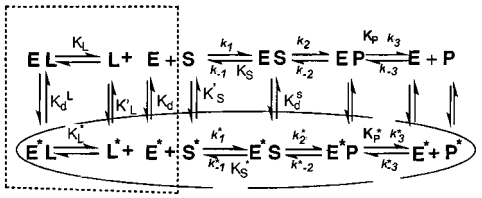

Figure 1. General kinetic paradigm for enzymology. As an extension of the classical Michealis–Menten paradigm, it includes the catalytic steps for independent turnover cycles in the aqueous phase and in the interface. The interacting species (enzyme = E*, or ligand L* = S*, or I*; other abbreviations in Tables 5 and 6 and section XV) localized in the interface (in the oval) and the corresponding interfacial constants are designated with an asterisk. In addition, the equilibria relating the species in the two phases control the interfacial processivity (number of catalytic turnovers while enzyme remains at the interface) as well as the substrate accessibility and replenishment. All equilibrium constants are for the dissociation reaction, either dissociation of a ligand from a complex such as E*L or EL or dissociation of a species from the interface such as E*, E*L, or L*. Such parameters and relations are useful for structure–function correlations. In this article we have reviewed analytical relations (Table 5), valid under suitably constrained conditions, that offer ways to extract the primary parameters (Table 6); for example, K_d for the dissociation of E* to E, inhibitor and substrate specificity, catalytic turnover events, and allosteric effects of the interface. The detailed balance constraint of the thermodynamic box (· · ·) is useful for understanding the relations between two- and three-dimensional equilibrium constants.

As a kinetic paradigm, Figure 1 shows the critical interactions between the various species that define the catalytic turnover cycle in the aqueous phase and in the interface. It emphasizes the kinetic and equilibrium relationships between an enzyme and the interacting ligands (L= S, P, or I) in a microscopically heterogeneous environment. It is also a general statement of the integrated relationships that in effect control the catalytic function of interfacial, matrix, and soluble enzymes. Note that Figure 1 does not specify the kinetic turnover path taken by an enzyme under specific conditions. As developed in this review, the challenge is to identify the assay conditions where the kinetic path for the turnover is unequivocally identified. For the interpretation of the reaction progress obtained from such assays, it is necessary to take into consideration the accessibility of the interface to the enzyme, the processivity of the successive interfacial turnover cycles, and replenishment of the substrate during the steady state. The microscopic variables for the kinetic path for the steady-state turnover are defined within such constraints. Having identified the events of the kinetic path, analyses under a variety of conditions provide the primary rate and equilibrium parameters useful for obtaining analytical tools and insights into the various kinds of structure–function correlations. Throughout this review the species and constants marked with an asterisk are for the reactants or constants localized in the interface, and the analytical relations (equations) refer to those in Table 5.

Interfacial enzymes carry out the catalytic turnover within the two-dimensional constraints of the interface because that is where their substrates are found. Pancreatic secreted phospholipase A_2 (sPLA2) has

Table 1. Examples of Interfacial Enzymes

interfacial enzyme	ref
secreted phospholipases A2	1−6, 9−11
cytoplasmic PLA2	12
phospholipase A_1	13
glyceride lipases]	14, 15
phosphatidyinositol-phospholipase C[a]	
bacterial and mammalian	16 and 17
phosphatidylinositol-3-kinases	18−20
bacterial acyltransferase	21
bacterial sphingomyelinase[b]	

[a] Exhibits low interfacial processivity. [b] Yu, Zakim, and Jain. Unpublished results.

served as the prototype of an interfacial enzyme,[9−11] and now the interfacial kinetic paradigm has evolved to include the sPLA2 family as well as many other enzymes involved in lipid metabolism and signal transduction pathways. In this review we critically evaluate the conceptual and analytical progress made since the publication of a comprehensive survey of sPLA2 by Verheij et al.[11] Our focus, within the paradigm of Figure 1, will be on methods to determine the primary parameters that describe the events of the interfacial turnover cycle. These are useful for quantitative structure−function correlation for specific reaction steps. Significant strides have also been made in the characterization of other interfacial enzymes (e.g., Table 1). Considering the volume and depth of the published literature, our coverage is limited to the conceptual progress in understanding sPLA2s, which continues to remain a viable paradigm for interfacial enzymology. It should be noted that establishing that a membrane-bound enzyme accesses its substrate from the aqueous phase (matrix enzyme) requires a pre-steady-state analysis, as accomplished only recently[7] for the enzyme platelet-activating factor (PAF) acetylhydrolase from blood serum.

II. The sPLA2 Paradigm for Interfacial Enzymes

A large variety of enzymes[11−35] are involved in the metabolism of a diverse group of nonpolar and amphiphilic solutes, including phospholipids, dietary fats, sterols, eicosanoids, carotenoids, and chlorophyll. Interfacial enzymes have evolved to deal with the biophysical realities of the molecular aggregates of amphipathic and nonpolar substrates in aqueous dispersions. An interfacial enzyme accesses the water-insoluble substrate partitioned in the interface to carry out the turnover cycle via the species localized in the interface (oval in Figure 1). The challenge of the kinetic characterization of interfacial enzymes comes from the fact that interfaces are microscopically dispersed. Therefore, one must consider the accessibility and exchange dynamics of the substrate and product molecules between the coexisting interfaces of the dispersed particles and the intervening aqueous phase. Generally, such exchange processes are not rapid on the time scale of the catalytic turnover. Therefore, numerous kinetic paths are possible depending on the contributions of the rates and equilibria that feed into the turnover cycle in one phase or the other. Such a dissection is not trivial.[5]

As developed below, the problem of ascertaining a definite kinetic path has been resolved under two sets of conditions: in the scooting mode, where the

Table 2. Members of the sPLA2 Superfamily[11,36−47]

group	MW (kDa)	disulfides	source[a]
IA	13−14	7	cobra and krait venom
IB	14	7	pancreas, lung, spleen
IIA	14−15	7	tears, synovial fluid, viper and rattle snake venom
IIB	14	6	gabon viper venom
IIC	15	8	mouse and rat testes
IID	14	7	mouse and human tissues
IIE	14	7	mouse and human tissues
IIF	17	7	mouse and human tissues
IIIA	18	5	bee and lizard venoms; human tissues
IIIB	14	5	scorpion venom
V	14	6	mouse and human tissues
IX	18[b]	6	cone snails
X	14	8	mouse and human tissues
XI		6	plants
XII	16	7	mouse and human tissues

[a] IB, IIA, IID-F, IIIA, V, X, and XII are present in the human genome. [b] A disulfide-linked heterodimer.[47]

Table 3. Conceptual Themes in Interfacial Enzymology of sPLA2 [Refs]

theme	ref
effect of the interface on the catalytic turnover by phospholipases	6, 9, 10, 48−50
problems of undefined interfacial processivity	5, 51
unequivocal evidence for interfacial processivity	1−4, 6, 52
extension of the Michaelis−Menten formalism to interfacial catalytic turnover	5, 6, 10, 14, 52, 53
His-Asp-Ca catalytic residues of sPLA2s	11, 54−56
interface preference	10, 49, 50, 57a,b
specificity: inhibitor; substrate; and neutral surface diluent, ND (see section V)	59−62; 58, 63, 64; 58, 59, 126
sPLA2 structures: X-ray (see also Figures 2 and 30 and NMR	65−70 and 71−76
model for interfacial binding supported by modeling; EPR; and the crystallographic dimer with five anions	66,77; 78; 79; 80
theory of interfacial enzymology and analytical foundation for the pathways in Figure 1	81; 5, 6, 14, 51−53

interacting species (enzymes, substrates, and products) do not exchange between the particles, and in the quasi-scooting mode, where the replenishment of enzymatically generated product by substrate from other aggregates is rapid on the time scale of the individual turnover event. Much of the pioneering work to resolve problems with characterization of the interfacial catalytic behavior in terms of the primary rate and equilibrium parameters (Figure 1) has been carried out with pig pancreatic sPLA2, and such studies have been extended to other members of the sPLA2 superfamily (Table 2).

A. Pig Pancreatic sPLA2 Prototype for Interfacial Enzymology

Pancreatic sPLA2 has served as the prototype for interfacial enzymology for much the same reasons that trypsin and lysozyme have come to represent solution enzymes. It is an abundant and stable small protein that can be readily purified. DeHaas and coworkers pioneered the systematic study of the 14-kDa pig pancreatic sPLA2,[9−11] which hydrolyzes the *sn*-2-ester bond in 1,2-diacyl- or 1-alkyl-2-acyl-glycero-*sn*-3-phospholipids.

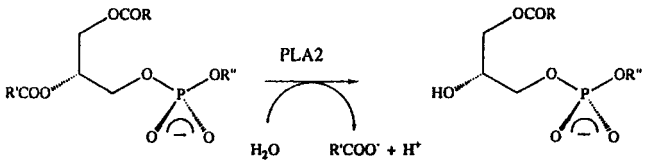

The conceptual themes in Table 3 are based on results[1−4,6,82−86] that have provided the analytical basis for the theory of interfacial enzymology.[81] sPLA2s were the first interfacial enzymes to have their X-ray structures determined.[65−70] Quite early it was recognized that phospholipases are efficient catalysts in the presence of substrate interfaces and that the catalytic turnover possibly occurs at the interface. A wide variation in the observed kinetics, with changes in the structure of substrate aggregates, suggests that interpretation of the observed kinetics requires not only an understanding of the catalytic specificity of the enzyme, but also the characterization of the interface preference, often called the "quality of interface" effects. These results set the foundation for the extension of the Michaelis−Menten paradigm for the turnover at the interface by relating the catalytic cycle events to the catalytic site and the interface preference to the i-face of the protein that makes contact with the interface. Yet the substrate specificity and interface preference could not be dissected because the interfacial processivity of the successive turnover cycles could not be adequately taken into consideration.[5,51] By interfacial processivity we mean the enzymatic hydrolysis of multiple phospholipids without dissociation of enzyme from the interface. Unequivocal evidence for the interfacial catalytic turnover cycle and also for the interfacial processivity of the successive turnover cycles came from the reaction progress in the scooting mode.[1−6] In the scooting mode, all phospholipids in the outer layer of the vesicle bilayer are hydrolyzed without dissociation of enzyme into the aqueous phase. Substrates present in vesicles that do not contain bound enzyme are not hydrolyzed in the presence of enzyme-containing vesicles. Clearly this rules out the mechanism in which vesicle-bound enzyme acts on the vanishingly small amount of phospholipid in the aqueous phase. These protocols provided results for quantitative analysis of the turnover events of the unequivocally defined kinetic path shown in the oval in Figure 1.

B. Structural Characteristics of sPLA2

The sequences of sPLA2s differ significantly; however, the three-dimensional structures have several features in common (Figure 2, Table 4). There are more than 40 sPLA2 entries in the Protein Data Bank. Structures of the native and complexed sPLA2 with substrate mimics (Figure 3) have helped in identifying the catalytic residues and the active site. The anion binding sites on the pancreatic IB sPLA2 also suggest a strong relationship to the surface of the enzyme that makes contact with the anionic interface, which we call the i-face (Figure 2B and C). As a class, sPLA2s contain about 120−170 amino acids in a single peptide chain (Table 2), except that group IX sPLA2 is a disulfide-linked heterodimer.[47] These sequences exhibit modest homology but differ in their disulfide architecture, chain deletions (60−70 loop), and insertions at the C-terminus. Rigid three-dimensional structures of sPLA2 are stabilized by 5−8 disulfide bridges.

As shown in Figure 2A, the bovine pancreatic sPLA2 is a small (22 × 30 × 42 Å) kidney-shaped molecule. About 50% of the residues are in α-helices, and 10% are in antiparallel two-stranded segments of β-structure. The structure is cross-linked by seven disulfide bonds. The His48-Asp99 pair forms the catalytic residues with calcium as the cofactor. The calcium ion is bound with five oxygen ligands provided by the protein (two oxygens of the Asp-49 side chain and backbone carbonyls of residues 28, 30, and 32). In addition, there are two coordinated water molecules, which are replaced by the oxygen ligands from the *sn*-2- and *sn*-3-substituents of substrate mimics. The catalytic residues are located at one end of the active site slot with hydrophobic walls lined with Leu-2, Phe-5, Ile-9, Ala-102, Ala-103, and Phe-106. The catalytic site is accessible through a remarkably flat i-face that acts as the interface binding region or site (Figure 2). All sPLA2 structures contain the same constellation of the catalytic residues His-Asp-Ca^{2+} in the architecture of the catalytic site. The features that differ between the sPLA2s are generally the i-face residues and other surface residues that are part of the recognition system for other functions.

C. The Catalytic Site versus the i-Face of sPLA2s

Insights and issues related to the structure of sPLA2 at the interface are still emerging. As shown in Figure 2, the substrate mimic must travel about 15 Å away from its position at the interface to bind in the catalytic site slot of interface-bound sPLA2. The apparent substrate specificity of sPLA2s is a combination of the interface recognition and catalytic

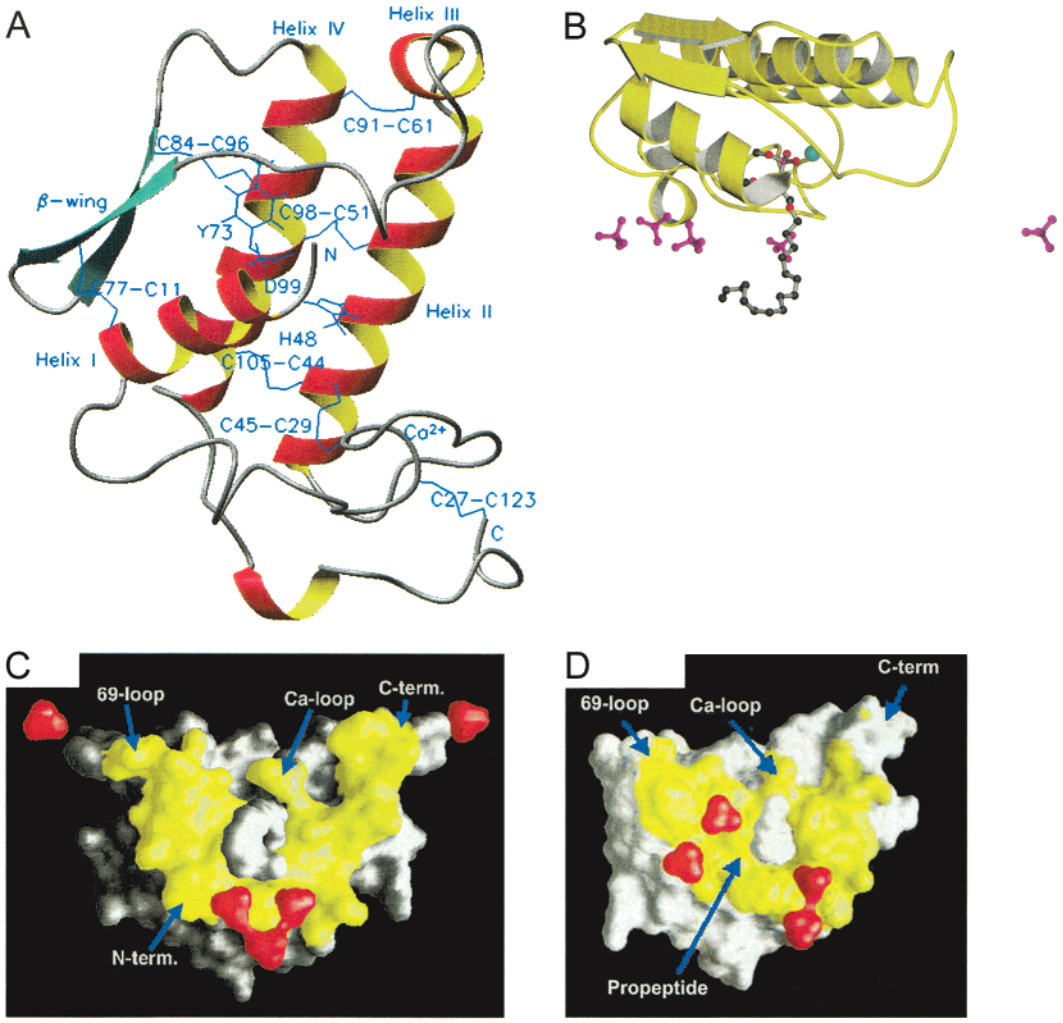

Figure 2. (A) Ribbon drawing of bovine pancreatic sPLA2 structure[67,71] showing the highly conserved[68,70] secondary structural elements, seven disulfide bonds, the D99-H48 catalytic pair, the Ca^{2+} binding loop, and the β-wing. The N- and C-termini are indicated. (B) Crystallographic structure of porcine pancreatic sPLA2 with five phosphate anions (pink ball–stick representation), the inhibitor MJ33, a mimic of the substrate-derived *sn*-2-tetrahedral intermediate (III in Figure 3), in the active site (gray balls).[87] The surface of the enzyme that contacts the interface (i-face) is along the horizontal plane passing through the bottom edge of the protein and perpendicular to the page. (C) The footprint of the anion-assisted-dimer subunit contact surface of pig pancreatic sPLA2 (GRASP display) shows the van der Waals surface (yellow), five bound phosphate anions (red), and the alkyl chain of MJ33 shown as the gray region in the middle.[80] As discussed in section XII, the contact face in this dimer is virtually identical to the model of the i-face proposed earlier.[77] The catalytic site architecture of virtually all sPLA2 is highly conserved. The regions that differ between the sPLA2s and show conformational flexibility are often along the i-face. PDB code IFXF. (D) The anion-assisted-dimer contact surface for pig pancreatic proPLA2 zymogen.[271] PDB code1HN4.

Table 4. Structural Features of Pancreatic sPLA2 Relevant to Interfacial Catalysis

cofactor pocket	Asp-49 and 26–34 loop bind calcium
catalytic site	His48/Asp-99 pair; Ca-loop; 69-loop of residues 59–74.
substrate pocket	hydrophobic face of the N-terminus helix (2, 5, 9) and 22, 103, 106
i-face	five anion binding sites; N- and C-terminus, 69-loop; 1500 Å^2 hydrogen-bonding and hydrophobic surface
k_{cat}* allosteric site	cationic residues 53, 56, and 120

site specificity. Operationally, in relation to the kinetic paradigm of Figure 1, two structural features are of functional interest: the catalytic site and the i-face which makes contact with several phospholipid molecules at the substrate interface. A conserved His-Asp-Ca^{2+} architecture as well as the active-site residues are involved in the substrate binding and the substrate specificity in the catalytic turnover cycle. Although not required for the binding of the enzyme to the interface, Ca^{2+} is an obligatory cofactor for the binding of the substrate in the catalytic site and also for the chemical step in the catalytic turnover cycle. The interface preference of sPLA2 is associated with the interaction along a site, the i-face, which is distinct from the catalytic site. For example, the pancreatic and Naja venom PLA2s when bound to the interface show little substrate specificity for the structure of the headgroup or the *sn*-2-acyl chain of naturally occurring phospholipids.[63,64] However, relative to pancreatic PLA2, the cobra venom enzyme binds about 3 orders of magnitudes more tightly to zwitterionic phosphatidylcholine interfaces.[107,108] All sPLA2s so far analyzed bind more tightly to anionic than to zwitterionic interfaces.[83]

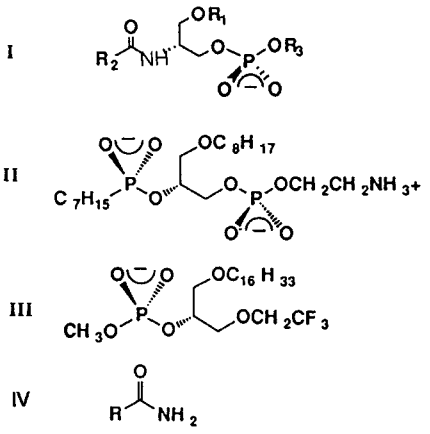

Figure 3. Subset of the substrate mimics cocrystallized with sPLA2. **I** = *sn*-2-amide analogue to modified pig pancreatic[88,89] and synovial sPLA2s.[90] **II** = *sn*-2-phosphonate analogue to bee venom,[91] Naja venom,[92] bovine pancreatic,[93] human synovial sPLA2s.[94] **III** = *sn*-2-phosphate analogue to bovine pancreatic[87] and as anion-assisted-dimer of pig pancreatic sPLA2[80] and its zymogen.[271] **IV** = Fatty acyl amide modeled in the active site of pig and bovine pancreatic PLA2.[95] His-48 alkylated pig pancreatic PLA2.[106] Synthetic substrate analogues: *sn*-2-amides,[96−102] fatty acid amides,[103] *sn*-2-phosphonate,[60,104] and *sn*-2-phosphates,[59] indole-derived amides,[105a] and other inhibitors.[105b,c]

D. Pathophysiological Significance of the Diversity of PLA2 Activity

Phospholipid *sn*-2-esterase activity is ubiquitous. It is found in most, if not all, living organisms and in virtually all cell types. Several evolutionarily nonrelated classes of proteins are known to exhibit PLA2 activity,[11,109] and some of these have found their way into the group classification.[40] In addition to the His-Asp-Ca^{2+}-based sPLA2s (Table 2), the catalytic serine-based *sn*-2-esterases of phospholipids include the 87-kDa cytosolic PLA2 with specificity for the arachidonyl chain,[12,110] the 46-kDa PAF-hydrolase that hydrolyzes truncated or oxidized chains,[7,8] and the 28-kD bifunctional lung enzyme that also has phospholipid peroxidase activity in addition to PLA2 activity.[111] Considering the ubiquity of phospholipids as well as their high compositional specificity in the various cellular compartments, it appears that the *sn*-2-esterases and acyltransferases play a critical role in mobilization and tailoring of the unsaturated fatty acyl substituents of phospholipids.

sPLA2s (Table 2) are found in numerous organisms including mammalian tissues, venoms, and plants. They are expressed and secreted into the extracellular milieu of tissues by secretory processes including secretion into the gastrointestinal tract where their primary role appears to be in the digestion of the phospholipid at the emulsion interface of dietary triglyceride particles.[28a,35] It is intriguing that sPLA2 inhibitors block the uptake of cholesterol;[28a] however, the cholesterol absorption efficiency does not change in knock-out mice deficient in IB sPLA2,[28b] suggesting that other sPLA2s can contribute to hydrolyses of phospholipids in the intestines.

At least some types of the sPLA2s are critical for defense and inflammatory responses in tissues. It is certain that their role in defense mechanisms includes liberating fatty acids from membrane phospholipids. It appears that arachidonic acid, present mainly in phospholipids, is mobilized for such functions by sPLA2s, at least under certain conditions. The eicosanoid pathways convert arachidonic acid to a diverse group of eicosanoids (prostanoids, thromboxanes, epoxyacids, leukotrienes, lipoxins) which are potent mediators of inflammation and other pathophysiological processes in response to specific signals and receptors.[30,112,113]

Some of the sPLA2s also exhibit toxicity, antibacterial action, and allergenic and immune responses. Structural origins of such effects may lie in certain epitopes; however, the catalytic and interface recognition functions are critical for many but not all of these biological responses. It is now known that humans contain at least 9 different sPLA2s, and at least 10 are present in the mouse. Although they have very similar catalytic sites, it is becoming clear that these enzymes display very different interfacial binding properties. For example, the initial velocity for the hydrolysis of phosphatidylcholine vesicles by human group X sPLA2 is several orders of magnitude larger than that for human group IIA sPLA2. Addition of small amounts of human group X (10 ng/mL) to mammalian cells also leads to rapid plasma membrane hydrolysis leading to arachidonate release and eicosanoid formation.[46,114] In contrast, mammalian cells are generally resistant to the action of exogenously added human group IIA sPLA2, presumably because it cannot bind to the phosphatidylcholine-rich outer leaflet of the mammalian plasma membrane. In effect, the physiological properties of human group IIA and X sPLA2s are controlled by their different interfacial binding specificities and not by their catalytic site specificity; both enzymes hydrolyze phosphatidylcholine and anionic phospholipids with similar efficiencies when enzyme is bound to the interface.[46,115]

Group IIA sPLA2 is the principal antibacterial agent in human tears.[116] It binds tightly to the phosphatidylglycerol-rich membranes of Gram-positive bacteria such that picogram per milliliter concentrations are sufficient to kill bacteria.[117] The activity against Gram-negative bacteria[118] is considerably enhanced in the presence of agents that disrupt their lipopolysaccharide coat.[119] The propensity of certain sPLA2s to bind to polyanions is not necessarily due to the interactions along the i-face.[120] In fact, such aqueous-phase complexes of certain sPLA2s, with sulfated-glycoconjugates and receptors present in the tissue environment, effectively reduce the fraction of the enzyme at the interface (Figure 1). In short, the equilibria for the distribution of the enzyme to the interface and in the complexes thus have a dramatic effect on the observed rates due to a change in the substrate accessibility and the interfacial processivity (see below).

III. Defining the Kinetic Path for the Analysis of Interfacial Catalytic Turnover

The pancreatic sPLA2 paradigm has extended the conceptual boundaries of enzymology in general. We

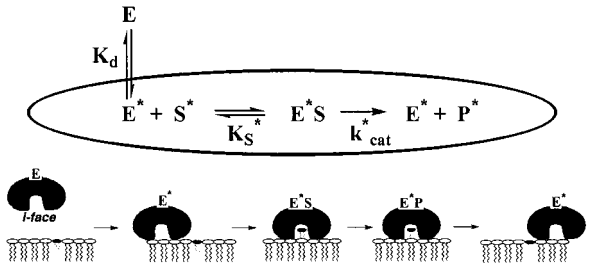

Figure 4. Schematic representation of the interfacial catalytic turnover steps mediated by the binding of the enzyme to the interface.

believe that this paradigm is likely to be conceptually and analytically useful for the study of other interfacial enzymes. It is also readily adopted for the characterization of other types of membrane-associated enzymes. As developed in this section, the field has benefited not only from the general progress in solution enzymology, but also from a better understanding of the organization and exchange properties of phospholipid interfaces which control the substrate accessibility and replenishment during the steady-state kinetic turnover.[81] With a full appreciation of the properties of microscopic dispersions and what the enzyme 'sees' during the steady-state turnover, it is possible to define unique kinetic paths which can be analyzed in terms of the primary rate and equilibrium parameters. Such information is useful for understanding the structural, catalytic, and allosteric relations between the enzyme and the interface.

Consider the catalytic turnover cycle at the interface (Figure 4). As a first step, the enzyme in the aqueous phase binds to the interface along the i-face that is different than the catalytic site, although as discussed later there may be regulatory cross-talk between the two. E to E* is the first step for the substrate accessibility. This is followed by the catalytic turnover events at the active site of the bound enzyme which include substrate binding in the catalytic site, chemical substrate hydrolysis, and release of products. The first kinetic event associated with the binding along the i-face is eliminated during the interfacial processive turnover cycles (Figures 4 and 5). This occurs if the equilibrium constant for the dissociation of enzyme from the interface $K_d = k_{off}/k_{on}$ is sufficiently small[1−4,6,77,83] such that during the reaction progress in the scooting mode, enzyme leaves the interface slowly compared to the time needed to hydrolyze all of the phospholipid in the enzyme-containing vesicle with its integrity retained (see below).

A. Processive Turnover Kinetic Path for the Interfacial Kinetic Analysis

Multiple kinetic paths are possible within the paradigm of Figure 1.[5,81] The challenge is to establish experimental conditions where the events of the successive catalytic turnover cycles occur processively through a single defined path. For the analysis of a defined kinetic path, it is necessary to identify the variables in the microenvironment of each interacting species. In solution enzymology, we take for granted

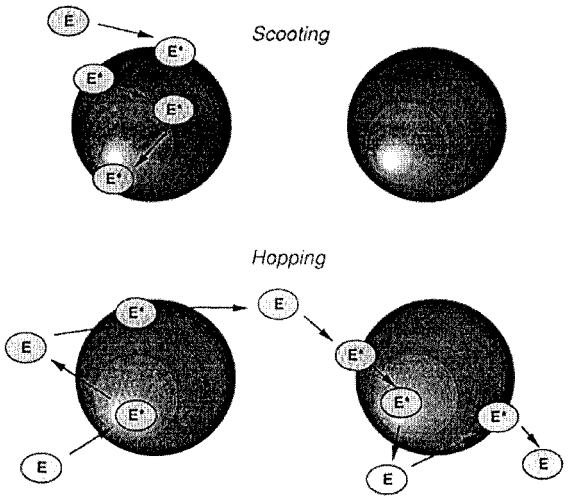

Figure 5. Cartoon to illustrate (top) the virtually infinite interfacial turnover processivity (scooting mode) versus (bottom) no interfacial processivity (fast hopping mode) where bound enzyme leaves the interface after each turnover cycle. Both of these two extreme cases can be analytically described. However, the problem is intractable under the conditions where the residence time of the enzyme at the interface is not known, or is not constant over the time course of the reaction progress, or the zero processivity (hopping) condition cannot be established. In vesicles of long-chain phospholipids, the intervesicle exchange of the substrate and the products of hydrolysis is negligibly slow. Also, in the scooting mode, the bound enzyme does not exchange between vesicles.

that every enzyme in the reaction 'sees' the same environment consisting of substrate and product molecules present at uniform concentrations through the entire reaction mixture (rapid mixing conditions). For assays of interfacial enzymes, substrates are packaged into an ensemble of aggregates (bilayer vesicles, micelles, or emulsion particles). In the hopping mode, the enzyme transfers between vesicles. In the ensemble of the interacting particles in the reaction mixture, each enzyme may be bound to vesicles of differing composition if the vesicle to vesicle transfer of the enzyme occurs on a time scale that is similar to the time needed for enzyme to change the composition of a vesicle by converting substrates into products. A similar change in the local environment will also result if substrates and products do not exchange quickly between aggregates on the same time scale as is the case for naturally occurring long-chain phospholipids. Obviously, such a situation greatly complicates kinetic analyses because differing vesicle composition is equivalent to differing reaction times for the turnover by the enzyme in such environments. This problem is eliminated under two extreme conditions. In the scooting mode, with at most one enzyme per vesicle, none of the interacting species (E*, E*S, E*P, S*, P*) leave the interface.[1−6] On average, all enzyme-containing vesicles behave similarly in time (as long as enzyme-containing vesicles have the same number of enzymes, which can be assured by Poisson law only for the limit of at most one enzyme per vesicle at the total enzyme/vesicle ratios of <0.15). Thus, the measurement of the product formed by the ensemble of enzymes reflects the behavior of any single enzyme

Table 5. Key Relations for Figure 1[a] in the Scooting or Quasi-Scooting Mode[6,53,81]

eq 1	initial rate[6,14,53] per enzyme	$v_0 = V_M{}^{app} = \frac{k_{cat}{}^* X_S}{X_S + K_M{}^*}$
eq 2	apparent calcium dissociation constant in the presence of an active-site-directed ligand L[122]	$K_{Ca}{}^*(L) = \frac{K_{Ca}{}^*}{1 + \frac{X_L}{K_L{}^*}}$
eq 3	competitive inhibition[6,53]	$\frac{v_0}{v_1} = 1 + \left(\frac{1 + \frac{1}{K_1{}^*}}{1 + \frac{1}{K_M{}^*}}\right)\left(\frac{X_I}{1 - X_I}\right)$
eq 4	apparent affinity (Michaelis constant) for the quasi-scooting hydrolysis of rapidly exchanging substrate at the interface[14,53]	$K_M{}^{app} = \frac{K_d K_M{}^*}{1 + K_M{}^*}\left(1 + \frac{K_S{}'}{K_M}\right)$
eq 5	detailed balance condition for the thermodynamic box in Figure 1[123]	$K_L{}' K_d K_L{}^* = K_L K_d{}^L$
eq 6	integrated Michaelis−Menten reaction progress[6]	$k_i t = -\ln[1 - P_t/P_{max}] + (k_i N_S/v_0 - 1)P_t/P_{max}$
		$k_i N_S = \frac{k_{cat}{}^*}{K_M{}^*(1 + 1/K_P{}^*)}$
eq 7	substrate specificity[64]	$\frac{v_{S1}}{v_{S2}} = \left(\frac{\left\{\frac{k_{cat}{}^*}{K_M{}^*}\right\}_{S1}}{\left\{\frac{k_{cat}{}^*}{K_M{}^*}\right\}_{S2}}\right)\left(\frac{X_{S1}}{X_{S2}}\right)$
eq 8	Poisson distribution of E over vesicle (V) population (F_0 = fraction of vesicles unhydrolyzed)[6,127]	$F_0 = \exp(-E/V)$

[a] The apparent parameters (eqs 1 and 4) apply under the quasi-scooting mode. The parameters and variables are defined in the text.

molecule on average, as is the case with solution enzymes under rapid mixing conditions.

The other extreme, which greatly simplifies the interpretation of the observed reaction kinetics, is the quasi-scooting mode analysis.[14,53] As described later in section III, here the enzyme and/or the substrate exchanges between aggregates quickly on the time scale such that the turnovers by the bound enzyme molecules do not significantly change the composition of an aggregate. This is the interfacial equivalent of the rapid mixing behavior by replenishment and exchange intrinsic to all steady-state kinetic analyses of soluble enzymes. For example, if enzyme dissociates from a vesicle after each turnover cycle (*fast hopping mode*), all vesicles will become hydrolyzed uniformly in time since rebinding of enzyme to the ensemble of vesicles occurs randomly as long as all vesicles have the same lipid composition at any point in time.

In addition to the ensemble averaging, one must also pay special attention to the substrate replenishment problem while setting up the interfacial kinetic assay. If enzyme is bound to an aggregate, the bound enzyme may deplete all of the substrate in the aggregate very quickly, and continued reaction progress requires replenishment of substrate in enzyme-containing microaggregates. Substrate replenishment is critical in the case of a detergent−phospholipid mixed-micelle that contains ~100 detergent molecules and ~5−10 phospholipid molecules. The kinetic consequences of such a situation will be discussed in more detail in section IV, where we consider the sPLA2-catalyzed hydrolysis of long-chain phospholipids dispersed in detergent micelles. Substrate replenishment is much less of a concern in bilayer vesicles over the period of minutes to hours needed for a bound sPLA2 to consume all of the substrate in the outer layer of a vesicle that contains several thousand or more phospholipids.

Table 5 lists the analytical relations that describe the interfacial kinetic behavior of an enzyme operating in the scooting or quasi-scooting modes with a defined kinetic path. The reader may note that these equations are quite similar to the corresponding equations used in solution enzymology. Included are the Michaelis−Menten equations for the integrated reaction progress and for the substrate mole fraction dependence of the initial steady-state rate as well as equations for dissociation constants of catalytic site ligands such as calcium, competitive inhibition, and substrates. Definitions of the constants are given in the text in relation to the appropriate limit for Figure 1. For random binding of enzymes to vesicles, the number of enzymes per vesicle is given by the Poisson equation (eq 8), which is useful to ascertain the fraction of enzyme-containing vesicles from the extent of hydrolysis in the scooting mode. Table 6 has values of the kinetic parameters for the action of pig pancreatic IB sPLA2 on aggregates of specific phospholipids.

Table 6. Primary Parameters (defined in Figure 1) for Pig Pancreatic sPLA2 at 24 °C

k_{cat}* (=k_2*) 400 s^{-1}, k_1* 350 s^{-1}, k_{-1}* 35 s^{-1} with K_M* 0.35 mole fraction for 1,2-dimyristoylphosphatidylmethanel (DMPM)[6]
k_{cat} < 0.03 s^{-1} for DC_6PC[121]
K_M^{app} 2.3 mM and V_M^{app} 450 s^{-1} for diheptanoylphosphatidylcholine (DC_7PC)[53]
K_P* 0.025 mole fraction for the products of DMPM[58]
K_I* 0.0008 mole fraction for active-site-directed inhibitor MJ33;[59] K_L' 0.009 mM for MJ33
K_{Ca}* 0.28 mM, K_{Ca} 0.33 mM, and apparent K_{Ca}* (DMPM) 0.09 mM[122]
K_d 3.2 mM and K_d^I 0.15 mM with MJ33 at phosphatidylcholine interface[123]
K_d is estimated as 10^{-13} M at the DMPM vesicle interface[83]
$K_d/K_d^I = K_I^*/K_I'K_I$ (eq 5) = 5−100 depending on the structure of the mimic[53,123]

B. Meanings of the Substrate-Concentration Variable

Concentration is a thermodynamic quantity. In a microscopically heterogeneous system its significance changes with the phase state as well as the nature of the interacting species for the underlying equilibria. For the present purpose, four different microscopic variables are generated from the total substrate amphiphile concentration, $[S_T]$, in mole per liter of the aqueous dispersion.

(a) The maximum monodisperse concentration of an amphiphile in the aqueous phase in equilibrium with the aggregate phase is defined as the critical micellization concentration (CMC). Excess phospholipid above the CMC is always present as the aggregate phase. The CMC can be in the millimolar range for the short-chain phospholipids; however, the concentration of solitary natural phospholipid molecules in the aqueous phase is typically in the subnanomolar range. Thus, the half-time for desorption of a long-chain phspholipid molecule from the bilayer interface is on the order of hours. Therefore, sPLA2s must directly access the substrate from the interface of the aggregated phospholipid (interfacial enzyme).

(b) The E to E* equilibrium depends on the concentration of interface accessible to the enzyme from the aqueous phase. It increases linearly with $[S_T]$ − CMC. It is most conveniently expressed as moles of phospholipid dispersed as the interface per liter (eq 4).

(c) The substrate concentration that E* 'sees' for the formation of the E*S complex is the number density, defined as the number of substrate molecules per unit area of interface. As a first approximation, within the limit of ideal and rapid equilibrium of mixing all such species that determine the E*S population, the substrate concentration variable for the formation of E*S is approximated as the substrate mole fraction, X_S, in the interface (eqs 1−3). In a single-component system, X_S has a maximum possible value of 1. In a codispersion of the substrate and inhibitor, products, or a different surface diluent, the sum total of the mole fractions of all the components is unity. Mole fraction units are further described in section IX.

(d) For an ensemble of enzymes and vesicles, the distribution of enzyme over vesicles, determined by the enzyme/vesicle (E/V) ratio, follows the Poisson law (eq 8). The concentration of vesicles is the total lipid concentration divided by the number of phospholipids per vesicle.

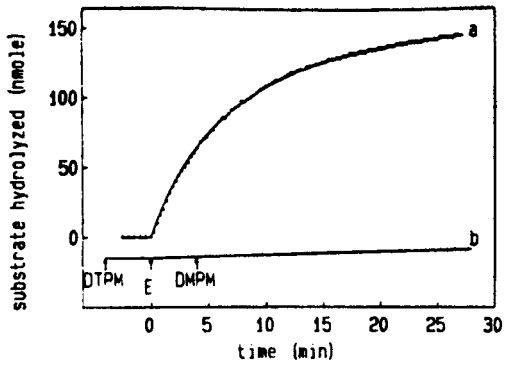

Figure 6. Reaction progress (pH-stat titration) for the pig pancreatic IB sPLA2-catalyzed hydrolysis (b) initiated by E added to large vesicles of DMPM or (b) DMPM vesicles were added to a mixture of the enzyme prebound to vesicles of nonhydrolyzable phospholipid 1,2-tetradecylphosphatidylmethanol (DTPM). Curve a is fitted to the integrated Michaelis−Menten equation (eq 6, Table 5). (Reprinted with permission from ref 6. Copyright 1991 American Chemical Society.)

C. Integrity of Vesicles Is Maintained during Processive Turnover

The simplest protocol for the unequivocal analysis of the interfacial turnover steps is based on the conditions where the successive interfacial turnover cycles occur only through the steps shown in the oval (Figure 1 or 4). The steady-state reaction progress in the highly processive scooting mode is observed at the anionic phospholipid interface with all sPLA2s that have been examined on arionic vesicles[83] and several other interfacial enzymes (Table 1). In the scooting mode the bound enzyme does not leave the vesicle and the integrity of the hydrolyzed vesicles is maintained, i.e., the content of the enclosed aqueous compartment does not leak out.[124−126] As suggested by results in Figure 6 and borne out by direct measurements, the rate of spontaneous vesicle-to-vesicle exchange of long-chain phospholipids is exceedingly slow, on the order of hours to days. Also, the monodisperse phospholipid concentration in the aqueous phase is insignificant. The products of hydrolysis do not exchange with substrate molecules present in the inner monolayer of the enzyme-containing vesicle or with the phospholipid present in excess vesicles. This is probably because the forces that stabilize the bilayer organization also prevent a change in the size or the transbilayer exchange that would require unfavorable interactions of the acyl chains.

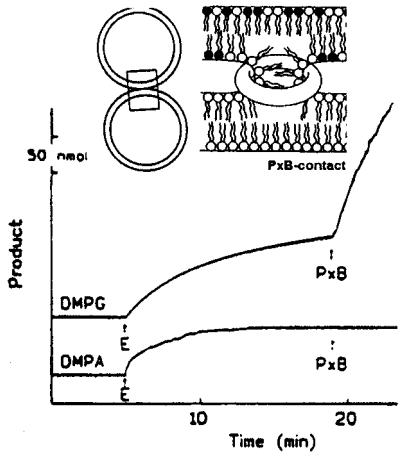

Figure 7. Reaction progress for the hydrolysis of dimyristoylphosphatidylglycerol (DMPG) or phosphatidic acid (DMPA) vesicles by pig pancreatic IB sPLA2 in the scooting mode. Addition of polymyxin B (PxB) promotes a direct vesicle-to-vesicle exchange of DMPG but not of DMPA. (Reprinted with permission from ref 129. Copyright 1996 American Chemical Society.)

D. Zero-Order Reaction Progress in the Scooting Mode

Analysis of reaction progress is considerably simplified if the enzyme-containing vesicles in the ensemble have at most one enzyme.[6] Product inhibition during the later part of the scooting mode reaction progress (Figure 6, curve a) is described by eq 6, where the K_P* term dominates because of an increase in X_P in a closed relationship $X_S + X_P = 1$ on the enzyme-containing vesicles. The initial zero-order phase of the reaction progress is significant only in large vesicles because X_S in small vesicles decreases over a relatively short period of time.

E. Apparent Activation due to Rapid Substrate Replenishment in the Scooting Mode

The apparent rate in the scooting mode reaction progress decreases as the turnover becomes limited by the mole fraction of substrate at the interface. Recall that excess unhydrolyzed vesicles do not have bound enzyme and are not accessible to enzyme bound to other vesicles. As shown in Figure 7, under such conditions a dramatic increase in the observed rate is seen after the addition of the polycationic cyclic peptide polymyxin B.[84] Independent studies show that polymyxin B mediates a rapid, selective, and direct exchange of monoanionic phospholipids through peptide contacts between enzyme-containing and enzyme-free excess vesicles.[127−129] Thus, polymyxin B leads to substrate replenishment in enzyme-containing vesicles, and this is the basis for its activating effect. These results underscore the fact that not all agents that lead to activation of an interfacial enzyme work by altering the intrinsic catalytic efficiency of the enzyme. The latter effects are selective and show strong structure−activity correlation. The novel biophysical phenomenon exhibited by polymyxin B is also exhibited by several other peptides and proteins including mellitin,[130] myelin basic protein,[131] and lung surfactant protein A.[132] This phenomenon may also be the basis for the antibacterial effect of polymyxin B and other cationic peptides, possibly through a direct effect on the hyperosmotic swelling (plasmolytic) response[133] controlled by the transcriptional effect on the *osmY* gene[134] in *E. coli*.

F. Constraints for the Microscopic Steady-State Condition in the Scooting Mode

The highly processive scooting mode reaction progress provides unequivocal proof for the true interfacial nature of the catalytic cycle events. Furthermore, the scooting mode reaction path is amenable to quantitative analysis. From the reaction progress it is possible to obtain a complete set of the primary kinetic parameters for the catalytic cycle (Table 6) because certain critical conditions are satisfied.[6]

(a) The kinetic path is unequivocally defined. Processive interfacial turnover on vesicles in the scooting mode is explicitly described by the interfacial steps of the turnover cycle with the initial binding of the enzyme to the interface as a pre-steady-state step (Figures 4 and 5).

(b) By choosing an excess of vesicles of narrow size dispersity over enzyme (eq 8), it can be assured that the microenvironment of each enzyme is identical through the course of the reaction progress. Thus, when a vesicle of, say, 10 000 phospholipids containing a single bound enzyme is 50% hydrolyzed, other vesicles of the same size and containing a single enzyme will be 50% hydrolyzed on average. The ensemble behavior of the system can be described simply in terms of the number of enzyme-containing vesicles. The reaction is initiated rapidly by mixing the enzyme with an excess of a monodisperse population of vesicles, which ensures a random Poisson distribution of at most one enzyme on each enzyme-containing vesicle if the vesicle-to-enzyme ratio is larger than 6.[1,6,81,127]

On the basis of these constraints, for the steady-state kinetic analysis of enzyme function it is assumed that all components are uniformly distributed in the reaction mixture and that the bulk-averaged conditions on the enzyme-containing vesicles correspond to the microscopic environment of each enzyme molecule. The constraints are necessary because the single turnover time is in milliseconds, and the steady-state reaction progress is measured over several minutes, i.e., information about the events of the single turnover cycle is inferred from the time-average and the ensemble-average of multiple turnover events under identical conditions.

G. Quasi-Scooting Mode Turnover with Rapid Substrate Replenishment

Under two sets of conditions, the catalytic turnover in the quasi-scooting mode occurs with rapid substrate replenishment from the excess aggregates. In one case, the rapidly exchangeable substrate also forms the interface where the turnover occurs.[53] The second case occurs if the rapidly exchanging substrate partitions into the interface of a diluent.[14] In

addition, the exchange of enzyme between vesicles would also give a similar reaction progress, which would be uninterpretable unless of course the processivity (Figure 5) or residence time of the enzyme on the interface is unequivocally established. If the exchange of enzyme is rapid on the time scale of the turnover, one does not need to know the residence time or the processivity; a knowledge of the affinity of the enzyme for the interface (K_d) is sufficient. This consideration is relevant to the case of sPLA2-catalyzed hydrolysis of long-chain zwitterionic phospholipid aggregates where the binding of the enzyme to the interface is of relatively weak affinity.

Since only the interface-bound enzyme carries out the turnover, the fraction of the enzyme at the interface depends on the bulk concentration of the interface. The dissociation constant of E* to E is defined as K_d, which is also a component of the apparent Michaelis constant, K_M^{app} (eq 4), that defines the dependence of the observed rate on the total substrate concentration. The steady-state condition for the bound enzyme is described unequivocally because the substrate depleted on the enzyme-containing micelle is rapidly replenished from the excess enzyme-free micelles via the monomer exchange. For example, a high critical micelle concentration (about millimolar range) of short-chain phospholipids ensures that the substrate exchange with excess micelles occurs on the microsecond time scale compared to the single catalytic turnover time of a few milliseconds,[135] as also supported by the mixing times for micelles of short-chain phospholipids.[136] The apparent parameters obtained from the bulk substrate concentration dependence are related to the primary parameters (Table 6) and reflect the fact that not all of the enzyme may be bound to the interface. Note that without independent evidence, the quasi-scooting mode reaction progress alone does not imply that the enzyme directly accesses the substrate from the interface.

To recapitulate, quantitative interpretation of the interfacial catalytic turnover is obtained under the (quasi)-scooting mode. Under these kinetic conditions, the variables in the microenvironment of the interface-bound enzyme can be unequivocally defined for the purpose of the ensemble-averaging and the time-averaging of all the events in the reaction mixture during the reaction progress. Kinetic interpretation requires that the intrinsic rate-limiting step and the kinetic path remain well-defined throughout the observed reaction progress. Otherwise, as considered in section IV, only uninterpretable kinetic results are obtained under the conditions with undefined kinetic paths for the steady-state turnover.

IV. Undefined Kinetic Path for Assays with Impaired Substrate Accessibility and Replenishment

In this section we outline limitations of some of the commonly used PLA2 assays where the kinetic path is not unequivocally defined and the microscopic variables cannot be established due to impaired substrate accessibility and replenishment. Although results from such assays can be rationalized in terms of Figure 1, the results do not provide unequivocal information about the primary events.

A. Assay Criteria for Kinetic Analysis

The challenge of interfacial kinetic analysis within the paradigm of Figure 1 is to identify assay conditions with a defined kinetic path where the microscopic variables can be unequivocally defined. Otherwise quantitative information about the primary functional events of the interfacial catalytic cycle is not obtained. Such information can be compromised for a variety of reasons including aggregate-to-aggregate exchange rates for the enzyme, substrate, and product, which can corrupt the interpretation of the observed reaction kinetics.

Resolution of the assay artifacts from parallel paths is critical for the evaluation of the events of interfacial catalytic turnover cycle. Of all the possible sources of difficulty, a change in the interfacial processivity due to a shift in the E to E* equilibrium has profound kinetic consequences. In fact, so much so that reaction progress curves with virtually any shape can be generated.[5] Note that it is not trivial to experimentally ascertain whether the bound enzyme stays at the interface for one or a few turnover cycles. Such considerations emphasize that a possible change in the E to E* equilibrium leads to a change in the processivity which makes analysis impossible. For a meaningful analysis, all equilibria feeding into the turnover cycle must remain invariant, or at least predictable, during the observed reaction progress.

B. Hydrolysis of Monodisperse Substrates

Use of a monodisperse substrate in the aqueous phase offers the possibility of studying the catalytic turnover through a monodisperse ES complex for the solution kinetic path in Figure 1. For such purposes it must be established that monodisperse ES exists and that the turnover proceeds in solution. Since interfacial enzymes are able to work at the interface of organized substrates, the possibility that they also work on a water-soluble substrate adsorbed on the reaction vessel surface or on micro air bubbles has to be considered. A protocol for eliminating the contribution of the reaction on all the surfaces in a reaction vessel is shown in Figure 8, and the method can also be adopted for identifying the contribution of the reaction at the air bubbles.[14,121] For the situation in Figure 8, the time course of hydrolysis of the monodisperse substrate, a short-chain phospholipid in this case, by pancreatic sPLA2 was monitored in the presence of a fluorescent pH indicator dye in the linear range of the signal.[121] The difference between the rate with and without stirring clearly shows that virtually all hydrolysis occurs on the cuvette walls because only the fluorescence from the center of the solution is measured. Thus, an upper limit estimate for the rate of hydrolysis of monodispersed substrate in the aqueous phase via ES complex is less than 0.03 s^{-1} compared to a rate of 4 s^{-1} under stirred conditions.

Note that even if a significant reaction rate is observed under the unstirred condition, it does not

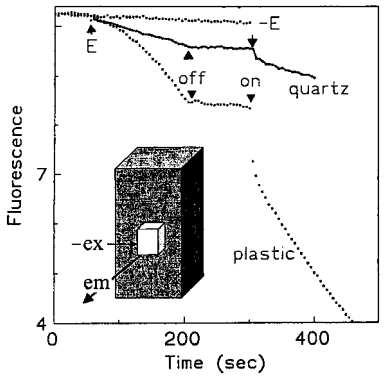

Figure 8. Effect of stirring on the reaction progress for the hydrolysis of monodisperse dihexanoyl-phosphatidylcholine (0.4 mM) by pig pancreatic sPLA2. A lack of significant product formation in the center of the cuvette in the unstirred solution shows that the observed reaction occurs only at the cuvette walls and/or stir bar surfaces. Arrows labeled "off" and "on" designate initiation and termination of stirring, respectively. Note that the reaction progress stops when the stirrer is turned off, and a product burst is seen when stirring is reestablished. Higher rates are also seen if air-bubbles are present in the reaction mixture. (Reprinted with permission from ref 121. Copyright 1999 American Chemical Society.)

necessarily mean that the reaction occurs through monodisperse ES because ES may combine with other substrate amphiphiles to form a premicellar aggregate. sPLA2s are known to form premicellar aggregates with short-chain amphiphiles below their CMC.[63,138−146] The aggregation behavior is probably due to the fact that the i-face of sPLA2s makes contact with the headgroup region of several phospholipids and thus changes their hydrophilic−lipophilic balance. Specific binding of an anionic amphiphile may nucleate the aggregation of other amphiphiles. Kinetic analysis with premicellar aggregates is difficult, if not impossible, to interpret because even with the simplest model the E/S ratio as well as the absolute concentrations of components would determine the fraction of the aggregate-bound enzyme. In short, it is extremely difficult to unequivocally establish that turnover occurs via a monodisperse ES complex.

Experience with monodisperse substrate also calls into question some of the observations that are at the basis for the dual phospholipid model for 'interfacial activation' via the ES complexes in aqueous phase. The first version of the model, with catalytically active dimeric enzyme at the interface,[24a] has been discounted by direct evidence that a single 14-kDa subunit of several sPLA2s is fully active at the interface.[83] In the current version of the dual phospholipid model,[147] the ES complex is composed of one enzyme with two single phospholipid molecules: one as the substrate bound to the catalytic site and the other at an allosteric site that controls the turnover events. This stoichiometry has never been determined directly. Since sPLA2s, particularly the *Naja* venom enzymes, exhibit a propensity for premicellar aggregate formation,[141,142] it is likely that the difference between the two classes of phospholipid amphiphiles reflects the tendency to form the premicellar aggregates.

C. Hydrolysis in the Water-Restricted Environment

The enzyme-catalyzed lipolysis of phospholipids and glyceride in organic solvents containing a small amount of water is useful for preparative purposes. Although these results have been interpreted for obtaining information about the product analysis,[150] the conditions and polymorphism for the kinetic analysis are not adequately defined.

D. Substrate Replenishment Becomes Rate-Limiting in Mixed-Micelles of Long-Chain Phospholipids with Detergent

To the best of our knowledge, detergent-dispersed substrates as mixed-micelles have not yielded primary kinetic parameters, although such conditions are extensively used for assays of interfacial enzymes.[24,50,148,149] One of the major limitations of mixed-micelles of long-chain phosholipids is that the rate of substrate replenishment, rather than the chemical step, becomes rate-limiting.[137] With less than 50 phospholipid molecules in a mixed-micelle containing 50−100 detergent molecules, X_S will drop to <0.2 in less than 0.1 s in the presence of an enzyme, such as sPLA2, with an intrinsic turnover rate of 500 s^{-1}. Thus, if the substrate replenishment rate is not much faster than the turnover rate, after a few milliseconds the apparent linear reaction progress is limited by the substrate replenishment rate and not by the catalytic efficiency of the enzyme. Thus, mixed-micelle kinetics[148,149] with long-chain phospholipids are more a measure of interaggregate exchange of components under the substrate-depleted conditons rather than a measure of the primary parameters that describe the catalytic action of the enzyme at the interface.

The replenishment rate for a long-chain phospholipid in mixed-micelles is expected to be, and is, exceedingly slow via the exchange mechanism where the phospholipid desorbs into the aqueous phase because the aqueous concentration is in the subnanomolar range.[151,152] The fact that the detergent exchange rate may be rapid between mixed-micelles of phospholipid is of no consequence for determining the substrate concentration that the enzyme 'sees' at the interface of a mixed-micelle.[85,137] What is critical is that the substrate and product exchange rates on the enzyme-containing micelle be rapid on the time scale of the intrinsic catalytic turnover rate. Mixing of long-chain phospholipids between mixed-micelles occurs mostly by a fusion−fission mechanism. As an initial step it requires collision of two micelles, and therefore, the mixing rate depends on the concentration of micelles. With millimolar concentrations of detergent and long-chain phospholipid, the half time of mixing of the components of mixed-micelles is in the range of seconds to minutes.[153,154] This is not rapid enough to replenish the substrate for an interfacial enzyme operating with a turnover time for the chemical step of 20 s^{-1} or an aggregate containing 100 substrates. It has been shown that the chemical step for hydrolysis of long-chain phospholipids by sPLA2s is rate-limiting for vesicle hydrolysis in the

scooting mode but not for the hydrolysis of the same substrates dispersed in detergent micelles. This is consistent with the rate in mixed-micelles being dominated by interaggregate exchange processes.

Other factors also come into play for the characterization of slow turnover enzymes using millimolar substrate dispersions. The E to E* equilibrium also depends on the micelle concentration. Thus, kinetic analysis would require characterization of the exchange rates on the enzyme-containing micelles, which could be even lower because a significant part of the surface of a small micelle would be covered by the enzyme, and this would lower the effective collisional probability for mixing. Kinetic analysis with mixed-micelles would also require assumptions about ideal mixing of the components at the interface and about the particle dispersity with changing S to detergent ratio. To the best of our knowledge, the analysis based on such assumptions has not been carried out.

E. Egg-Yolk Assay

High concentrations of egg yolk or phospholipids emulsified with bile salts are an adequate substrate for pancreatic sPLA2 but few other sPLA2s.[155] This pH-stat titration assay with a significant background drift can be readily set up for determining the amount of active enzyme with the help of a calibration curve. With an equimolar mixture of phosphatidylcholine and bile salt, it has also been adopted for the assay of inhibitors.[97−101] However, for the characterization of mutant sPLA2s, results from this assay do not correlate well with other assays.[156−158] The major problem is that the primary parameters needed for the structure−function correlation cannot be extracted from the kinetic results unless the organization and exchange properties of the interface are known and taken into consideration. This has not yet been achieved.

F. Anomalous Activating Effect of the Reaction Products Accumulated in the Interface

In the absence of rapid substrate replenishment, the product accumulation at the enzyme-containing interface has significant consequences on the course of the reaction progress.[5,51a,107,159,160] For example, pig pancreatic sPLA2-catalyzed hydrolysis of zwitterionic vesicles follows a complex reaction progress with an initial delay followed by the onset of a steady-state phase (Figure 9). The key result is that the product-containing zwitterionic vesicles do not exhibit the initial delay and that the binding of the enzyme, E to E*, to the ternary vesicles containing the products of hydrolysis is more enhanced. The delay decreases with increasing calcium concentration[161,162] and also in the presence of other anionic amphiphiles or with anionic phospholipid vesicles.[1−4,83,107,163−165] The reaction progress is also affected by a variety of nonpolar solutes and amphiphiles.[49,51,159,163−169] The most dramatic of such anomalous reaction progress curves is the effect of the gel−fluid phase transition of the bilayer on the reaction progress on phosphatidylcholine[51] but not with anionic vesicles.[3,164] These results clearly provide the kinetic basis for the apparent effect of the phase transition temperature on the hydrolysis of phosphatidylcholine vesicles carried out as a single-point assay.[170] A sharp increase in the apparent rate is seen as the delay reaches a minimum at the transition temperature.

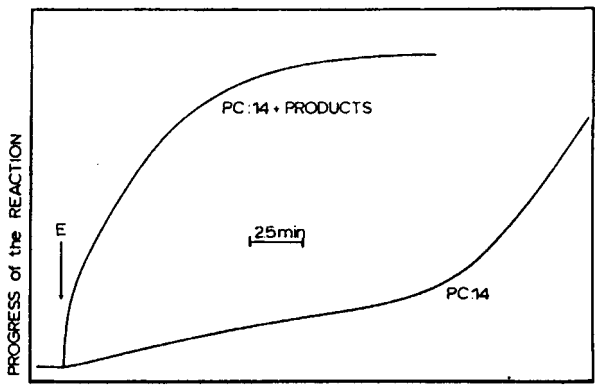

Figure 9. Reaction progress for pig pancreatic sPLA2-catalyzed hydrolysis of dimyristoyl phosphatidylcholine vesicles alone (PC:14) or with co-vesicles containing 10 mol % of the products of hydrolysis. (Reprinted with permission from ref 107. Copyright 1982 Elsevier.)

These results strongly suggest that the onset of the rapid phase following the initial delay is due to the effect of the accumulated product.[107] Together such observations leave little doubt that the complex reaction progress on phosphatidylcholine vesicles is due to the effect of accumulated product mole fraction, which changes with the reaction progress, on binding of the enzyme to the interface.[108] In addition, as described later, build up of the interfacial anionic charge also induces allosteric k_{cat}* activation of pancreatic sPLA2 (section V). The inhibitory effect of the product due to its binding to the active site (classical product inhibition) is also important in addition to the surface dilution of X_S. However, the first two effects are considerably larger during the delay phase because the affinity of the enzyme for the zwitterionic interface is very low. These results also show that the effect of the products is on the E to E* binding equilibrium and not on the kinetic rate constant for the E to E* step (sometimes called the penetrating power of the enzyme).

Contrary to the assumption made in many of the theoretical treatments to account for the lag period with zwitterionic vesicles and monolayers (see below), the delay is not a simple one-step primary kinetic event. Even under the best of conditions it involves a shifting equilibration time due to accumulaion of the product. Quantitative analysis of the results in Figure 9 is possible with several variables,[5] only if other independent information is included and additional assumptions are made. The concentration of the product on the enzyme-containing vesicles changes the position of the E to E* equilibrium during the reaction progress. Also, fusion of the product-containing vesicles is promoted by a millimolar concentration of calcium.[161,162] At some stage of this analysis it may be necessary to make assumptions about the effects of nonideal miscibility of the products[108,167] and the consequent changes in the phase properties of the

bilayer during the reaction progress.[171−174] Also note that the delay to steady-state has also been accounted for by a kinetic model in which desorption of the enzyme from the interface is promoted by the products of hydrolysis,[160b] although the assumption is inconsistent with independent measurements. Considering the contributions of such variables along with the turnover parameters, the study of sPLA2s that display the long-delay phenomenon on zwitterionic phosphatidylcholine vesicles is unlikely to provide unequivocal information about the primary events.

G. Kinetic Artifacts of Change in Processivity due to a Shift in E to E* Equilibrium

Within the kinetic paradigm of Figure 1 there are several ways in which the observed rate can increase or decrease. Nonspecific inhibition is induced by a variety of solutes in the interface that shift the E to E* equilibrium in favor of E.[5,164,175,176] Likewise, nonspecific activation occurs if the additive causes a higher fraction of the enzyme to bind to the interface. In addition to the cationic amphiphiles (mepacrine, quinacrine), hydrophobic solutes in general have a dramatic effect on the miscibility of the dispersed anionic amphiphiles that control the fraction of the interface-bound enzyme. On the other hand, such artifacts are not observed with vesicles of anionic phospholipids because enzyme remains tightly bound to the interface even in the absence of additives. These concepts have been discussed in detail elsewhere.[58,62,82,177]

H. Origin of the Delay in the Monolayer Reaction Progress

Phospholipid monolayers at the air−water interface have been used to study sPLA2s and other interfacial enzymes.[10,48,57,178−182] The reaction progress is monitored as a change in the surface pressure (first-order conditions). It is also possible to monitor reaction progress as a change in the surface area (zero-order conditions) using a movable barrier to measure the change in the number of amphiphiles at the interface as a function of time. With the assumption that the products rapidly leave the monolayer, the delay in the onset of a linear phase of the reaction progress for the hydrolysis of phosphatidylcholine monolayers (Figure 10) has been attributed to slow penetration of the enzyme into the substrate monolayer. As it turns out, this interpretation is not valid as shown in Figure 10 and outlined below.

Several factors come into play because of the monolayer trough geometry, and for a variety of reasons it is not possible to determine the microscopic variables. For example, a 100-μm thick unstirred aqueous layer in contact with the monolayer interface introduces a diffusion-dominated delay; for enzyme to equilibrate in the monolayer through the unstirred aqueous layer requires about 2−5 min,[5] as is apparent in curve a in Figure 10 at low surface pressure. Critical tests show that longer delays in the appearance of the rapid phase of the reaction progress at

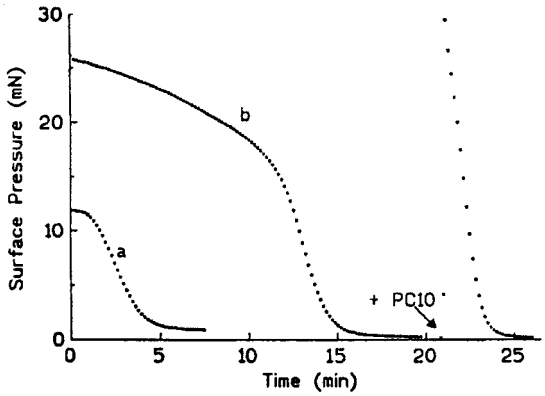

Figure 10. Reaction progress for the hydrolysis of didecanoylphosphatidylcholine (PC10) as a monolayer at the air−water interface at constant area (38 cm^2) by pig pancreatic sPLA2 added at 0 min: (a) at 12 mN initial pressure, (b) at 26 mN initial pressure and then at the end of the reaction progress the same amount of PC10 was added again at 21 min marked (with an arrow). (Reprinted with permission from ref 178a. Copyright 2000 American Chemical Society.)

higher surface pressures (curve b) is due to accumulation of the products that remain in the monolayer.[178] This is reminiscent of the long delay seen with zwitterionic vesicles (Figure 9) where products present in the interface allow more enzyme to bind to the interface. As also shown in the later part of curve b, the delay is not seen if the monolayer is spread over the subphase containing the products of hydrolysis. At least qualitatively, these results clearly show that the product accumulation in the interface during the delay leads to an apparent increase in the rate. The maximum steady-state rate of hydrolysis of the didecanoylphosphatidylcholine monolayer, at the end of the delay, is less than 1 s^{-1}, compared to a rate of >500 s^{-1} for the micellar and bilayer dispersions of the same substrate. Thus, it seems clear that only a small fraction of the total sPLA2 added to the subphase is bound to the monolayer. Coupled with the fact that it is difficult to quantify the amount of enzyme on the monolayer, it is unlikely that the intrinsic turnover rate at the monolayer can be directly determined.

Detailed analysis of the results in Figure 10 and also of the results obtained under zero-order conditions shows that the microscopic steady state at the monolayer interface has several additional contributions which cannot be quantitatively resolved.[178b] The delay in the onset of the steady state in the reaction progress is not a first-order process, presumably due to multiple quantitatively unresolved contributions to the onset of the apparent steady-state reaction progress. The equilibrium partitioning of the product shows a biphasic dependence on the surface pressure of the monolayer, which accounts for a complex dependence of the delay and the turnover on the surface pressure. Finally, it is quite intriguing that the products of hydrolysis alone do not form a stable monolayer,[57a] yet depending on the surface pressure, a significant amount of the product is retained in the substrate monolayer at equilibrium as well as during the steady-state reaction progress. In short, the monolayer assay is unlikely to yield the catalytic

parameters because the rate-limiting step is in a step other than the chemical step.

I. Dispersions of Immobilized Cross-Linked Lipids

Pyrene-labeled phospholipids are used in several sensitive and convenient assays.[183−185] By including serum albumin to bind released fatty acid to increase the quantum yield, this assay permits quantitative detection of less than 1 pmol of sPLA2.

Cho and co-workers championed the use of laterally cross-linked (polymerized) phospholipid as the matrix for the pyrene-labeled phospholipid substrate to obtain an apparent rate parameter.[186] The significance of the rate parameter in terms of the primary kinetic events is questionable. The assay mixture consists of serum albumin and 1−5 mol % non-cross-linked pyrene-labeled substrate (0.1 μM in the matrix of 9.9 μM cross-linked phospholipids). It is unlikely that long-chain substrate exchanges between vesicles. With an enzyme/vesicle ratio >5, virtually all vesicles have one or more bound enzymes. The observed initial rates are typically 1 s^{-1} with a short zero-order region. The time course is fitted to a first-order rate progress curve, which divided by the total enzyme concentration gives the apparent k_{cat}/K_M value. For the interpretation of this parameter, consider the conditions for the reaction path. For the turnover calculations it is assumed that all the enzyme is bound to the interface. With an enzyme/vesicle ratio $\gg$1, the apparent first-order rate constant is related to an ensemble-averaged number of enzymes per vesicle. Thus, the experimental reaction progress curve is actually a sum of different first-order curves, each with a different time constant related to the number of enzymes per vesicle. Ideal mixing of substrate and product within the polymerized matrix is assumed. It is quite likely that the degree of polymerization of the matrix would influence the mixing and lateral distribution of the enzyme as well as the substrate and product. With another kind of polymerized lipid there are indications that the matrix has an inhibitory effect on the hydrolysis of partitioned substrate,[187,188] as if the matrix is not an ideal diluent (section V).

J. Fatty Acid Binding Protein Assay

A sensitive assay for sPLA2 uses natural phospholipid substrates, and released fatty acid is monitored by fluorescence as it displaces a fluorescent fatty acid analogue bound to a fatty acid binding protein in the aqueous phase.[189] Typically, rates of 0.1 nmol/min are obtained, which makes it attractive for quantifying small amounts of enzyme. The fatty acid binding protein assay as well as the pyrene−phospholipid assay cannot be used for monitoring the reaction rate at high vesicle concentration because the fatty acid is drawn away from the respective sinks (fatty acid binding protein or albumin) into the vesicle interface. This opens the possibility that some of the enzyme may be bound to extraneous surfaces.

V. Equilibria at the Interface

Three types of interfacial equilibria have been determined for the interpretation of the observed catalytic turnover.[58,81,122,123,126] (a) The dissociation constant for E* from the interface, K_d, determines the fraction of bound enzyme as a function of the bulk interface concentration expressed as moles of phospholipid per unit volume of the aqueous phase. The apparent value of K_d for virtually all sPLA2s for the scooting mode turnover on DMPM vesicles is estimated to be in the subpicomolar range.[1,6] Note that in this case the bound enzyme exists as a mixture of E*, E*S, and E*P species; thus, K_d is an apparent constant. The apparent K_d values for the various sPLA2s on phosphatidylcholine vesicles and micelles are in the range from <0.01 to 20 mM.[108,115,126]

(b) K_L' is the bulk concentration of the interface at which one-half of the total ligand (L = inhibitor, substrate, or product) is partitioned from the aqueous phase into the interface.[123] For the micellar amphiphiles, K_L' is the CMC.

(c) Binding of an active-site-directed ligand in the interface to E* to form E*L in the interface is defined by the two-dimensional equilibrium dissociation constant (K_I*, K_P*, K_S*) expressed in units of mole fraction. Thus, when $X_L = K_L$*, [E*] = [E*L].[56,58,123,126,192,193]

A. Neutral Diluent as a Two-dimensional Interfacial Solvent

Measurement of the primary interfacial equilibrium constants is possible with a suitable surface diluent which permits a systematic change in X_L between 0 and 1. A surface neutral diluent is conceptualized as an amphiphile which as a two-dimensional solvent changes X_L and also provides an interface for the E to E* step.[58] If the diluent has significant affinity for the active site of E*, i.e., if $K^*_{diluent}$ for the diluent amphipile is <1, the diluent and the ligand molecules will compete with each other for the binding to E* and the measured K_L* will be an apparent value whose magnitude depends on the identity of the surface diluent. Such nonideal surface diluents can be used for the equilibrium measurements under suitable conditions as long as $K^*_{diluent}$ is not $\ll$1.[126] For an ideal neutral diluent (ND), $K^*_{diluent} \gg 1$.

Amphiphiles such as 1-hexadecyl-propanediol-3-phosphocholine and 2-hexadecyl-glycero-3-phosphocholine in aqueous dispersions have served as useful neutral diluents for the pancreatic sPLA2, i.e., their aqueous dispersions provide an interface for the E to E* step, but the diluent amphiphile does not bind to the catalytic site of E*.[58] On the other hand, structurally related lysophosphatidylcholine has considerably higher affinity with K_L* = K_P* = 0.06 mole fraction. As expected, the same amphiphile does not necessarily serve well as a neutral diluent for different interfacial enzymes.[115,126] Neutral diluents are useful for studying the properties of the enzyme at the interface and also for changing the surface concentration of an active-site-directed ligand to monitor the E* to E*L equilibrium (see below).

Note that a two-dimensional diluent may also have an allosteric effect on the bound enzyme. Similarly, the dispersity of the diluent aggregates may have a significant effect on the replenishment rates for the

observed turnover without a significant effect on the equilibrium process.[58,123] In effect, neutral diluents are interface-forming amphiphiles that are also very poor inhibitors. For sPLA2s, the polar group of the amphiphile essentially distinguishes an active-site-directed binder from a neutral diluent amphiphile.[53,123] The transfer of a nonpolar chain from the interface to the active site has little or no significant energetic advantage because the hydrophobic effect in both cases would be comparable, and in the water free environment the difference would be dominated by the van der Waals contacts.

B. Binding of Enzymes to the Interface

Binding of a sPLA2 along the i-face involves contact with a number ($n = 20-40$) of phospholipid molecules at the interface.[2,108,138,194−197] In terms of the excluded area effect, the binding of one enzyme molecule makes n phospholipid molecules inaccessible for the binding of the next enzyme. Under the conditions where K_d is much smaller than the total phospholipid concentration, only the value of n can be determined from the binding isotherms, as is the case for the binding of sPLA2 to anionic vesicles.[3,197] When K_d for the E to E* equilibrium can be measured, it is equal to the bulk concentration of amphiphile at which one-half of the enzyme is bound to the interface. The excluded-area effects can be neglected as long as the number of binding sites on the bilayer vesicle (total phospholipid/2n) is much greater than the number of bound enzyme molecules. Usually a three-parameter fit is necessary for obtaining n, K_d, and the maximum signal when all the enzyme is bound;[108,138] however, even with the three-parameter fit the binding isotherm is not hyperbolic (see section XI).

C. Two-Dimensional Equilibrium Constants

X_L can be systematically varied by adding a neutral diluent to the interface with the assumption of ideal mixing. Such a shift in the E* + L* to E*L equilibrium permits determination of K_{Ca}*, K_S*, K_P*, and K_I*.[58,59,122,126] To distinguish E* from E*L, one takes advantage of the fact that, with most L*, E*L reacts >100 times slower with an active-site-directed alkylating agent.[54,58] At least for pancreatic sPLA2 the rate of alkylation is comparable for E in the aqueous phase and E* at the neutral diluent interface. It may be noted that the partitioning of alkylating agent into the interface does not affect the rate of enzyme alkylation since the factors that favor transfer of alkylating agent from the aqueous phase to the interface are canceled by the factors required for transfer of alkylating agent from the interface to the catalytic site of E*. This protocol thus provides a basis for distinguishing neutral diluents from the active-site-directed mimics. Other measures of the occupancy of the active site can also be designed under suitable conditions.[123,197]

D. Sequential Equilibria

Two or more equilibrium steps in Figure 1 may be sequentially related and characterized as apparent dissociation constants. Also in the case of sPLA2s, the E to E* equilibrium shifts with the ligand binding to the active site of E* (mass action). Similarly, the binding of an active-site-directed substrate mimic obligatorily depends on the calcium binding (not shown but implied in Figure 1), which gives an apparent dissociation constant for calcium at a given substrate concentration (eq 2). Also, the apparent calcium dissociation constant depends on the fraction of enzyme at the interface, K_d, since interfacial binding is required for the E* + S → E*S equilibrium. Under certain conditions such coupled equilibria can be readily resolved.[122,126] Again, the use of a neutral diluent ensures that the primary rather than apparent equilibrium constants are being measured.

E. Quantification of sPLA2 Interfacial Binding

Studying the structure−function for the binding of sPLA2 requires a reliable method for measuring the equilibrium constant for the enzyme−vesicle complex dissociating to free enzyme and vesicles (K_d). Measuring K_d values seems simple enough by assuming that the E to E* is a single-step event. However, several problems are intrinsic in the available methods.[197a−c] The most commonly used method relies on the change in intrinsic tryptophan fluorescence[1,2] or the energy transfer from tryptophan residues on or near the i-face and a trace amount of dansylated phospholipid present in vesicles.[197a] While such methods are reliable under certain specific conditions, we have found that the Trp environment changes significantly when distal mutations are introduced and that the efficiency of energy transfer varies dramatically with the vesicle composition. For example, cobra venom sPLA2 binds tightly to anionic phosphatidylmethanol vesicles leading to a readily detectable energy transfer signal. However, no signal was detected when the same enzyme was added to phosphatidylcholine vesicles even though other methods clearly show that cobra venom sPLA2 binds tightly to such vesicles (K_d in the low micromolar range). Such differences are expected if the enzyme contact surfaces are different at the anionic versus the zwitterionic interfaces. Also, the differences can be rationalized in terms of the Forster equation where the efficiency of the energy transfer depends on the distance, orientation, and dielectric of the medium separating the donor−acceptor pair and their relationship to the local quenching groups.

The binding of most, if not all, sPLA2s to vesicles composed mainly of anionic phospholipids is tight (K_d ∼ nanomolar or lower). Values of K_d in this range are very difficult to measure because experiments require the use of low phospholipid concentration (∼1 nM) and even lower sPLA2 concentrations (low pM because each enzyme covers about 50 phospholipids and roughly 50% of the phospholipids are on the inner leaflet of vesicles). All sPLA2s that we have studied undergo nonspecific absorption to the reaction vessel (plastic or glass, siliconized or not) at concentrations below 10−100 nM. It has therefore not been possible to measure values of K_d in the subnanomolar to nanomolar range (see also ref 121).

Surface plasmon resonance (SPR) has been used in an effort to remedy this problem.[197c] For this

technique, a phospholipid bilayer within about 10 nm of a gold surface is required. Protein binding to the bilayer is detected by a change in the bulk refractive index within a ~50-nm thick layer next to the gold surface. Intact phospholipid vesicles are placed close to the gold surface by using the biotin-streptavidin technology. Experimental conditions were optimized such that captured vesicles were intact, vesicles were packed close together on the surface, and vesicles did not leave the surface after extensive washing with buffer. By raising the enzyme concentration in the flow solution, the SPR signal reaches a maximum (measured to occur with 1 sPLA2 per 40−70 outer layer phospholipids). The concentration of sPLA2 was decreased until the SPR signal dropped to one-half its maximal value. At this point 50% of the enzyme binding sites on the vesicle contain bound enzyme and the concentration of free and protein-bound sites on vesicles are equal with the assumption that the extraneous surfaces are saturated with the enzyme (see below). Under this condition, K_d is given simply by the concentration of sPLA2 in the aqueous phase. Since pM concentrations of sPLA2 can be measured by sensitive enzyme assays, this SPR method should be suitable for measuring values of K_d in the pM range. Note that nonspecific binding of sPLA2 to all surfaces of the closed circulation loop other than the supported vesicles is of insignificant consequence since only enzyme bound near the gold is detected. However, nonspecific binding of sPLA2 to surfaces other than vesicles near the gold surface will cause problems if it is comparable in amount to that bound to vesicles. We used this method to determine a value of $K_d = 0.6 \pm 0.2$ μM for the dissociation of cobra venom sPLA2 to vesicles of dioleyl phosphatidylcholine in the presence of saturating Ca^{2+} (diether phospholipid used to prevent enzymatic hydrolysis).[197c] Recall that no fluorescence energy transfer was detected when this enzyme was bound to phosphatidylcholine vesicles.

The SPR method is useful for measuring high-affinity interfacial binding. For many applications, measuring K_d values under weaker affinity conditions is suitable. sPLA2s typically bind much tighter to vesicles of anionic phospholipids than to zwitterionic phosphatidylcholine vesicles. Thus, it occurred to us that we could adjust the K_d over a broad range by incorporating various amounts of anionic phospholipid in phosphatidylcholine vesicles. For this approach the K_d was measured using the method of McLaughlin and co-workers,[197b] where vesicles are loaded with sucrose by extrusion and then diluted into buffer containing near physiological salt concentration (0.1 M NaCl). Such vesicles are readily pelleted by ultracentrifugation. A fixed amount of sPLA2 is added to various concentrations of vesicles, and the amount of nonvesicle-bound sPLA2 is measured by enzyme assay of the supernatant after ultracentrifugation. We have been able to carry out this experiment with phospholipid concentrations of 0.1−4 mM (lower phospholipid concentrations are avoided because of loss of sPLA2 to the vessel walls). For each sPLA2, we simply adjust the mole fraction of anionic phospholipid in the phosphatidylcholine vesicle so that the K_d is in the measurable range (~0.2−2 mM). Although we cannot quantify higher affinity interfacial binding with this method, we do obtain information about the effect of anionic phospholipid on the binding of sPLA2s to phosphatidylcholine vesicles, and this information is extremely valuable in understanding the behavior of sPLA2s on mammalian cells (next two sections). The sucrose-loaded vesicle method also avoids costly SPR equipment.

VI. Events of the Interfacial Catalytic Turnover Cycle

In this section the focus is on the events of the interfacial catalytic cycle in the scooting mode which permits determination of virtually all primary rate parameters.[6,58,81]

A. Integrated Reaction Progress Curve

Reaction progress in the scooting mode provides unequivocal evidence for the interfacially processive turnover cycles. Since the substrate depletion and product formation on each vesicle are correlated, the substrate affinity and product inhibition parameters are related to the substrate and product mole fraction at the interface. The analysis is further facilitated because the measurements can be carried out with a monodisperse population of vesicles containing at most one enzyme per enzyme-containing vesicle. Within such constraints the integrated reaction progress in the scooting mode is described by eq 6.

B. The Role of Calcium in the Turnover

There is an absolute requirement of calcium for reaction progress.[11] Other divalent cations can substitute for calcium for the substrate binding[56] and also for the chemical step with certain substrates.[122] The kinetic mechanism for the divalent ion requirement is sequential binding of the cation followed by substrate binding. The crystallographic structures suggest that the active-site-directed mimics provide one or two ligands for coordination with calcium, which is probably the basis for an obligatory requirement of the metal ion for the susbtrate binding. The role of the metal ion in the chemical step is proposed in terms of the ligand coordination geometry during the transition state.[56] Whether or not the protein undergoes a functionally significant structural change on calcium binding remains to be established; however, it is clear that the role of the cation is not allosteric on the catalytic turnover steps.

C. Monomer as the Minimum Catalytic Unit of sPLA2s

Most sPLA2 are monomeric in dilute solutions, and they do not show an anomalous increase in the rate as a function of the enzyme concentration. In the scooting mode with at most one enzyme per vesicle, the maximal possible extent of hydrolysis per enzyme, N_S, is the number of substrate molecules on the outer layer of each vesicle. If the vesicle size is known, the maximal amount of product formed, P_{max},

provides a count of the number of catalytically active molecules in the reaction as long as the bound enzyme hydrolyzes all of the substrate present in the outer monolayer of the vesicle. Since the mass of enzyme present in the reaction is known, one obtains the MW of the catalyst. All sPLA2s examined by this method are found to display full activity as monomeric proteins.[83,127] With excess enzyme over vesicles, P_{max} provides a measure of the fraction of the lipid exposed to the bulk aqueous phase under the conditions where the inner layer lipid does not exchange on the time scale for the hydrolysis of the outer layer lipid. Independent measurements also show that the resonance energy transfer between fluorophore-labeled 14-kDa sPLA2 subunits is not seen until the vesicle surface is crowded with sPLA2s.[83]

D. Interfacial Kinetic Parameters

The interfacial Michaelis constant K_M* is obtained from the dependence of the initial rate on X_S. The latter is varied by adding a neutral diluent such that the bilayer structure remains intact.[58] The same value of K_M* has also been obtained from the apparent dependence of the rate on the presence of a competitive inhibitor (eq 3), or the product (eq 6), or calcium (eq 2) with independently determined K_I*, K_P*, or K_{Ca}* at the interface of a neutral diluent. The interfacial turnover number k_{cat}* is calculated from K_M* and v_o, the observed rate at the maximum possible mole fraction of the substrate, $X_S = 1$ (eq 1). These relations are based on the assumption that the binding of the enzyme to the interface is a step distinct from the binding of a ligand (S, P, I, or Ca) to the active site. For pig pancreatic sPLA2, calcium is not required for the binding of the enzyme to the interface but is an obligatory cofactor for the binding of the substrate or mimics to the catalytic site of enzyme in the interface[122] and for the chemical step (as discussed above).[56] These conditions are also satisfied in the quasi-scooting mode with rapid substrate replenishment.

E. Substrate Specificity

The substrate specificity for the catalytic site of an interfacial enzyme, which is not influenced by the interface preference, is determined by carrying out a competitive substrate analysis on co-vesicles where the interface-bound enzyme is allowed to choose between multiple substrates.[64] The ratio of the products formed under these conditions is dictated by the ratio of the specificity constant k_{cat}*/K_M* for the turnover cycle in the interface (eq 7). For example, human group IIA sPLA2 binds several orders of magnitude more tightly to phosphatidylserine vesicles than to phosphatidylcholine vesicles, which is reflected as a large difference in the initial rates seen with vesicles of single phospholipid. However, these two phospholipids are hydrolyzed at similar rates when enzyme is bound to a vesicle containing both of these lipids in an equimolar ratio.[115] Additional independent evidence has been also developed for micellar substrates to discern the effect of surface charge on K_M* and k_{cat}*.[53] The literature contains numerous apparent substrate specificity studies of interfacial enzymes in which catalytic site and interfacial binding specificity are not deconvoluted.

F. The Chemical Step Is Rate-Limiting and Essentially Irreversible

Isotope effects and other measurements show that the enzyme−product complex at the interface dissociates to the enzyme plus products faster than it goes through the reverse of the ester hydrolysis step.[86] The element (oxy/thio) effect on the turnover parameters for the hydrolysis of the *sn*-2-oxy-ester versus the −thioester substrate provides significant insight. This element effect on k_{cat}* in the scooting mode is about 10 in favor of the oxyester for pig pancreatic sPLA2.[85] This ratio remains invariant when measured with mutants with lower k_{cat}*.[56,192] Since k_{cat}* by definition is the compound rate for all steps after formation of the E*S complex, these results provide evidence that the chemical step is rate-limiting for the interfacial reaction cycle in the scooting mode. On the other extreme, a change in the oxy/thio element effect toward a value of unity would show that the chemical step is no longer rate-limiting. Thus, catalytic turnover in the scooting mode is not limited by product desorption from the active site of the bound enzyme (see also section X). Note that there is no element effect on V_m^{app} for the observed kinetics on mixed micelles of long-chain phospholipids and detergents. Since V_m^{app} (eq 1) is the compound rate for all reactions after enzyme−interface binding (E* formation), this shows that a step other than the chemical step, probably substrate replenishment, is rate-limiting[137] in this case, as also discussed in section IV.

G. Interfacial Rate and Equilibrium Parameters Do Not Change with the Phase State of the Interface

The gel−fluid phase transition has no noticeable effect on the interfacial processivity and turnover rate by pancreatic sPLA2 on DMPM vesicles.[3,198] The catalytic parameters in the bilayer and micellar interfaces are also comparable.[53] Also, the equilibrium parameters determined in zwitterionic neutral diluents[58] are completely in accord with the processive kinetic parameters in anionic vesicles and micelles obtained under a variety of conditions.[52] Such convergence and correlation show that the phase state of the interface has little effect on the values of the interfacial parameters. This is not totally unexpected because, as discussed later (section XI), the close contact of the i-face with the interface creates its own microenvironment. Moreover, virtually all anomalies associated with the phase state have been attributed to changes in the variables that influence either the E to E* equilibrium or the substrate accessibility and replenishment rate. Thus, regardless of the organizational phase state of the interface, the chemical step is always slower than lateral diffusion of interacting species in the interface.

Although it seems counter intuitive, this assertion is also consistent with the fact that the i-face of the bound sPLA2 creates its own dehydrated microenvironment with the interface[197a] (also section XI).

H. Active-Site-Directed Competitive Inhibitors

As summarized in Figure 3, mechanistically important inhibitors with *sn*-2-amide or *sn*-2-tetrahedral substituents have emerged as active-site-directed substrate mimics. X-ray crystallographic results show that C═O or P═O of the *sn*-2-substituents replaces the axial water coordinated to calcium. Also, the amide-NH or the other nonbridging oxygen of phosphate is directly or indirectly hydrogen bonded to δNH of the catalytic residue His-48. In addition, from the large number of analogues that have been synthesized (Table 3) there are other subtle interactions which impart modest selectivity toward sPLA2s. Complete kinetic analysis of several of these classes of competitive inhibitors has been carried out.[58,59,177] The mole fraction of inhibitor required for 50% inhibition under the zero-order conditions (X_S constant), $X_I(50)$, is related to K_I^* and K_M^* (eq 3, in Table 5). For determining if the inhibition is competitive, one takes advantage of the differential effect of the inhibitor under the zero-order conditions at constant X_S and the first-order conditions where X_S changes with the reaction progress. A ratio of 1:7 is obtained for the 50% inhibitory mole fraction of an inhibitor for the hydrolysis of pig pancreatic sPLA2 on DMPM under the zero-order versus the first-order conditions.[4,58] This is theoretically predicted,[6] and it is also in accord with independently determined values of $N_S k_i$ and v_o in relation to eq 6.[58,59]

I. Interfacial Partitioning of Competitive Inhibitors

The effect of partitioning of inhibitors on the $X_I(50)$ value is a rather complex function (Figure 11) that fits well to the experimental behavior.[53,177] For such analysis, the problem is best defined as a thermodynamic box (square box in Figure 1) relating the detailed balance condition discussed further in section VIII for a set of equilibria that are connected in a closed cycle.[123] For the hydrolysis of micellar dioctanoylphosphatidylcholine, two limits are of particular interest (Figure 11).

(a**)** The dependence of inhibition by substrate mimic *rac*-MJ33 on the bulk substrate concentration, [S*], gives the fit with $K_I^* = 0.0014$ mole fraction using the independently measured $K_M^{app} = 0.31$ mM. The inhibitor is virtually completely partitioned into the interface with a value of CMC $= K_I' = 0.009$ mM. The CMC of the substrate dominates the behavior at low substrate concentration, whereas at high substrate concentration the behavior is the same as with a bilayer interface.

(b**)** The dependence of inhibition by *rac*-MJ72, a shorter C_8-chain homologue of MJ33, gives the fit shown with $K_I^* = 0.0005$ mole fraction, $K_M^{app} = 0.31$ mM, and $K_I' = 0.3$ mM in deoxy-LPC.[123]

These results show that the difference in the observed inhibitory effect of the two homologous inhibitors is dominated by the difference in the aqueous-to-vesicle partitioning of the homologous inhibitors, whereas the K_I^* values are comparable. In a different study it was shown that differential interaction of inhibitor with phospholipids in the interface, and not within E*, determine the relative inhibitor potency.[104] These effects result from the fact that the percent inhibition of enzyme at the interface depends on the value of X_I in relation to K_I^*. Thus, it is more difficult to interpret relative potencies of PLA2 inhibitors in terms of enzyme−inhibitor binding because the observed degree of inhibition will, in general, be a function of K_I^* and K_I'. It is also possible that inhibitor binds to E in the aqueous phase. Theoretical analyses have been reported that describe the quantitative contributions to the overall inhibition from the binding of inhibitor to both E and E*.[14,53,81,123,177] Some aspects of this are presented in section VIII.

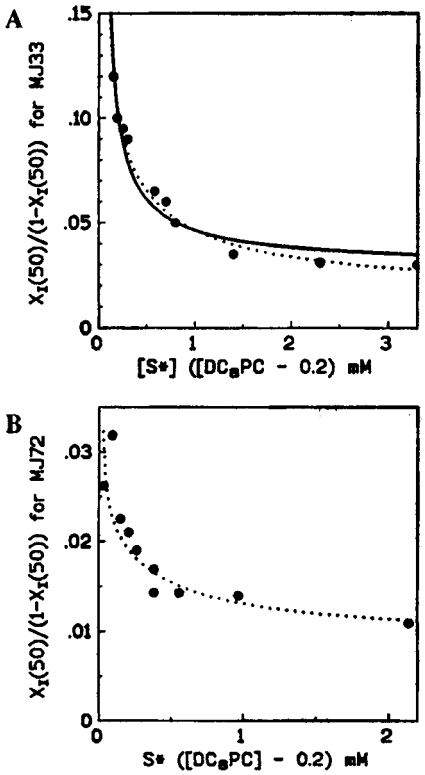

Figure 11. Dependence of $X_I(50)$ values for homologous competitive inhibitors (A) MJ33 (1-hexadecyl-) and (B) MJ72 (1-octyl-3-(trifluoroethyl)-*rac*-glycero-2-phosphomethanol) on the micellar concentration of DC_8PC micelles. The dotted curve shows the best fit to independently determined parameters as discussed in the text. The difference is attributed to a difference in the partition coefficient of the inhibitors. (Reprinted with permission from ref 53. Copyright 1997 American Chemical Society.)

VII. Interfacial Allostery

In this section we outline the evidence that has shown that, by eliminating the kinetic contributions of substrate accessibility and replenishment, it is possible to identify the allosteric effect of the interface on sPLA2 catalytic activity. These results show a coupling between the catalytic and interfacial binding events. They constitute the basis for the effect of the interface on the substrate binding to the catalytic site

(K_S* allostery) and the effect of the interfacial anionic charge on the chemical step (k_{cat}* allostery).

A. Interfacial Activation: Enzyme versus Substrate Model

The phenomenological basis for interfacial activation was suggested from the observation that triglyceride lipase is significantly more active on tributyroylglycerol substrate when present above its solubility limit than with monodisperse substrate below its solubility limit in the aqueous phase.[14,15] More than any other result, an increase in the observed rate at the CMC of short-chain phosphatidylcholines by sPLA2s[9,10,53,194] has provided the grail for the formulation of Figure 1 for enzymology. Early attempts to account for the activation fall in two categories. Variations of the theme of the pure "substrate model" range from a high substrate density (local concentration) at the interface to a preferred conformation or orientation of the substrate at the interface. In contrast, the "enzyme models" invoke a change in the enzyme upon binding to the interface which makes it catalytically more efficient. These models have not been adequately tested, and they have little predictive value. Most likely, the conformation of the substrate mimics in the active site is not significantly different than it is in solution or at the interface.[70] Similarly, the observation that conformationally restricted analogues of phospholipids exhibit higher activity[199] or the result that substrate specificity for the turnover at the interface lies in k_{cat}*[200] are at best consistent with the substrate models. Certainly, such evidence does not rule out the possibility that the active-site pocket of the enzyme also changes with the structure of the substrate. In all such cases there is always the issue of the reference state against which the active substrate conformer is evaluated. The fact remains that there is little evidence for a unique or restricted substrate conformation at the interface.

In support of the enzyme-conformation models for interfacial activation, there is considerable circumstantial evidence that subtle changes occur in the regions that are near or are part of the i-face. For example, the regions that differ significantly between the various sPLA2 structures[68,74−76,87,89,106,145,193,205−208] include the calcium-loop, 69-loop, and the N- and C-terminus domains (Figure 2). These are also the regions that are flexible in the NMR structure[73] and become more ordered in the crystallographic structures or on binding of the enzyme to the interface. Under suitable conditions, such structural signatures can be correlated with the specific events such as the binding of the enzyme to the interface, calcium binding, occupancy of the active site, and the charge compensation associated with the k_{cat}* allosteric site.

As a possible surrogate for activation by covalent enzyme modification by substrate,[201a−d] fatty-acid-acylated sPLA2s are presumably 'activated' due to their enhanced binding to the interface.[182,202,203] Other motifs for high-affinity interactions of proteins with membrane interfaces have also been reviewed.[20,204a−d]

B. Contributions to the Allosteric Effect of the Interface

As a prelude to the formulation of the activation problem for the following discussion, our ultimate concern is about the substrate affinity and catalytic efficiency of E*S. Such effects are related by the detailed balance constraint of the thermodynamic box to the state of ES, E*, S*, and other states intrinsic in Figure 1. Such functional dissection in terms of the primary events would be developed, correlated, rationalized, and understood in terms of the sPLA2 protein structure at the interface versus the aqueous phase. It is clear that sPLA2s do not have a lid covering their active sites that could open upon interfacial binding, as seen with several triglyceride lipases which are serine hydrolases.[209,210]

Although interfacial recognition by sPLA2 has been a dominant theme for three decades, the effect of the interface on the intrinsic properties of the enzyme could not be tested directly until recently when suitable methods and analytical protocols became available. Pursuing the observations that the anionic charge at the interface is a critical determinant for enhanced rate at the interface,[107] evidence has converged on three critical issues best appreciated in the context of Figure 1. Enhanced interfacial binding of the pancreatic sPLA2 occurs at the anionic interface. Having dissected the kinetic effects of the E to E* step, the problem of interfacial activation has been recast on the basis of the allosteric effect of the interface on the events of the catalytic turnover cycle.[53,123,193] The model for k_{cat}* activation is shown in Figure 12, and the basis for K_S* activation is outlined later (section IX). These model-based analyses permit identification of the changes in the equilibrium binding parameters by dissecting out the changes associated with the dimensionality or the local concentrations of interacting components. In addition, specific structural changes on the enzyme, introduced by site-directed mutagenesis, are convinc-

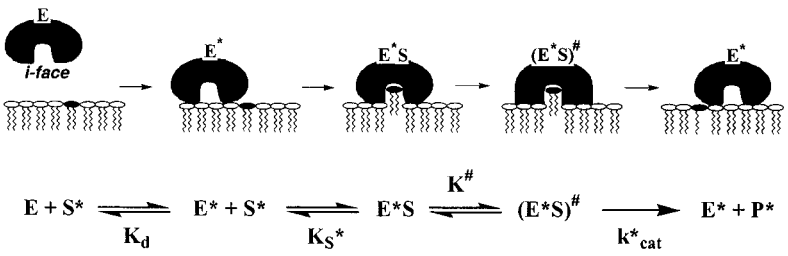

Figure 12. Two-state model for k_{cat}* activation. (Reprinted with permission from ref 193. Copyright 2000 American Chemical Society.)

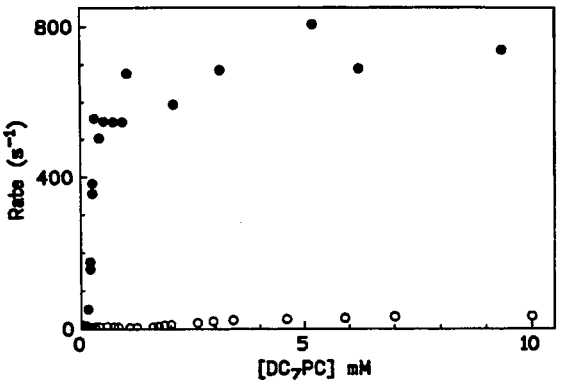

Figure 13. Substrate concentration dependence of the rate of hydrolysis of diheptanoylphosphatidylcholine by pig pancreatic sPLA2 without (○) or with 4 M NaCl (●). (Adapted from ref 53.)

ingly correlated to the functional change, suggesting the existence of discrete states of the enzyme.

C. Analytical Basis for Interfacial k_{cat}* Allostery

For an appreciation of the phenomenon of interfacial activation consider the fact that the pancreatic sPLA2-catalyzed rate of hydrolysis of premicellar monodisperse dihexanoylphosphatidylcholine is <0.03 s^{-1}.[121] In contrast, the observed rate with saturating concentrations of the micellar dispersions is about 10 s^{-1} in the absence of NaCl compared to 240 s^{-1} with 4 M NaCl.[53] On the basis of such evidence, the overall rate enhancement has two components. First, the effect of the binding to the zwitterionic interface, and second, an additional effect of added NaCl on k_{cat}* of the bound enzyme.

The magnitude of the first effect can only be estimated. The monomer rate is an upper limit estimate because it could include contributions for catalysis of premicellar enzyme−substrate aggregates (section IV). The rate at the zwitterionic micellar interface in the absence of added NaCl is also a limit estimate because in this case it is not possible to rule out an effect of the anionic charge on the target micelle due to the steady-state accumulation of the product formed in situ. As developed later (section VIII), there is a significant increase in the affinity of the bound enzyme for the binding of the substrate to the active site; however, K_S* activation is not significantly different at the anionic interface or at the zwitterionic interface in the presence or absence of NaCl.

D. Effects of Charge Compensation

As shown in Figure 13, the rate of hydrolysis of diheptanoylphosphatidylcholine micelles increases in the presence of added NaCl. The overall enhancement of the observed rate in the presence of added NaCl is attributed to three factors which have been quantitatively dissected.[53] First, added NaCl lowers the substrate CMC due to the hydrophobic salting-out effect. Second, the binding of the enzyme to the interface is promoted in part due to the salting out of the enzyme from the aqueous phase. Third, there is an allosteric effect on the rate-limiting chemical step (k_{cat}* allostery) by the anionic charge induced in the interface by preferential partitioning of chloride over sodium ions into the zwitterionic interface. The preferential partitioning of chloride anion into the zwitterionic interface is not widely appreciated. For example, electrophoretic mobility data of Tatulian[211] show preferential binding of anions over cations to zwitterionic interfaces, imparting a net negative charge to them. Selective binding of anions over cations to zwitterionic interfaces is indicated by other measurements as well.[53,212a−i]

The salting-out effect diminishes the interactions of ionic solutes with hydrophobic groups. Dissection of the salting-out effect from the effect of the interfacial anionic charge on the events of steady-state catalytic turnover cycle has been possible with an analysis of the effect of added NaCl on the observed rate as a function of the substrate concentration. As shown in Figure 13, the maximum rate at saturating substrate concentration increases about 50-fold in the presence of 4 M NaCl. Although not obvious from this plot, the observed rate of hydrolysis increases only above the substrate CMC, which is about 1.5 mM and decreases to 0.2 mM in 4 M NaCl. Thus, two apparent parameters are obtained by fitting the observed rate to the micellar substrate concentration (eq 1 and 4 in Table 5). For the results in Figure 13, the major effects of added NaCl are to lower K_M^{app} from 3 to 0.2 mM and to increase V_M^{app} from 16 to 660 s^{-1} for the pig pancreatic sPLA2-catalyzed hydrolysis of diheptanoylphosphatidylcholine micelles. Comparable results have been obtained with other zwitterionic substrates. The effect on K_M^{app} has been attributed to a change in the K_d term largely due to the anionic charge induced by the selective partitioning of chloride.

Analysis in terms of the detailed balance condition shows that when going around a full cycle of changes in the thermodynamic box (Figure 1), salt effects that appear in one branch are fully compensated for in some other branch(es), so that the overall free energy change is zero. Thus, the effect of added NaCl on K_L' is compensated for by a change in K_L.[53] Similarly, the effect of NaCl on K_d is compensated for by an effect on K_d^L. There is no significant effect of added NaCl on K_L* or K_M*. It appears that the catalytic mechanism does not change with added NaCl because the oxy/thio element effect (section VI) on the chemical step remains the same.

Together, the effects of added NaCl on the zwitterionic interface suggest that the k_{cat}*-activating effect of the interfacial anionic charge is due to charge compensation of certain cationic residues on pancreatic sPLA2. This is in accord with the observation that the pancreatic sPLA2-catalyzed rate of hydrolysis of anionic phospholipid aggregates is high and is not influenced by added NaCl. This assertion is consistent with a model in which the Michaelis complex at the interface becomes catalytically competent after the charge compensation of certain cationic residues.

E. Charge Compensation for k_{cat}* Activation Is Mediated by Specific Cationic Residues

The effect of added NaCl is observed with certain sPLA2s.[193] For the 12 cationic residues present in bovine pancreatic sPLA2, only 3 are common to all the sPLA2s that show the NaCl-induced k_{cat}* activation. Also, these three cationic residues are not conserved in the sPLA2s that do not show the effect of added NaCl, although some sPLA2s contain as many as 17 other cationic residues. The comparison clearly suggests that the charge compensation of three cationic residues 53, 56, and 120 in bovine pancreatic sPLA2 could account for the effect of NaCl.

Indeed, site-directed mutagenesis results show that the charge compensation by Lys to Met substitution in bovine pancreatic sPLA2 accounts for most of the k_{cat}* activation by the anionic charge.[53] The individual mutations have an incremental effect on the maximum rate seen in the absence of NaCl, although the maximum rate in the presence of 4 M NaCl remained unchanged within a factor of 2. Also, the rate at the anionic interface is not influenced by the mutations. The incremental contributions of the substitution of the individual residues on k_{cat}* is energetically additive. Data also shows that Lys to Met substitution promotes the binding of sPLA2 to the interface as well as an effect on the substrate binding to the enzyme at the interface. These results are consistent with the model for k_{cat}* activation shown in Figure 12, where the Michaelis complex exists in two forms E*S and $(E^*S)^{\#}$ The complex $(E^*S)^{\ddagger}$ that undergoes the chemical step is formed by charge compensation of specific cationic residues. The presence of methionines in place of cationic residues presumably allows catalytically productive interaction of the substituted regions of sPLA2 with the interface in the absence of interfacial anionic charge. Analysis of the incremental changes in the kinetic parameters shows that the charge compensation of Lys-53 and -56 contributes to the k_{cat}* activation, and in contrast, Lys-120 contributes only to the structural change that promotes the stability of the Michaelis complex at the interface.

F. Structural Reciprocity between Distal Regions of Pancreatic PLA2

Structural and spectroscopic studies with Lys-to-Met substitutions show that in the E, E*, and E*L form of the enzyme at the zwitterionic interface the environment of Trp-3 on the i-face has changed.[53] Such changes appear to be induced by the substitutions in the 53/56 as well as in the 120 region, both of which are far separated from the position of Trp-3. The crystal structure of the K53,56M mutant shows several interesting features compared to that of the wild-type enzyme. In these isomorphous crystals the backbone foldings are virtually identical. Yet significant changes in the side chains of certain residues, away from the site of mutation but including Trp-3 and other residues at the i-face, are discernible. Such reciprocity is expected because a structural change that perturbs the interfacial binding could also affect the i-face, i.e., the face along which sPLA2 makes contact with the interface. As described later where we present our proposal for the location of the i-face on the surface of sPLA2, residues 120/121 are probably part of the anion binding site on the i-face. Lys-53 and -56 are not involved directly in the anion binding. Since they are at the edge of the i-face but somewhat removed from the contact surface, the charge compensation effect may be related to a change in the helix on which the catalytic His-48 and the calcium binding Asp-49 are also located.

VIII. K_S Allostery and the Detailed Balance Constraint*

The transition from the three-dimensional space (bulk phase) to the two-dimensional surface of the interface raises fundamental issues about the volume and entropy effects of confinement in the interface. Such concerns are intrinsic[213] in the basic questions including the following: What is the concentration of the substrate in the interface? Is the search for the substrate more rapid at the interface than in the aqueous phase? What are the variables and the units for the processes at the interface? Such basic biophysical issues are also part of interfacial enzymology. In this section we outline the considerations that have helped us in the formulation of issues that bear on the equilibrium processes at the interface as well as across the interface.

A. Choice of Concentration Units and the Reduction of Dimensionality

For the analysis of the equilibria in the square box in Figure 1, consider the situation where an active-site-directed ligand (L = substrate, product, or inhibitor) can partition into a preformed interface while the enzyme can bind to the interface[53,123]

$$\begin{array}{ccc} E + L & \underset{K_L}{\rightleftharpoons} & EL \\ K_d \updownarrow \downarrow \uparrow K_L' & & K_d^L \uparrow\downarrow \\ E^* + L^* & \underset{K_L^*}{\rightleftharpoons} & E^*L \end{array}$$

Enzyme−ligand complexes can form either in solution or in the interface. The equilibrium distributions can be analyzed in a straightforward way to give all concentrations of all species in the system. However, first it must be decided what units should be used for the concentrations of the species in the interface. For computational simplicity, the most practical choice is to use mole fraction units (X_L) for L* and moles per volume of aqueous solution for E* and E*L. As a consequence, the units for the corresponding dissociation constants are per mole fraction for K_L', mole fraction for K_L*, and molar units (M) for K_d and K_d^L. The choice of units does not influence the form of the equilibrium relations for the individual steps. However, when the actual concentrations of the

various species are to be calculated from the total amounts, the choice is important.

However, a thermodynamic definition of the equilibrium constants must be based on the chemical potentials, which in turn are defined from the densities relative to an accessible volume. For the species in aqueous solution, this automatically leads to the choice of molar units. The accessible volume in the interface corresponds to the interfacial surface area times the distance that the molecules are allowed to "bob" up and down perpendicular to the interface, i.e., the root-mean-square (rms) perpendicular fluctuation distance as determined by the shape and strength of the interaction potentials. Only in the limit of very tight binding, when the rms distance is smaller than the thermal wavelength of the molecule, will a degree of freedom, i.e., a degree of translational entropy, actually be lost upon binding of ligand from the aqueous phase to the interface and the maximal effect on interaction of ligand with enzyme at the interface as calculated by Page and Jencks[214] be reached. Such tight ligand binding in the interface is not expected for membrane adsorption.[215] Thus, the "reduction of dimensionality" when a molecule binds in the interface consists primarily of a reduction of accessible volume. Apart from a multiplicative constant corresponding to this distance of perpendicular freedom, the thermodynamic choice of concentration units in the interface would be surface density (moles per unit surface area). This choice allows a direct identification of the free energy of interaction from the equilibrium constants. However, surface density is related to the mole fraction by a multiplicative constant only when all molecules in the interface contribute to the surface area by the same amount. If not, the conversion factor will depend on the composition of the interface, and therefore, it will depend on how many ligands are already partitioned. This complicates the calculations,[81] and for simplicity of discussion, we will assume that the molecules partitioned in the interface are all of comparable size.

B. Detailed Balance and Allosteric Cooperativity

A detailed balance condition appears for the equilibrium constants in any reaction diagram where the same state can be reached through different paths. For the scheme above it can be expressed as follows (eq 5 in Table 5)

$$\omega_{\mathrm{coop}} = \frac{K_{\mathrm{d}}}{K_{\mathrm{d}}^{\mathrm{L}}} = \frac{K_{\mathrm{L}}}{K_{\mathrm{L}}' K_{\mathrm{L}}^*}$$

$K_{\mathrm{d}}/K_{\mathrm{d}}^{\mathrm{L}}$ expresses how much better the E*L complex binds to the interface than does E*, while the right-hand side expresses how much better L binds to E* than to E. Thus, either ratio is a measure of the cooperativity between interface binding and catalytic-site binding. This cooperativity could either be an allosteric effect where the interface binding stabilizes an enzyme conformation that binds the ligand better or come from residual interface interactions where the ligand, which is also in the E*L complex, retains some of its interface interactions and thereby helps to "anchor" the complex. For pig pancreatic sPLA2 it was found that the cooperativity factor is between 5 and 100, depending on the headgroup of the ligand, and is independent of its chain length.[53,123] This suggests that the anchoring effect is small and cooperativity is primarily allosteric. When the ligand is the substrate, this cooperativity implies K_{S}^* allostery by the interface.

There are also other implications of the detailed balance condition. In fact, any change in the system must affect two or more of the equilibrium constants in a compensatory manner to preserve the detailed balance relation. For instance, if a certain ligand binds more strongly than a different ligand in the interface (smaller K_{L}'), it will also be more difficult for the ligand to dislodge and be pulled into the active site of E* (i.e., larger K_{L}^*). As a consequence, changing the interface properties so that the ligand partitioning becomes more favorable will also make it more difficult to form the E*L complex from E* and L* in a way such that $K_{\mathrm{L}}'K_{\mathrm{L}}^*$ is invariant. Alternatively, if the ligand does not need to be dislodged to enter the catalytic site, the compensation for the decreased K_{L}' will come in as a decreased $K_{\mathrm{d}}^{\mathrm{L}}$, i.e., anchoring of E*L relative to E* to the interface.

One could also ask how much the total enzyme−ligand complex concentration changes when an interface is added to the system. This issue determines whether more inhibition occurs if enzyme is mostly bound to the interface versus mostly present in the aqueous phase. Without interface, there is only the EL complex present, while in the presence of an interface, both EL and E*L contribute. From the binding scheme above, one finds that the condition under which the presence of an interface will actually increase the total amount of ligand-bound enzyme complexes (EL + E*L) is

$$0 < \frac{[M^*]}{K_{\mathrm{L}}'} < \frac{K_{\mathrm{d}}}{K_{\mathrm{d}}^{\mathrm{L}}} - 1 - \frac{K_{\mathrm{d}}}{K_{\mathrm{L}}'}$$

where [M*] is the molar concentration of interface molecules calculated per unit volume of aqueous solution. The basic criterion is that the right-hand side must be greater than zero; otherwise there can be no interface concentration for which there is more complex formation than without. The condition can be written as

$$\omega_{\mathrm{coop}} = \frac{K_{\mathrm{d}}}{K_{\mathrm{d}}^{\mathrm{L}}} > 1 + \frac{K_{\mathrm{d}} + [M^*]}{K_{\mathrm{L}}'}$$

which shows that cooperativity is a necessary requirement for increased complex formation in the presence of an interface. However, with too much interface present the local concentrations of the reactants will become too dilute in the interface and complex formation must decrease.

C. Scaffolding Effect

It has been suggested[214, 217] that one of the major functions of an enzyme is to bring and hold the reactants together in a small volume of the catalytic site, where they can react. A similar effect can be

calculated for interfacial activation, where interface binding can concentrate both enzyme and substrate. This is the case of scaffolding where enzyme and substrate are held in the interface in orientations that are particularly suitable for interaction. The maximum cooperativity factor is achieved if the ligand remains fully attached in the interface even when it is bound at the catalytic site. Then the E*L complex is held with the combined interface interactions of L* and E*, i.e., L* contributes to the anchoring of the complex. This gives[81]

$$\frac{K_d}{K_d^L} = \frac{\{M^*\}}{K_L'} \cdot \frac{1}{\delta\Omega_{L^*}} = \omega_{coop}^{scaff}$$

where {M*} is the local concentration of interface molecules (moles per accessible volume as defined above; {M*} ≈ 5−8 M) and $\delta\Omega_{L^*}$ is the orientation factor, i.e., the relative fraction of solid angles that the main orientation axis of the substrate is allowed in the interface. The orientation factor appears if the interface holds the substrate in the correct orientation for binding to E*; this entropy loss associated with L* binding to E* does not have to be "paid again" when the substrate binds the catalytic site.[214] For instance, if $\delta\Omega_{L^*} \approx 10^{-1}-10^{-2}$ and $K_L' = 1$ mM, the maximal cooperativity factor is of the order of 10^5-10^6. This significant effect could be the basis favoring the interaction of two proteins anchored to a cell membrane versus the binding of one of the proteins from the aqueous phase to the other protein anchored to the membrane (i.e., in the control of cellular signal transduction processes at cell membranes). This is the "reduction of dimensionality" effect (also called increase in entropy effect or the increase in local concentration) that gives the maximal gain in enzyme rate if both substrate and enzyme are held in optimal orientations. If there is an allosteric effect as well, this can further increase the cooperativity factor.

In contrast, sPLA2 seems to pull a significant part of the long-chain phospholipid substrate out of the interface for reactions in the active site.[92] As a consequence, any gain from the increased local concentration is in large part compensated for by the difficulty of pulling the substrate out of the interface for binding to E*. In this case there can be no anchoring and E* and E*L, in the absence of allosteric effects, would be bound to the interface with the same affinity so that $K_d = K_d^L$. Thus, no scaffolding effect remains, and the cooperativity factor is

$$\omega_{coop} = \frac{K_d}{K_d^L} = 1$$

The cooperativity factor of about 5−100 for the pig pancreatic IB sPLA2 was interpreted as an allosteric effect[123] rather than anchoring, since it depends on the nature of the headgroup and is insensitive to the length of the hydrophobic chain.

D. Diffusion Effects in the Interface

Concentrating the reactants, enzyme, and substrate in the interface will also affect the rate constants for enzyme−ligand complex formation and break-up. If complex formation is diffusion limited, it can be much more efficient to confine the search to a 2D surface than to search through all of 3D space. This is sometimes referred to as a rate enhancement due to a reduction of dimensionality.[213] However, as in the case of the equilibrium constants discussed above, the rate enhancement is due primarily to a reduction of the space that needs to be searched. There would be no interfacial rate enhancement, quite the contrary, if the whole 3D reaction solution were spread out into a thin 2D layer.

Describing a diffusion-limited reaction rate in 2D has complications from the fact that there is no stationary solution to the diffusion-reaction equation in 2D. This is because the depletion zone around the target continues to grow, while in 3D the depletion zone remains finite. As a consequence, there exists no true rate constant, but a diffusion-limited association rate "constant" that depends on the concentration (mole fraction X_S) of substrate in the interface can be calculated.[5,216] One finds

$$k_1^* = \frac{4\pi D_2}{a_{M^*}(\ln(1/X_S) - 1)} \text{ (mole fraction)}^{-1}\ s^{-1}$$

where D_2 is the sum of the two-dimensional diffusion rates for substrate and enzyme in the interface and a_{M^*} is the surface area of an interface molecule. The expression holds only for small values of X_S. For $a_{M^*} = 50$ Å^2 and $D_2 = 10^{-8}$ cm^2 s^{-1} one finds that the rate constants for binding of substrate in the interface to E* in the interface k_1^* are 7×10^6 (mole fraction)$^{-1}$ s^{-1} at $X_S = 0.01$ and $k_1^* = 3 \times 10^6$ (mole fraction)$^{-1}$ s^{-1} at $X_S = 0.0001$. Thus, the rate constant of binding in the interface can be very fast, except when the interface is large and substrate molecules are very sparse. For sPLA2 it was found experimentally that $k_1^* = 10^3$ (mole fraction)$^{-1}$ s^{-1} (Table 6), and the substrate−enzyme association is probably not diffusion-limited in this case. Note, this conclusion cannot be obtained from the significant element effect on k_{cat}^* (section VI) since this constant is for reaction steps after binding of substrate of enzyme.

The main consequence of the fast 2D diffusion is that for most enzymes with a turnover rate commonly much less than 10^5 s^{-1}, substrate distribution in the interface has time to equilibrate between turnover events. Thus, there will be no expansion of the local depletion zones around each enzyme during catalysis, and a steady-state description will hold also for the 2D diffusion, except at very low surface densities of enzyme and substrate. Such a limiting condition may be reached with substrates poorly partitioned into monolayers.

If all enzyme and substrate are in solution, the overall diffusion-limited rate of complex formation is given by the Smoluchowski[218] expression

$$J_3 = 4\pi D_3 b N_{Av}[S_T]$$

where D_3 is the diffusion rate in 3D, b is the target radius, N_{Av} is Avogadro's number, and $[S_T]$ is the

concentration of substrate. If all enzyme and substrate are in an interface

$$J_2 = k_1{}^*X_S = k_1{}^*[S_T]/[M^*]$$

To get a faster association rate in 2D than in 3D, i.e., $J_2 > J_3$, requires that the interface is not too large thereby reducing the substrate density

$$[M^*] < \frac{D_2}{D_3}\cdot\frac{1}{b a_{M^*} N_{Av}(\ln(1/X_S) - 1)} \approx \frac{D_2}{D_3}\cdot 0.5\ \text{M}$$

The approximate equality holds if the target radius $b = 10$ Å, $a_{M^*} = 50$ Å^2, and $X_S = 10^{-3}$. As the diffusion rates may be 100-fold slower in the interface than in solution, the interface concentration should be below 5 mM or so for a rate enhancement to be possible.

IX. Catalytic Mechanism of SPLA2

In this section we summarize the findings obtained with a number of mutants of pancreatic sPLA2 that have revealed its structure−function features. The conserved architecture of the His-48/Asp-99/calcium motif for the catalytic site provides the structural basis for the chemical step in sPLA2s.[11,54] The identity of the catalytic residues is affirmed by the biochemical,[58,222] biophysical,[56,190,221] crystallographic (Figure 3), and site-directed mutagenesis (section X) studies. It is also consistent with simulations and molecular dynamic calculations.[89,95,219−22] IR results show that the carbonyl oxygen of the *sn*-2-amide analogue of phospholipid is polarized when bound to the catalytic site.[223] Typically, in the cocrystals of sPLA2 with the active-site-directed substrate mimics, a C═O or P═O oxygen, corresponding to the *sn*-2-ester carbonyl of the substrate, is coordinated to the bound calcium. A significant part of the stability for the interaction of a *sn*-2-amide or -tetrahedral substituent also comes from the hydrogen bonding with the catalytic His-48. These results are in accord with the H48N and H48Q mutants. Although they have only 0.01% residual activity, the binding of calcium and the *sn*-2-amide analogue occurs with a modest change in the affinity attributable to a change in the H-bonding ability to δNH of His-48.[190]

A. Plasticity of the Active-Site Interactions

The primary amides of fatty acids (Figure 3) are also potent competitive inhibitors of sPLA2s, whereas their *N*-methyl derivatives are 50-fold weaker.[103] Calculations in the Eulerian space of the docked amide suggest that the carbonyl oxygen can coordinate with calcium without replacing either of the two Ca^{2+}-coordinated water molecules.[95] This structure with eight oxygen ligands in square antiprism geometry for the coordination environment of calcium had several interesting features. Not only was the carbonyl oxygen the eighth ligand to calcium, but both the amide hydrogens are in favorable hydrogen bonds: one with δNH of His-48 and the other with the equatorial water. This structure also provides an explanation for the curious observation that the *N*-methyl fatty acyl amide is 50-fold weaker as an inhibitor, presumably because it can form only one of the two hydrogen bonds. These calculations raised the possibility that the equatorial water molecule, which was still coordinated to calcium, could be the potential nucleophile for the chemical step.

B. Catalytic-Triad versus the Calcium-Coordinated Oxyanion Mechanism

In analogy with the mechanism for serine proteases, Verheij et al.[54] proposed that Asp-99, His-48, and a water molecule form a "triad" in which water is "activated" by His-48 as the general base (Figure 14). Besides the lack of the serine, another feature of the Asp-99/His-48 pair in sPLA2s is that the syn hydrogen bond of the carboxylate is with ϵNH (Figure 14). The *sn*-2-ester carbonyl coordinates with calcium and polarizes it for the nucleophilic attack. In the consensus mechanism that emerged from this suggestion, the rate-limiting step is presumed to be the formation of the tetrahedral intermediate during which δN of His-48 is protonated. The decomposition of the tetrahedral intermediate gives an alcoholate that is protonated by δNH^+ (pK_a 6.0).

On the basis of the observations about the flexibility of the calcium coordination environment and other observations outlined below, an alternative mechanism was entertained.[56] In this mechanism a Ca-coordinated oxyanion (Figure 14), formed by the attack of the equatorial water (*w5*), is connected to δN of His-48 through another water molecule (*w6*). His-48 is protonated during the formation of the tetrahedral intermediate; however, due to the activation of the *w5* oxyanion, the activation energy in this step is significantly lower such that the rate-limiting step now lies during the decomposition of the tetrahedral intermediate.

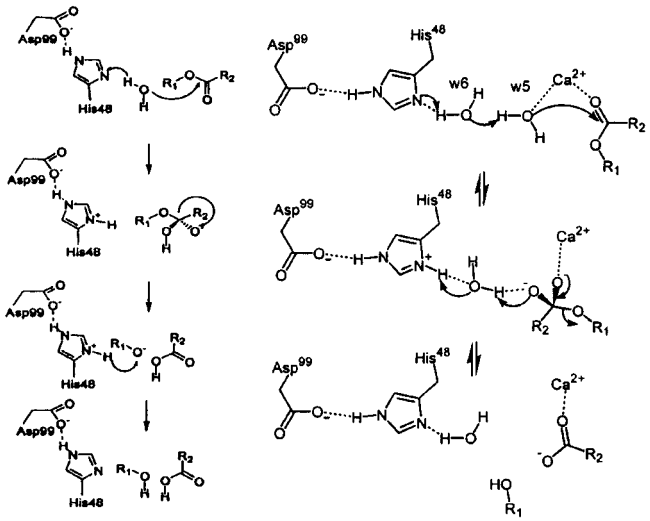

Figure 14. (left) "Triad"- and (right) calcium-coordinated oxyanion mechanism for the chemical step of secreted sPLA2. Formation of the tetrahedral intermediate occurs by the nuceleophilic attack of a water molecule, possibly *w6*. In the first mechanism, His-48 acts as a general base and the rate-limiting transition state is during the formation of the tetrahedral intermediate. In the second mechanism, the catalytic water *w5* is coordinated to the calcium cofactor, which also polarizes the ester carbonyl, and the rate-limiting transition state lies during the decomposition of the tetrahedral intermediate. (Adapted from ref 56.)

There is considerable similarity between the two mechanisms, and the major difference is in the direct role for the calcium cofactor in the formation of the oxyanion. This is in fact critical for ascertaining the rate-limiting transition state. In the oxyanion mechanism, the Ca^{2+}-coordination environment changes from seven to eight. Thus, divalent ions that resist such an expansion of the coordination environment are likely to be catalytically inert. This expectation is generally consistent with the observation that divalent Cd, Zn, and Cu ions can only bind the substrate but not catalyze the reaction.[56] In contrast, the competitive cofactor like Co and Ni cations supports the substrate (mimic) binding and also catalyzes the reaction as well as calcium does. These roles are consistent with the fact that the smaller cations are likely to have a more flexible coordination environment. Additional evidence is summarized below.

(a) In the oxyanion mechanism, during the rate-limiting transition state the *sn*-3-phosphate of the substrate replaces the calcium-bound axial water molecule (w12). This is consistent with the observation that the substrate specificity for a variety of *sn*-3-phoshates, phosphonates, and arsonates lies in the k_{cat}* step.[200] Since OH of Tyr-69 is also bonded to the *sn*-3-phosphate, the Tyr-69-Phe mutant would be k_{cat}*-impaired as is found to be case.[56]

(b) Activation of the oxyanion coordinated to the calcium is also consistent with the observation that the k_{cat}* for the Asp-99-Asn mutant is about 5% of the value for WT sPLA2.[55,224,225] In contrast, the Asp-102-Asn mutant of trypsin has only 0.01% activity, as expected if the attack of the nucleophile is rate-limiting. Thus, the 'activating' effect of Asp-99 is lower because it is not as critical for the transfer of the proton from δNH^+ to alcoholate. The possibility that the residual activity is due to partial spontaneous conversion of Asn-99 to Asp-99 is ruled out by the scooting mode analysis which confirmed that such a conversion does indeed occur with Asn-49 substitution.[243]

(c) The oxy/thio effect of 10 in k_{cat}*,[85] described in section VI, suggests that the rate-limiting transition state is unlikely to be during the formation of the tetrahedral intermediate. This is because a nucleophilic attack on a thioester is as favored as on an oxyester. It may be argued that release of a thiolate ion in solution is favored more than that of an alcoholate, which only implies that even with that contribution in the active site the activation energy is still in the proton-transfer step from the protonated His-Asp pair.

(d) As discussed in section X, substitution of His-48 by Gln, Lys, or Ala gives mutants with significantly lower activity. However, there is significant residual activity in His to Asn substitution mutants, which is about 0.01% in the pancreatic IB PLA2[190,242,243] and 2% in IIA sPLA2.[118c] These results suggest that the amide NH of Asn could participate in the chemical step. According to the oxyanion mechanism, the H-bonding of the assisting water w6 with the Asn side chain could significantly lower the pK_a of *w6* and thus retains its function in the decomposition of the tetrahedral intermediate.

(e) Mutants with unnatural amino acids have also been constructed: the His-48 at the active site of porcine pancreatic PLA2 has been replaced by 1,2,4-triazole-3-alanine. The other two histidine residues, His-17 and His-115, were replaced by Asn. This mutant displayed low activity from pH 3 to 6,[222] presumably in the unprotonated form due to the low pK_a < 3.3 in the protein. The wild-type is virtually inactive at pH 3, and its maximum activity at pH 7 is only 4-fold higher with the thiophospholipid substrate. The inhibitory effect of *sn*-2-amide inhibitor I (in Table 3) is the same, which suggests that the modest effect is on the chemical step. These results are consistent with the oxyanion mechanism (Figure 14) in which His-48 is the proton donor to the alcoholate during the decomposition of the tetrahedral intermediate. These results are also consistent with the role of δNH as a general base for the activation of nucleophilic water.

(f) The calcium-activated oxyanion mechanism is analogous to the mechanism favored for zinc-dependent hydrolases.[226] Their quantum chemical calculations for sPLA2 also support the oxyanion mechanism.[227] The QM/MM calculations show that in the triad mechanism the activation energy barrier is indeed during the formation of the tetrahedral intermediate. However, if the calcium coordination and other features of the protein environment are included in the calculation, the relative energy for the formation of the tetrahedral intermediate decreases dramatically and the rate-limiting transition state shifts to the decomposition step. For the QM/MM calculations only one water molecule coordinated to calcium and His-48 was used with the atomic coordinates for human IIA sPLA2. For several reasons we believe that two water molecules may in fact be involved in the chemical step. Our docking results suggested that two water molecules adequately bridge the distance between His-48 and calcium in pig pancreatic sPLA2.[95] The solvent deuterium isotope effect for the chemical step is about 10. The proton inventory effect (Figure 15) also suggests multiple hydrogen-bonding interactions involved in the chemical step.

It may be a coincidence, but in the present context it is remarkable that the assisting water *w6* is seen in the structure obtained from the cocrystals of PLA2 with MJ33 and five sulfate or phosphate anions. As discussed later in sections XI and XIII, a water molecule corresponding to *w6* in the Ca-coordinated water-assisted mechanism is seen in the recent crystallographic dimer structures of pig pancreatic sPLA2 but not in the proPLA2 structure. Note that the water connects the tetrahedral *sn*-2-phosphate to His-48, while the other oxygen of the phosphate is still coordinated to calcium. These results clearly show that there are no steric constraints to accommodating *w6* in the catalytic site region.

Another functionally critical comparison is relevant here. In an earlier structure,[87] one of the O═P of MJ33 (Figure 3) was directly coordinated to calcium and the other P═O oxygen was also in direct contact

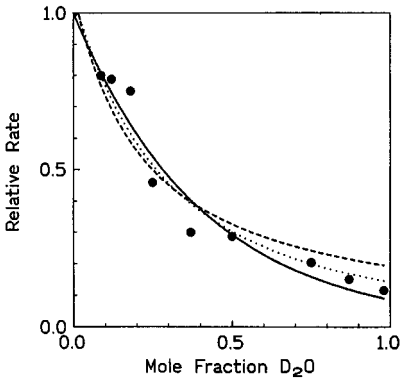

Figure 15. Relative initial rate (v_o) of hydrolysis of 1,2-dimyristoylphosphatidylmethanol vesicles by pig pancreatic sPLA2 in the aqueous phase containing varying mole fractions of D_2O in H_2O. Since the $X_I(50)$ value for MJ33 does not change under these conditions, it is suggested that the solvent isotope effect is primarily on k_{cat}*. Although the isotope effect is large, the data points could not be adequately fitted (curves) to the simple models considered by Quinn and Sutton.[228] Such a behavior suggests multiple fractionating transition states, i.e., solvent-accessible proton transfer plays a role in two or more substeps of the rate-limiting steps (suggested by Professor Dan Quinn). Results from ref 3 but unpublished in this form.

with His-48. This difference in the two crystal forms is very intriguing. The difference is attributed to the active-site difference between the catalytically 'inert' and the 'active' forms in the model (Figure 12) for the k_{cat}* activation by the charge compensation of cationic Lys-53, -56, and -120.[193]

X. High-Resolution Structure–Function Relationships for sPLA2

As shown in Figure 2, the structure of sPLA2 is characterized by several features: High disulfide bond content, preponderance of α-helices, high stability, an Asp-99···His-48 catalytic pair (dyad), a hydrogen-bonding network connecting the interfacial binding site and catalytic site, and a catalytic calcium site. Other conserved features include the three helices and a β-wing. These structural features have been investigated in depth and correlated with the functional properties of sPLA2. As described below, the sPLA2 protein has provided a system to demonstrate the full integration between structural and functional roles of specific residues.

sPLA2s have been subjected to semisynthesis and site-directed mutagenesis studies (Table 7). Over 200 mutants of pig and bovine pancreatic IB, human synovial IIA, and bee venom IIIA PLA2 have been made. For the following discussion we focus on the bovine sPLA2 for which a complete set of the primary parameters is available.[191] However, the partially resolved effects reported for mutants of other sPLA2 are generally consistent with the conclusions summarized in this section, which are based on the results for the bovine mutants. There is a general agreement about the identity of the catalytic site, and a consensus has emerged that the close contact of the enzyme with the interface occurs along a large flat surface, the i-face (Figure 2), rather than a 'lid' or a protruded site that 'penetrates' in the interface. Although the observed incremental effect of the substitutions in the catalytic site may be more than 100-fold, the effects of single substitutions in other regions are typically <10-fold. With use of suitable methods some surprising results have also emerged about the tendency of Asn-49 to spontaneously change to Asp-49,[243] the structural role of the catalytic residues,[224,242] and the allosteric effects of certain charged residues.[193] In short, primary parameters with site-directed mutants continue to help in resolving the coupling between the active site and interface binding events as developed in the rest of this review.

A. General Approaches

More than 100 porcine and bovine pancreatic PLA2 mutants have been characterized.[191,265] As summarized in Table 7 and pointed out in the following discussion, mutants of human synovial and bee venom sPLA2 have been designed for specific questions. Most of the mutants of bovine pancreatic sPLA2 have been subjected to rigorous structural analyses to ensure proper interpretation of the functional data. The structural analysis was performed by three major approaches. (i) One-dimensional NMR and 2D NOESY experiments were used to assess whether the global conformation of the mutant has been perturbed. (ii) For selected mutants,

Table 7. Reported Mutagenesis Sites on sPLA2

consensus site	role/effect
N-terminus (1−10)	substrate binding,[229] interface binding[79,229−235]
16, 17	interface binding[119]
19, 20	substrate and interface binding[236, 237]
30	lower rate[238]
31	lower rate;[239] interface binding;[240] k_{cat}*[192]
42, 46	headgroup specificity[241]
48	k_{cat}*[55,190,224,242]
49	calcium binding[243,244]
52,73	lower rate;[246] substrate binding[245]
53, 56	charge preference;[157,247−249] k_{cat}* activation[193]
69-loop	interface binding;[206,250−252] k_{cat}*[56]
Asp66/Glu71/92	second calcium site[254]
Asp99	lower rate;[55,224,242,255−258] k_{cat}*[225]
22, 102, 106	substrate binding[259]
C-terminus	lower rate[146,161,235,260,261] and k_{cat}* allostery[193]
disulfides	lower activity of the analogues of sPLA2s,[262] and Cys-Ala substitutions[255]
cationic	Lys to Arg,[157,248] to Met,[193,247,248,263] to Glu[233, 253, 264]

high-resolution crystal structures have been determined to examine detailed structural changes. (iii) The conformational stability of the mutants, $\Delta G_d^{H_2O}$, has been measured by guanidinium chloride-induced denaturation as monitored by CD spectroscopy.[266] The kinetic data of the mutants have been interpreted only if the global conformation of the mutant has not been perturbed.[267] As described later in this section, some of the mutants were found to display serious structural perturbations.

For some of the mutants displaying interesting functional properties, the crystal structure has been solved at high resolution in order to examine the structure−function relationship in depth. The mutants whose crystal structures have been solved to date include the following. (i) Bovine pancreatic PLA2, Q4E;[229] K56M;[247b] D99N;[256,257] D99A and H48Q;[258] D49E;[268] Y52F/Y73F;[269] K120A/K121A;[260] K53M/K56M;[193] Y52F/Y73F/D99N;[225] and K56M/K120M/K121M.[270] (ii) Pig pancreatic PLA2: Y52F and Y73F;[246] Δ62−66;[88] F63V.[252]

B. The Asp-His Dyad (Pair) Plays both Structural and Catalytic Roles

His-48 is hydrogen bonded to Asp-99. The pair is located near the calcium-binding site (Figure 16), where the carboxylate of Asp-49 provides two oxygen ligands, and it is involved in the substrate binding. This relationship is affirmed by the results shown in Figure 17 for the pig sPLA2, which are comparable to those discussed below for the bovine pancreatic sPLA2. The Asp-99/His-48 clearly plays the key role in catalysis. The His-48-Ala or Asp-99-Ala mutants have less than 0.001% catalytic activity without a significant change in calcium binding or in the binding of the enzyme to the interface. Both of these residues also contribute significantly to structural stability of the enzyme. For example, the conformational stability $\Delta G_d^{H_2O}$ decreases from 39 kJ/mol for WT to 18.5 and 26.5 kJ/mol for Asp-99-Ala and His-48-Ala mutants, respectively.[73,190,242,243] Their importance in maintaining the structural integrity of PLA2 is reasonably accounted for by the model that the amide nitrogen atoms of Asn and Gln could mimic the δNH and ϵNH of His-48, respectively. Kinetic analysis indicated that in bovine PLA2 His-48-Asp retains 6×10^{-5} of the original activity, which is very low but is significantly higher than undetectable activity with H48Q and H48A. These results support the catalytic role of the δN atom of His-48. On the other hand, two-dimensional NOESY spectra suggest that the global conformation is largely retained in His-48-Gln but not in His-48-Ala or His-48-Asn and the conformational stability $\Delta G_d^{H_2O}$ is not perturbed for His-48-Gln but decreases by 12 kJ/mol for the other two mutants. These results suggest that the H-bond of Asp-99 to ϵN of His-48 plays an important structural role.

C. H-Bonding Network Is More Important for Structure than for Catalysis

The hydrogen-bonding network (Figure 16), linking Ca^{2+} and His-48 in the catalytic site to the residues

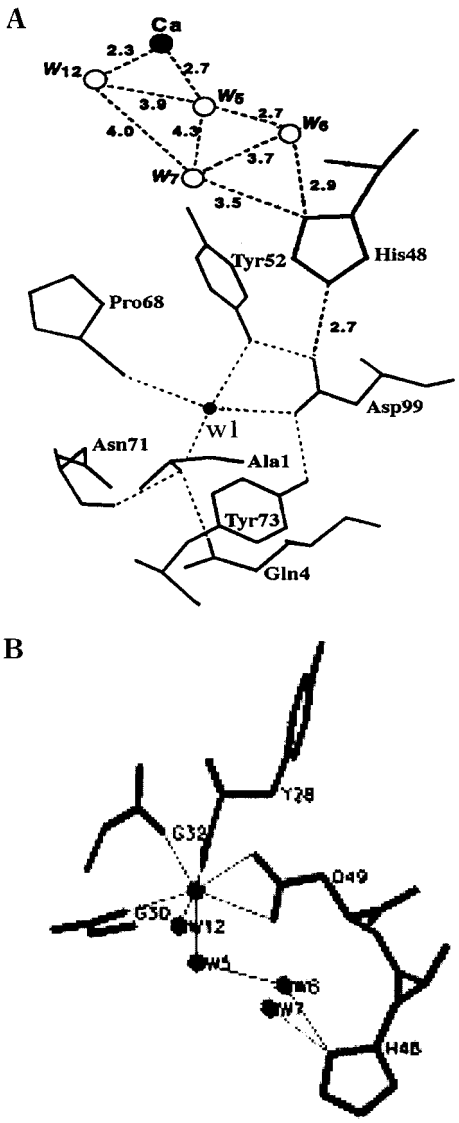

Figure 16. Highly conserved features of sPLA2. (A) The catalytic site motif and the hydrogen-bonding network in sPLA2s. The network connects the active-site residues and the interfacial binding region at the N-terminus in crystal structure of bovine pancreatic PLA2. The waters *w5* and *w12* are directly coordinated to calcium and *w6* and *w7* are in the outer sphere. (B) Calcium binding ligands of bovine PLA2 (Figure 3). (Adapted from results in refs 56, 67, 70, 87, 93, and 225.)

involved in the interfacial binding, is one of the salient features in the crystal structures. It involves a highly conserved structural water molecule (*w1*), the catalytic dyad (His-48/Asp-99), the N-terminal region (Ala-1 and Gln-4), and several other conserved residues (Tyr-52, Tyr-73). The conserved water (*w1*) is not present in the catalytically inert zymogen of pig PLA2.[271] The detailed balance condition for the thermodynamic box for the experimentally measured equilibrium dissociation constant of an inhibitor (independently measured K_I^* values in mole fraction units) and the conformational stability of the His-48 mutants (Figure 17) is consistent with the role of His-48 in the inhibitor binding, and it is clearly dissected from the role of His-48/Asp-99 in the stability of the protein. Additional results summarized below also suggest a structural role for the other components of H-bonding network.

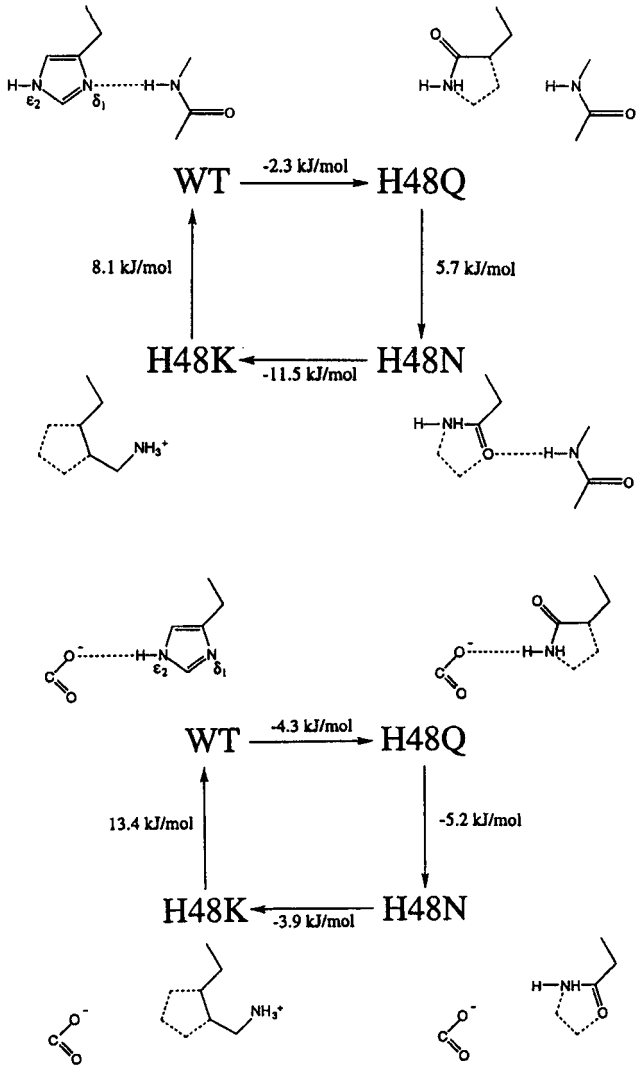

Figure 17. Detailed balance condition for binding of pig sPLA2 mutant (top) for the binding (K_I*) of a competitive inhibitor I (Figure 3) or (bottom) for the conformational stability. These relations demonstrate a role of the two H-bonding groups of His-48. The hydrogen-bonding relations invoked here are inferred from the crystallographic results with WT. (Reprinted with permission from ref 190, which also has the activity results. Copyright 1999 Oxford University Press.)

(a) Tyr-52 and Tyr-73 are absolutely conserved in all known group I and II PLA2s. However, deletion of the phenolic OH group of *either or both* residues did not affect the catalytic activity, which suggests that the hydrogen bonds involving Tyr-52 and Tyr-73 are not essential for catalysis by PLA2.[245,246,273] Consistent with the above results, the Tyr-52-Phe/Tyr-73-Phe/Asp-99-Asn is a triple mutant with a 20-fold lower k_{cat}* in the scooting mode on DMPM vesicles, which is same for the Asp-99-Asn single mutant.[225]

(b) On the other hand, the conformational stability $\Delta G_d^{H_2O}$ decreases from 40 kJ/mol for WT to 31, 21, and 16.5 kJ/mol for Tyr-52-Phe, Tyr-73-Phe, and Tyr-52-Phe/Tyr-73-Phe mutants, respectively, suggesting that the H-bonds are important for the conformational stability of PLA2.[245] The crystal structures of the Try-52-Phe/Tyr-73-Phe double mutant[269] and the Tyr-52-Phe/Tyr-73-Phe/Asp-99-Asn triple mutant[225] indicate a substantial disruption of the H-bonding network.

(c) The high-resolution NMR structure obtained at neutral pH allowed direct observation (at 11.1 ppm) of the H-bond between Asp-99 and Tyr-73. Analysis of a series of mutants by NMR and CD showed that the existence of the Tyr-73···Asp-99 H-bond correlates directly with the conformational stability of the mutant. Loss of this H-bond results in a loss of 8−12 kJ/mol in the conformational stability of the protein.[72,224]

D. Environment of Ca^{2+} Cofactor

Ca^{2+} ion is required for catalysis by sPLA2 but not for binding of the enzyme to the interface. Figures 16 and 18 show detailed structures of the calcium-binding site. The free sPLA2 clearly shows the presence of a seven-coordinated Ca^{2+} ion in the vicinity of the D99-H48 pair. Two of the coordinating ligands are water molecules, one axial (*w12*) and the other equatorial (*w5*). The five ligands provided by the protein are the two carboxylate oxygens of Asp-49 and the backbone carbonyl oxygen atoms of residues 28 (apical), 30, and 32 in the calcium-binding loop (residues 26−34). Key observations for the roles of the Ca^{2+} ion are as follows.

(a) The critical role for Asp-49 in calcium binding, first suggested by chemical modification studies,[274] is confirmed by mutagenesis studies.[36,243] Even a conservative replacement by Glu led to a lower affinity to Ca^{2+} by a factor of 12 and a dramatic decrease in catalytic activity by a factor of 4.3×10^4. The crystal structure of Asp-49-Glu mutant indicates that Ca^{2+} is coordinated to only one of the carboxylate oxygens of Glu, resulting in only four ligands (instead of five) from the protein.[268] On the other hand, these mutants (Asp-49 to -Asn, -Glu, -Gln, -Lys, and -Ala) fully retain the affinity for binding to the surface of zwitterionic micelles and anionic vesicles and also the conformation and stability. Together these observations suggest that Ca^{2+} is not required for binding to the interface[122] or for stabilizing the structure of PLA2.[243]

(b) PLA2 from different sources showed a very high degree of stereoselectivity toward the Rp isomer of phosphorothioate analogues of phospholipids.[275] The results of metal-ion dependence in stereoselectivity led to the suggestion that Ca^{2+} coordinates the *pro*-S oxygen of the *sn*-3-phosphodiester.[276] This was subsequently demonstrated by crystal structures of E−I complexes (references in Figure 3), which show that the axial water ligand of Ca^{2+} in the free enzyme is replaced by the *pro*-S-oxygen of the *sn*-3-phosphate. The phenolic hydroxyl of Tyr-69 forms a H-bond with the *pro*-R oxygen of the *sn*-3-phosphodiester. Replacement of Tyr-69 by Phe led to some relaxation of stereoselectivity toward the phosphorothioate analogues.[250b]

(c) In the crystal structure of the cocomplexes of PLA2 with a *sn*-2-tetrahedral mimic (II and III), in which the *sn*-2 carboxylic ester is replaced by a phosphonate or phosphate group, the *pro*-S oxygen of the phosphonate replaces the other water ligand (the equatorial water) of Ca^{2+} and the *pro*-R oxygen

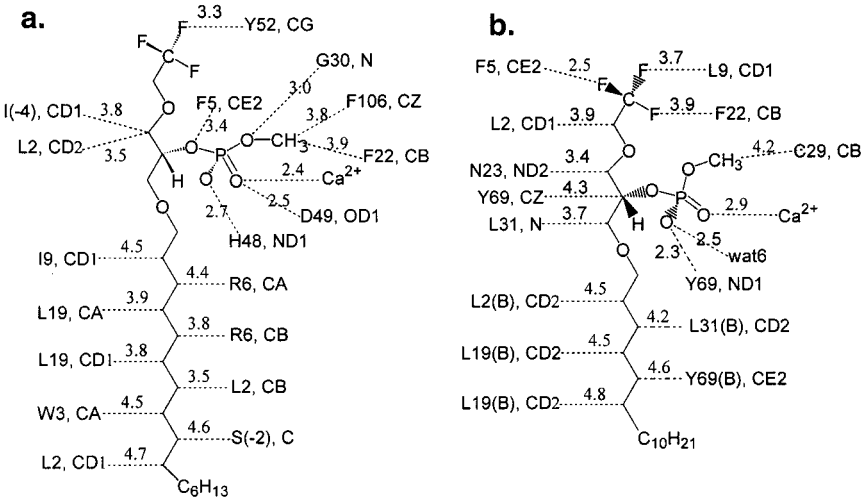

Figure 18. Schematic of the major contacts of MJ33 made within pig pancreatic IB (a) proPLA2 or (b) PLA2. Several interactions of MJ33 with the subunit B of the divalent anion-assisted-dimer are note by a "B" next to the residue. (Reprinted with permission from ref 271. Copyright American Chemical Society.)

of the phosphonate forms a H-bond with His-48 (references in Figure 3). This supports the role Ca^{2+} in polarizing the carbonyl oxygen and the chemical step as discussed in section IX.

(d) In addition to the catalytic calcium ion, a second Ca^{2+} ion with 10-fold lower affinity has also been observed in several 14-kDa PLA2 enzymes.[91] It seems to play a modest yet undefined role on the turnover at zwitterionic interfaces.[277] A major unanswered question is why the second Ca^{2+} ion is found in the porcine pancreatic IB sPLA2 but not the bovine sPLA2 which share >85% sequence identity. It has been suggested that Glu-71, which binds the second Ca^{2+} ion, is mutated to Asn in the bovine sPLA2.[254]

E. Residues at the "Hydrophobic Channel" for the Substrate Binding

The "hydrophobic channel" was identified by the first crystal structures of E−I complexes (references in Figure 3). As shown in Figure 19, it is comprised of a "wall" of hydrophobic side chains that provide access to and stabilization of substrates. For bovine pancreatic PLA2, these residues include the side chains of Leu-2, Phe-5, Phe-22, Asn-23, Leu-31, and Tyr-69. The following results support contributions of specific residues.

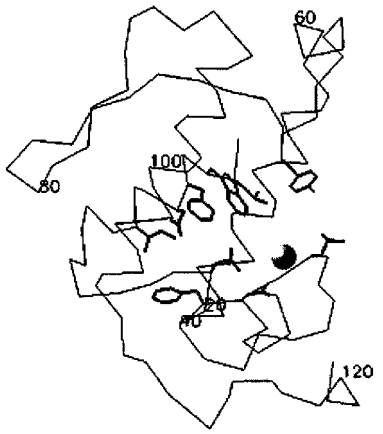

Figure 19. The hydrophobic channel residues and interfacial binding site residues. The i-face is along the perpendicular plane to the right edge of the molecule.

(a) Phe22, located at the wall of the channel, forms a face-to-face aromatic pair with Phe-106 and an edge-to-face pair with Tyr-111, which are likely to be structurally important. However, the results of structure−function analyses suggest that the primary role of Phe-22 is in catalysis, not in structural stabilization of PLA2. Substitution of Phe-22 by hydrophobic residues Tyr or Ile did not perturb the catalytic activity, while substitution by the less hydrophobic Ala resulted in lower activities by factors of 10−200 attributed to impaired substrate binding.[259]

(b) Unlike Phe-22, Phe-5 appears to contribute to both structure and function. The mutants Phe-5-Ala (-Val, -Tyr, and -Trp) showed a significant decrease in catalytic activities by factors of 15−200.[229] NMR analyses indicate that the conformations of all mutants, except Phe-5-Tyr, are perturbed, which suggests that the edge-to-face aromatic pair between Phe-5 and Phe-106 is structurally important.

(c) Leu-2 is located near the surface entrance to the hydrophobic channel, and it is involved in the chain-length specificity. When it is replaced by a bulkier residue (Trp) or a hydrophilic residue (Arg), the activities of substrates with shorter acyl chains (C_8) are only slightly affected, while those with longer acyl chains (C_{14}) decrease significantly by factors of 100−500.[229]

F. Roles of Disulfide Bonds in Structure and Activity Are Modest

The large number of disulfide linkages in PLA2 makes it an excellent system to examine structural and functional roles of disulfide bonds in enzymatic catalysis. It is a general perception that disulfide bonds are important for stabilizing protein folds. In agreement with this, bovine pancreatic PLA2, with seven disulfide bridges, displays a remarkable stability against denaturation ($\Delta G_d^{H_2O}$ = 40 kJ/mol). However, when the roles of the disulfide bonds were

probed by replacing a disulfide Cys-Cys pair with a pair of alanines, five of the seven double mutants displayed relatively modest changes in the conformational stability of the protein ($\Delta\Delta G_d^{H_2O} = +8$ to -12 kJ/mol).[255] Only one mutant, C11A/C77A, exhibits a large decrease in $\Delta\Delta G_d^{H_2O}$ (-26 kJ/mol), and another mutant, C84A/C96A, could not be purified, possibly due to misfolding. Furthermore, the activities of the mutants, including C11A/C77A, are only perturbed modestly (<10-fold) relative to that of WT, with the exception of C29A/C45A, which showed a 20-fold decrease in activity.

The 14-kDa sPLA2s differ in their disulfide architecture. Using the primary sequence of pig pancreatic PLA2, Janssen et al.[262] engineered the disulfide analogues of group IIA, IIC, V, and X sPLA2s. Preliminary characterization suggested that the effect of the disulfide architecture on the observed rates is less than 20-fold, which is in general agreement with the observations from the disulfide mutants of bovine pancreatic PLA2 described above.

G. Molten-Globule Structure of PLA2 Mutants

Although the bovine pancreatic PLA2 is very stable and rigidly held together by seven disulfide bonds, its structure appears to be very sensitive to point mutations. Many mutants of bovine pancreatic PLA2 (>20), constructed to test specific functional roles of active-site and interfacial site residues, display highly perturbed structural properties.[225,229,242,245,255,259] Typically, these mutants exhibit broad NMR resonances, narrow chemical shift dispersion, loss of slowly exchanging NH protons, and a significant loss of NOE cross-peaks. These features from NMR experiments, along with the retention of secondary structure as indicated by far-UV CD spectra, are apparently characteristic of a molten globule state. The molten globule state of a protein is generally considered as an intermediate state in the folding pathway, when most of the secondary structure has been formed but the tertiary structure is not yet in place. In almost all other proteins, strongly acidic conditions are required to convert the native state of a protein into a molten globule state.[278,279] However, unlike classical molten globules, these PLA2 mutants still retain some fixed side chain−side chain interactions and still undergo cooperative denaturation induced by guanidinium chloride.

Structural changes in certain regions of PLA2 are also suggested by NMR, fluorescence, and circular dichroism methods. The results indicate that the tertiary structure is not completely lost in these mutants.[72] As shown in Figure 20, the residual structure is localized in the structural domain that contains the N-terminus and stabilized by some of the disulfide bonds. However, most of the functional residues (the active site, the hydrophobic channel, the interfacial binding site, and the calcium binding loop) reside in the remainder of the protein, where the tertiary interactions are disrupted. It is unexpected and unprecedented that a protein with such a high disulfide content and high thermodynamic stability is so easily converted to a molten-globule state. A possible explanation consistent with the results described in this section is that PLA2 has evolved to involve full integration between different residues and between structural and functional roles. Thus, mutation of a single residue is sufficient to tip the balance and result in significant structural perturbation in distal regions.

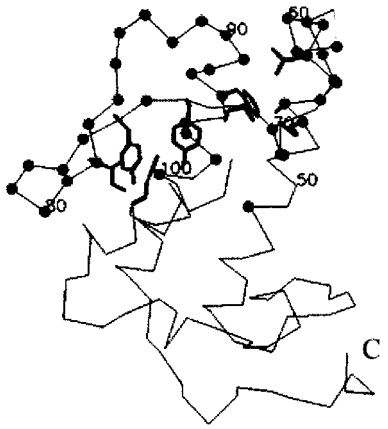

Figure 20. Backbone of the PLA2 solution structure showing the residues in the regions where the tertiary structure is retained in the "molten globule-like structure" of PLA2. The four disulfide bonds (C51−C98, C61−C91, C84−C96, and C11−C77) could be responsible for the retention of partial tertiary structure. (Reprinted with permission from ref 72. Copyright 1999 American Chemical Society.)

H. Change of a Single Residue Led to Change of Biological Function

The functional diversity of the 14-kDa sPLA2 is unparalleled. Some of these proteins or their catalytically inert natural isoforms also exhibit toxicity, allergenic, heparin-binding related to the binding to endothelium, and cytoplasmic receptor-binding. Due to the extreme functional diversity, this class of protein provides an excellent system to investigate the structure−function relationship of proteins. Tsai and collaborators[280] converted bovine pancreatic PLA2 into a competitor of neurotoxic PLA2 by replacing Phe-22 (conserved in pancreatic PLA2) with Tyr (conserved in neurotoxic PLA2). This mutation, however, did not affect the catalytic activity of the bovine PLA2.

XI. sPLA2 at the Interface

In this section we review the evidence for pancreatic sPLA2. A structural relationship between the active site and a possible interfacial recognition site (i-face) at the entrance to the active site was clearly pointed out on the basis of the crystallographic results.[66a] Evidence for modeling the i-face,[77] as the face of the enzyme that makes a close contact with the substrate interface, comes from a range of observations. Structural information about the i-face is useful for understanding many aspects of the interactions of an interfacial enzyme at the interface including interfacial preference, turnover processivity, and allostery. In support of the idea of an i-face it was found that on the binding of pancreatic sPLA2 to micelles of alkylphosphocholine there is a signifi-

cant spectral perturbation in the environment of Trp-3 and possibly Tyr-69.[195] Calorimetric titration[196] coupled with ultracentrifugation studies suggest formation of a particle containing two pig pancreatic sPLA2s with about 70 amphiphiles.[138] Since pancreatic sPLA2 has only one tryptophan residue and it is located on the i-face, the spectral changes have been quite useful in developing the functional significance of such binding along the i-face of sPLA2 containing Trp-3.

A. Binding Correlates with the Catalytic Efficiency

The observation that the presence of the products of hydrolysis eliminates the delay in the reaction progress on phosphatidylcholine interfaces (Figures 9 and 10) is consistent with the enhanced binding of the enzyme to dialkylphosphatidylcholine bilayers in the presence of the products of hydrolysis.[108] These results showed that the apparent K_d for dissociation of E* from the interface decreases by a factor of about 30, to 0.2 mM in the presence of 0.15 mole fraction products. The fit of the binding isotherm according to the relation

$$E + nA \rightleftarrows E^* + E^*L$$

provides a value of $n = 30-35$, i.e., in the E to E* step the amphiphile to enzyme stoichiometry is far greater than 1. Also, the interfacial affinity of sPLA2 from the venom of *Naja melanoleuca*, which does not exhibit the delay phase on phosphatidylcholine vesicles,[107] was significantly higher even in the absence of the products.[108] These results show a clear relationship between enhanced interfacial binding and higher turnover rate of sPLA2 at the anionic bilayer interface; however, the number and nature of bound enzyme species could not be addressed.

B. Binding Under the Scooting Mode Conditions

Virtually all sPLA2s exhibit scooting mode reaction progress on vesicles of anionic phospholipids.[1,83] The high-affinity binding isotherm of pancreatic sPLA2 with ditetradecylphosphatidylmethanol vesicles shows that K_d is in the submicromolar range. Also, as noted above, the binding of one enzyme molecule to the interface typically excludes about 30 phospholipid molecules for the binding of the next enzyme molecules to the same vesicle.[2,108,197] This is consistent with the 1750 Å^2 area of the putative i-face (Figure 2, bottom) and the cross-sectional area of 50 Å^2 per phospholipid molecule. This model is also consistent with the calorimetry results, which showed that the binding of one sPLA2 to the interface eliminates the cooperative gel−fluid transition due to 35−40 phospholipid molecules. These results support the conclusion that the anionic charge at the interface is critical for establishing optimum binding of pancreatic sPLA2 for the processive interfacial catalytic turnover. Other factors related to the size of the headgroup and a partial charge neutralization may also be at work in controlling the binding and the orientation along the i-face.

C. Close Contacts Along the i-Face

A close contact of the substrate interface with the enzyme was first conceived to account for the high interfacial processivity. The assertion is if the enzyme must pick up the highly water-insoluble substrate from the interface, the contact along the i-face must not be significantly exposed to the aqueous phase. Fluorescence and calorimetry measurements show that both the anionic substrate interface as well as the Trp-3-containing face of the enzyme are not in contact with bulk solvent water.[2,4,197] Additional results showed that Trp-3 in the bound enzyme is not accessible to fluorescence quenchers from the aqueous phase.

Substitutions at residue 30 of pancreatic sPLA2 lower the turnover rate.[238] Leu-31 substitutions have only a modest effect on calcium binding to the E form but not to E*. The Leu-31-Trp mutant is modestly k_{cat}*-impaired.[192] The solvent accessibility results with the W3F/L31W double mutant show that Leu-31 is not a part of the i-face. Although a modest effect on the Trp-31 environment is seen on inhibitor binding, the chemical step is also significantly impaired with the Trp-31 substituent in this double mutant.

High-affinity binding of sPLA2 to the interface occurs without disruption of the bilayer organization. The binding is not influenced by the gel or fluid phase organization of the bilayer. In fact, the gel−fluid transition is not seen in the bilayer to which sPLA2 is bound,[4] although the bilayer organization is retained.[125,126] The results support the independent conclusion that the bound enzyme creates its own microenvironment along the i-face contact. Also, the emission and quenching characteristics of the dansyl fluorophore of *N*-dansyl-phosphatidylethanolamine localized at the interface show that the microinterface between the interface and the i-face is protected from the bulk solvent. Fluorescence properties of Trp-3 of the pancreatic sPLA2 show that the microenvironment at the contact face is dramatically different than it is when the i-face is in contact with the aqueous phase in the *E* form. The pre-steady-state binding of pig PLA2 with a variety of phospholipid dispersions shows that the desorption rate of the enzyme bound to the anionic interface is $\ll 0.001$ s^{-1}. However, the diffusion-limited second-order association rate is followed by a first-order constant of 4 s^{-1} independent of the concentration of the enzyme.[198] This suggests that the enzyme initially bound to the interface may undergo a slow relaxation to its 'settled' state on the interface. However, such a slow process cannot be a part of the steady-state catalytic turnover characterized by the much larger constant $k_1^* > 1000$.

D. Model of the i-Face

The results outlined above clearly support the kinetic results and show that during the processive turnover at the anionic interface sPLA2 remains in close contact with the bilayer interface. The contact presumably occurs with about 30−40 phospholipid molecules along the face from which the catalytic site

is readily accessible, but the contact region is not accessible to the bulk aqueous phase. Starting with the model of the interface recognition site,[66] several possibilities were explored by Ramirez and Jain.[77] Since the Coulombic interactions are not strongly distance dependent, the region of interest on the protein was the face of the enzyme that is less than 5-Å thick, which has hydrophobic and hydrogen-bonding groups along with cationic residues. Such a region could accommodate a sharp transition that occurs at the bilayer interface from the high polarity of the aqueous phase to the low polarity of the acyl chains of the phospholipids at the interface. Leu-31, Lys-56, and Tyr-69 were suggested to be part of the interface recognition site;[66a] however, they are not directly on the i-face that makes a close contact with the interface but are at the edges and are somewhat removed from a direct contact with the interface.[77] The original suggestion for the interfacial recognition site has now been revised on the basis of a 0.97 Å resolution structure,[66b] which conforms better to the view of the i-face[77] and the anion-assisted-dimer contact surface (Figure 2C). A method involving site-selective spin-labeling and electron paramagnetic resonance spectroscopy demonstrates that sPLA2 sits on the membrane surface rather than digging or penetrating into the membrane.[79] It has also been described in section IV that the slow onset of phospholipid monolayer hydrolysis when sPLA2 is added to the subphase is not due to slow interfacial penetration but rather due to the slow accumulation of reaction products which drives the E to E* shift.

In short, among other features, the putative i-face is remarkably flat with an area of about 1700 Å^2. Contact along a flat surface would exclude bulk water from the contact region that may also be desolvated. Such interactions along the i-face would minimally disrupt the lateral packing of the phospholipid molecules at the bilayer interface. It is clear that a hydrogen-bonded network of water with the polar groups and the glycerol−ester oxygens of phospholipids keep this interface region immobile relative to the surface or the interior; however, the cooperativity of the gel−fluid phase transition would be lost for the phospholipid molecules in direct contact with the i-face.

E. Components of the i-Face Interactions

Kinetic evidence leaves little doubt that the high-affinity binding of sPLA2 to the anionic substrate interface is critical for the processive catalytic turnover at the interface. On the basis of the exchange time of the enzyme with excess anionic vesicles, on the order of hours, our estimate for the apparent dissociation constant of pig pancreatic sPLA2 at the anionic DMPM vesicle interface is in the subpicomolar range. The estimated −15 kcal/mol binding energy would be for standard states of 1M for interface molecules and for enzyme. As discussed earlier in section VIII, the actual interaction strength may be significantly larger since some of the interactions are used up to constrain the enzyme in the surface leaving one degree of rotational and two degrees of translational freedom.

The binding to the interface along the i-face could involve several contributions. On the basis of the model at hand, these involve Coulombic and hydrogen-bonding interactions coupled with hydrophobic drive for removing a relatively large flat surface area from the aqueous phase. In addition, specific hydrogen bonding and coordination of the anionic groups and the uncharged groups at the i-face are involved. Since the contact apparently occurs along a large surface area, individual weak interactions are mediated through several residues and the contribution from individual amino acid residues is always modest, as reaffirmed by results from mutagenesis of the i-face residues.[191]

E. Hydrophobic Effect Is Related to the Water-Exposed Area of a Residue

One of the features of the interactions along a flat i-face is that the incremental contribution of the residue substitution would be correlated with the change in residue area.[281,282] As shown in Figure 21, such a correlation is found with substitutions in the N-terminal region of bovine pancreatic sPLA2. The correlation is consistent with the suggestion that as a part of a flat i-face these residues play a role in the hydrophobic effect that involves the enzyme's surface contact. The contribution of single-residue substitution to the binding to the interface is modest; however, a monotonic correlation with the change in the area is significant, especially because no correlation was seen with the *trans*-bilayer partitioning or binding of hydrophobic helices.[191] The results suggest that the important factor governing interfacial binding is the surface area of the side chain in the context of the i-face that is exposed to aqueous solvent rather than the total surface area of residue as a separate entity.

F. Role of the Cationic Residues

The preference of sPLA2 for the anionic interface suggests a role for the cationic residues in the i-face interactions. Three different site-directed mutagenesis approaches have been used. (a) A cationic residue

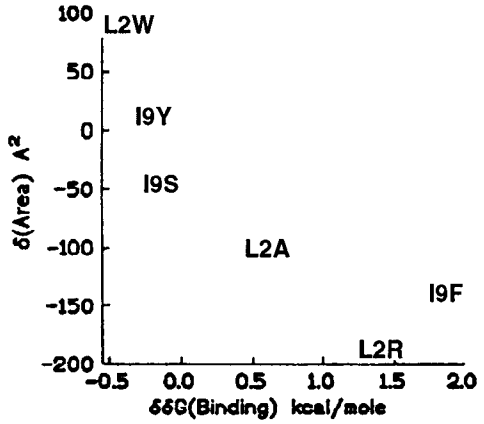

Figure 21. Relationship between the change in the hydrophobic area due to residue substitution and the binding of bovine pancreatic sPLA2 to the zwitterionic interface with only the *E* to *E** step. (Reprinted with permission from ref 191. Copyright 1999 American Chemical Society.)

is substituted by another, Lys-Arg, which probably compensates for close-ranging packing differences and the pK_a shifts. (b) The cationic-to-anionic charge-reversal mutants have an added effect of electrostatic repulsion which lowers the magnitude of the observed effect. (c) The charge compensation by isosteric Lys-Met substitution increases the observed activity. These approaches have shown that the incremental effect of such substitutions occurs in the expected direction; however, the overall electostatic contribution is maximally about 0.5−1 kcal per charged residue, and much smaller effects are observed for some cationic residues as noted below.

Electrostatic profiles of sPLA2s show a marked sidedness;[283−285] however, it does not seem to correspond to the evidence that long-range electrostatic interactions do not dominate the binding along the i-face. Results of charge-reversal mutagenesis also clearly show that electrostatic interactions of the anionic interface with specific cationic residues on sPLA2 plays only a modest role. The most dramatic example of this has been observed with the sPLA2 from bee venom.[286] The face of this enzyme that includes the opening to the catalytic site slot contains five basic residues (Lys and Arg). The five-site mutant in which these basic residues were mutated to glutamates (charge-reversal) still displays scooting kinetics on anionic phosphatidylmethanol vesicles. Although K_d for the wild-type and mutant were not measured, this result clearly shows that electrostatic interaction of basic residues with the anionic interface is not the main reason for high-affinity interfacial binding to anionic membranes. Also, enzyme could not be dissociated from anionic vesicles in the presence of high salt. Another example is human IIA sPLA2 where charge reversal mutagenesis of basic residues on its putative i-face reduced its affinity for anionic vesicles somewhat, but the multisite charge reversal mutant still displays high-affinity binding to anionic vesicles.[233] Basic residues appear to contribute to the binding of *Agkistrodon piscivorus piscivorus* venom sPLA2 to anionic interface, but again, multisite charge reversal mutagenesis reduced interfacial binding by less than 1000-fold.[287]

Results with the charge-reversal mutants are also consistent with the binding results with the charge-compensation mutants in which the charge on lysine was compensated by substitution with isosteric methionine. In these mutants a modest 20-fold increase in the binding affinity toward zwitterionic micelles and vesicles was seen.[193,263] However, as described before, a much larger k_{cat}* activation was also observed at the zwitterionic interface without a significant effect on k_{cat}* at the anionic interface. Together, results with charge-reversal and charge-compensation mutants show that the contribution of the electrostatic interaction toward the binding of sPLA2 to the interface is modest relative to the overall binding energy and in the range of 1−3 kcal/mol.

It is intriguing that virtually all sPLA2s exhibit the scooting mode reaction progress at the interfaces of anionic phospholipids,[83] and none exhibits high interfacial processivity on phosphatidylcholine vesicles. The apparent K_d for sPLA2s toward zwitterionic interfaces are in the range of 0.01−10 mM.[108] These results suggest that in addition to the charge-compensation effects, certain types of more important close-range specific interactions of the anionic headgroups at the interface with the protein residues along the i-face are involved. Indeed, as also developed below, such interactions are suggested to be close-range ligand coordination of the interfacial anionic groups through the hydrogen-bonding protein groups, as also seen for the binding of anions to proteins.[288]

G. Simulation Studies for the i-Face

Direct methods to obtain atomic level details of the i-face are not available. Molecular simulations support a tight-binding orientation of the i-face of sPLA2 with desolvation of the microinterface.[78] In the bilayer docking simulations with human group IIA sPLA2,[78a] the desolvated lipid interface interacts with the hydrophobic residues 2, 3, 18, 19, 24, 31, and 70. Several cationic (34, 53, 57, 69, 92, 123, and 124) and anionic (16, 56, 89) residues in the consensus sequence are also found in the collar surrounding the hydrophobic rim. Refinements with predictive insights remain to be developed.

XII. Atomic-Level Details of the i-Face from the Anion-Assisted-Dimeric sPLA2

Totally unexpected evidence in support of the contacts at the i-face has emerged from the structure of the crystallograhic dimer of pig pancreatic sPLA2 with one substrate mimic, MJ33, and five sulfate or phosphate anions shared between the two protein monomers.[80] These crystallization conditions were selected with an appreciation of the fact that the anionic binding sites on the protein play a role in the various functions of sPLA2. Therefore, the crystallization conditions included divalent anions to identify the anion binding sites. The crystallographic asymmetric unit contains five coplanar phosphate anions. Furthermore, only one molecule of the inhibitor MJ33 is shared between the subunits of the dimer such that the *sn*-2-phosphate of the polar headgroup is bound to the A subunit and the alkyl chain extends into the active-site slot of the B subunit across the subunit−subunit contact surface. Remarkably this subunit contact face (Figure 2C) is virtually identical to the model of i-face proposed 10 years earlier.[77] If this is truly the face of sPLA2 that makes contact with the interface for the processive turnover, by providing the atomic level details of the i-face and the anion binding sites, the anion-assisted-dimer contact results are useful for resolving some of the remaining questions.

(a) The two subunits in the crystallographic dimer are packed with a large hydrophobic and desolvated surface symmetrically provided by the same face of the two subunits. The interactions with the anions are dominated by close-range hydrogen-bonding interactions with polarizable ligands including the backbone NH and water molecules, as also seen in other proteins.[289] In no case is the charge on the

anion fully neutralized. These results show that while the anionic charge at the interface is required for the binding of sPLA2, it does not necessarily follow that the charge is always or completely compensated by the cationic residues. This helps to explain why interfacial binding is not dominated by Coulombic electrostatic interactions between cationic residues of sPLA2 and anionic phospholipid headgroups as described above.

(b) The environment of the headgroup of MJ33 shows the presence of a water molecule between the *sn*-2-phosphate and His-48. In the oxyanion mechanism (Figure 14) the assisting water molecule w6 is virtually in the same position as the w6 in relation to the tetrahedral intermediate in the reaction coordinates. It is certainly intriguing that this water molecule was not seen in an earlier structure where the crystallization conditions did not include the anions and the crystallographic asymmetric unit consisted of only one protein.[87] This difference raises the possibility that the structure with the assisting-water w6 is the charge-compensated activated form of the activated Michaelis complex $(E^*S)^{\#}$ (Figure 12), whereas the earlier structure may be close to the E*I form in this k_{cat}* activation mechanism.

(c) Certain regions, disordered in the earlier NMR and crystallographic structures, are clearly identifiable in the dimer structure. For example, the electron density of the residues in the 69-loop is clearly defined. Also, the side chains of the residues in N-terminus helix and the calcium-binding loop are well defined. Since the disorder in the ensemble of the solution structures is also reduced on binding to the interface, it is likely that the ordered side chains in the dimer structure may represent one view of the interfacial structure of the activated enzyme.

(d) Note that residues 69 and 31 are involved in k_{cat}*. Residues 59−75 form a loop connecting two helices. It is disordered in the NMR structure and remains so in most crystallographic structures. It is somewhat more ordered in the structures of the complexes with substrate mimics. The whole loop and side chains are clearly defined in the crystallographic dimer structure with bound divalent anions.[80] Also, in some sPLA2s residues 62−66 are deleted. Mutagenesis results suggest that the loop plays a role in the apparent turnover at the zwitterionic interface. In addition to the structurally significant Tyr73, the 59−75 loop also contains the catalytically significant Tyr-69. The phenolic side chain appears to swing over a distance of 6 Å in different structures. Although it is not a conserved residue, a role for this residue in the chemical step is also supported by the observation that Tyr-69-Phe mutant is k_{cat}* impaired by 10-fold.[56] In cocrystals the phenolic OH is hydrogen bonded to the *pro*-S-oxygen of *sn*-3-phosphate of substrate mimics. On the other hand, in the structures with MJ33 in the active site, the OH is bonded to the diester oxygen[87] or to the *pro*-S oxygen[80] of the *sn*-2-phosphate.

Both Tyr-69 and Leu-31 are closely positioned and are part of separate but somewhat flexible neighboring loops and have an effect on k_{cat}*, and they are part of the substrate−mimic binding. Tyr-69 is in the contact surface in the dimer structure. Residues at 31 and 69 are not conserved. Often lysine is found in one or the other of these positions but never in both. It appears that residues 31 and 69 influence the chemical step by controlling the plasticity of the catalytic site environment rather than through a direct participation in the catalytic mechanism.

It is interesting that residues 53 and 56 are not part of the i-face. Our current thinking is that these basic residues at the edge of the i-face remain in the aqueous phase and make only the long-range (5−10 Å) nonspecific electrostatic interaction with the interface. This could however trigger a change in the orientation of the 59−71 loop that makes contact with the interface and the substrate. Other hydrophilic residues on the i-faces of sPLA2s can make close contact by donating hydrogen bonds to the phosphate portion of the polar headgroup of phospholipids at the interface. Such hydrogen bonding is facilitated by the numerous hydrophobic residues on the i-face, which are thought to penetrate only slightly into the membrane interface, perhaps into the region that includes the glycerol ester region of phospholipids. In the context of this model, the relatively poor binding of sPLA2s to phosphatidylcholine vesicles may be due to the presence of the bulkier choline group that could sterically interfere with the type of protein−phospholipid hydrogen-bonded structure described above.

It has been shown that tryptophan is an important residue for supporting interfacial binding to anionic and charge-neutral vesicles.[289] Tryptophan contains an aromatic side chain and a hydrogen-bond-accepting indole NH. Thus, intermediate hydrophobicity may be ideal for the close-range apposition with the region of the membrane that includes the glycerol esters. Many snake venom enzymes, especially those from cobra species, display relatively high affinity among sPLA2s for phosphatidylcholine vesicles. Cobra venom sPLA2s contain at least two tryptophan residues on their putative i-faces, and recent mutagenesis studies have shown that these residues as well as other aromatic amino acid side chains play an important role in supporting binding to phosphatiylcholine vesicles.

XIII. Summary and Outlook

Figure 1 is a road map for identifying the kinetic path of interest. However, with so many possible branches, it is a challenge to identify the assay conditions with unequivocally defined kinetic path. Figure 1 is a general paradigm for enzymology that provides the kinetic paths for the soluble, matrix, and interfacial enzymes. Roughly one-half of the proteins in cells are membrane associated, and most of these remain to be functionally characterized.

The pancreatic sPLA2 paradigm is based on constraining the reaction system so that the turnover cycles occur in the scooting mode or in the quasi-scooting mode. Only in these ways can the primary parameters for the interfacial binding and turnover events be dissected out. These results provide significant kinetic and structural insights into workings of an interfacial enzyme. The sPLA2 problem has

yielded to rigorous analysis by separating the interfacial binding from the catalytic turnover events. Their spatial relationship is implicit in the structural features of the catalytic site versus the i-face, and a temporal resolution of the underlying events is carried out during the reaction progress in the scooting mode. With a full appreciation of the factors that control high interfacial processivity, it is now possible to have an appreciation of the intrinsic difficulties of the kinetic analysis under the conditions where the substrate accessibility and replenishment are not suitably controlled.

With a set of primary parameters for the events of the catalytic turnover cycle, new insights have emerged into the catalytic mechanism of sPLA2. Even more remarkable is the fact that the allosteric effect of the interface on the catalytic turnover events can be clearly delineated. The analysis clearly shows that the effect of the interface on the two-dimensional ligand binding equilibrium is the basis for the K_S* allostery. An additional k_{cat}* allosteric contribution of the interfacial anionic charge is also analyzed for pancreatic sPLA2 and attributed to a structural change due to charge compensation of specific cationic residues.

Protein structure determination at the interface is a major unsolved problem. The last lucky break that contributed to the pancreatic sPLA2 paradigm emerges from the structure of the anion-assisted-dimer. Certainly the evidence is circumstantial, yet one cannot help but notice the way pieces seem to fall together. The five coplanar anion-binding sites are at the rim of the putative i-face. The substrate-binding slot and the catalytic site is accessible through the opening in the hydrophobic water-exclusion area surrounded by the anion-binding sites. This is generally consistent with the view of efficient binding of a protein to the interface by taking advantage of numerous weaker interactions and the hydrophobic effect. It is a remarkable coincidence that the difference in the binding environment of the *sn*-2-tetrahedral phosphate of the substrate mimic MJ33 bound to pancreatic sPLA2 in the two structures with and without the anions also point to mechanistically relevant differences as a possible basis for the k_{cat}* allostery.

Consequently, with the structural and analytical progress made with the sPLA2 paradigm, it is now possible to study other interfacial enzymes in order to interpret their role in the cellular environment. Obviously, the aqueous-phase perspective is not adequate for such purposes. In short, what matters depends on what the enzyme 'sees'.

XIV. Abbreviations

CMC	critical micelle concentration
DC_nPC	1,2-diacyl-*sn*-glycero-3-phosphocholine
deoxy-LPC	1-hexadecylpropanediol-3-phosphocholine
DMPM	1,2-dimyristoyl-*sn*-glycero-3-phosphomethanol
DTPM	1,2-ditetradecyl-*sn*-glycero-3-phosphomethanol
i-face	the interfacial contact face of sPLA2
L	S (substrate), P (product), I (inhibitor), or imperfect diluent (ND)
MJ33	1-hexadecyl-3-(2,2,2-trifluoroethyl)-*rac*-glycero-2-phosphomethanol
ND	neutral (surface) diluent form interface but has no affinity for the active site
PC	phosphatidylcholine
sPLA2	14-kDa secreted phospholipase A_2

XV. Acknowledgment

The work from the authors laboratories was supported by grants from the U.S. National Institutes of Health GM29703 (M.K.J.), HL36235 and HL50040 (M.H.G.), and GM 41788 (M.D.T.), and from the Swedish Natural Science Research Council (O.G.B.). We take this opportunity to thank our co-workers for their contributions mentioned in this review.

XVI. References

(1) Jain, M. K.; Rogers, J.; Jahagirdar, D. V.; Marecek, J. F.; Ramirez, F. *Biochim. Biophys. Acta* **1986**, *860*, 435.
(2) Jain, M. K.; Maliwal, B. P.; de Haas, G. H.; Slotboom, A. J. *Biochim. Biophys. Acta* **1986**, *860*, 448.
(3) Jain, M. K.; Rogers, J.; Marecek, J. F.; Ramirez, F.; Eibl, H. *Biochim. Biophys. Acta* **1986**, *860*, 462.
(4) Jain, M. K.; de Haas, G. H.; Marecek, J. F.; Ramirez, F. *Biochim. Biophys. Acta* **1986**, *860*, 475.
(5) Jain, M. K.; Berg, O. G. *Biochim. Biophys. Acta* **1989**, *1002*, 127.
(6) Berg, O. G.; Yu, B.-Z.; Rogers, J.; Jain, M. K. *Biochemistry* **1991**, *30*, 7283.
(7) Min, J. H.; Jain, M. K.; Wilder, C.; Paul, L.; Apitz-Castro, R.; Aspleaf, D. C.; Gelb, M. H. *Biochemistry* **1999**, *38*, 12935.
(8) Min, J. H.; Jain, M. K.; Gelb, M. H. *Biochim. Biophys. Acta* **2000**, *1488*, 20.
(9) De Haas, G. H.; Bonsen, P. P. M.; Pieterson, W. A.; van Deenen, L. L. M. *Biochim. Biophys. Acta* **1971**, *239*, 252.
(10) Verger, R.; de Haas, G. H. *Annu. Rev. Biophys. Bioeng.* **1976**, *5*, 77.
(11) Verheij, H. M.; Slotboom, A. J.; de Haas, G. H. *Rev. Physiol. Biochem. Pharmacol.* **1981**, *91*, 91.
(12) (a) Bayburt, T.; Gelb, M. H. *Biochemistry* **1997**, *36*, 3216. (b) Leslie, C. C. *J. Biol. Chem.* **1997**, *272*, 16709.
(13) Higgs, H. N.; Glomset, A. A. *J. Biol. Chem.* **1996**, *271*, 10874.
(14) Berg, O. G.; Cajal, Y.; Butterfoss, G. L.; Grey, R. L.; Alsina, M. A.; Yu, B.-Z.; Jain, M. K. *Biochemistry* **1998**, *37*, 6615.
(15) Sarda, L.; Desnuelle, P. *Biochim. Biophys. Acta* **1958**, *30*, 513.
(16) (a) Volwerk, J. J.; Filthuth, E.; Griffith, O. H.; Jain, M. K. *Biochemistry* **1994**, *33*, 3464. (b) Lewis, A. A.; Garigapati, V. AR.; Zhou, C.; Roberts, M. F. *Biochemistry* **1993**, *32*, 8836. (c) Griffith, O. H.; Ryan, M. *Biochim. Biophys. Acta* **1999**, *1441*, 237.
(17) (a) Boguslavsky, V.; Rebecchi, M.; Morris, A.; John, D. Y.; Rhee, S. G.; McLaughlin, S. *Biochemistry* **1994**, *33*, 3032. (b) Williams, R. L. *Biochim. Biophys. Acta* **1999**, *1441*, 255.
(18) Barnett, S. F.; Ledder, L. M.; Stirivant, S. M.; Ahern, J.; Conroy, R. R.; Heimbrook, D. C. *Biochemistry* **1995**, *34*, 14254.
(19) Burden, L. M.; Rao, V. D.; Murray, D.; Ghirlando, R.; Doughman, S. D.; Anderson, R. A.; Hurley, J. H. *Biochemistry* **1999**, *38*, 15141.
(20) Hurley, J. H.; Misra, S. *Annu. Rev. Biophys. Biomol. Struct.* **2000**, *29*, 49.
(21) Jain, M. K.; Krause, C. D.; Buckley, J. T.; Bayburt, T.; Gelb, M. G. *Biochemistry* **1994**, *33*, 5011.
(22) Borgstrom, B.; Brockman, H. L. *Lipase*; Elsevier: Amsterdam, 1984; p 527.
(23) Carey, M. C.; Small, D. M.; Bliss, C. M. *Annu. Rev. Physiol.* **1983**, *45*, 651.
(24) (a) Dennis, E. A. *The Enzymes* **1983**, *16*, 307. (b) Roberts, M. F. *FASEB J.* **1996**, *10*, 1159.
(25) Derwenda, Z. S. *Adv. Protein Chem.* **1994**, *45*, 1.
(26) Ferrato, F.; Carriere, F.; Sarda, L.; Verger, R. *Methods Enzymol.* **1997**, *286*, 327.
(27) Gelb, M. H.; Jain, M. K.; Hanel, A. M.; Berg, O. G. *Annu. Rev. Biochem.* **1995**, *64*, 653.
(28) (a) Homan, R.; Jain, M. K. In *Intestinal Lipid Metabolism*; Mansbach, C. M., Tso, P., Kuksis, A., Eds.; Kluwer Academic Press and Plenum Publ.: New York, 2000; p 81. (b) Richmond, B. L.; Boileau, A. C.; Zheng, S.; Huggins, K. W.; Granholm, N. A.; Tso, P.; Hui D. Y. *Gastroenterology* **2001**, *120*, 1193.
(29) (a) *Esterases, Lipase, and Phospholipase: from Structure to Clinical Significance*; Mackness, M. I., Clerc, M., Eds.; Plenum Press: New York, 1994; p 279. (b) Moreau, P.; Cassagne, C. *Biochim. Biophys. Acta* **1994**, *1197*, 257. (c) Mansbach, C. M. *J. Clin. Invest.* **1977**, *60*, 411.

(30) Smith, W. L. *Biochem. J.* **1989**, *259*, 315.
(31) Upton, C.; Buckley, J. T. *Trends Biochem. Sci.* **1995**, *20*, 178.
(32) Vrielink, A.; Lloyd, L. F.; Blow, D. M. *J. Mol. Biol.* **1991**, *219*, 533.
(33) Waite, M. *The Phospholipases*; Plenum: New York, 1987.
(34) Wittcoff, H. *The Phosphatides*; Reinhold Publishing Corp.: New York, **1951**; pp 99−115.
(35) *Lipases: Their Structure, Biochemistry and Application*; Woolley, P., Petersen, S. B., Eds.; Cambridge University Press: Cambridge, 1994; p 363.
(36) Van den Bergh, C. J.; Slotboom, A. J.; Verheij, H. M.; de Haas, G. H. *J. Cell. Biochem.* **1989**, *39*, 379.
(37) Davidson, F. F.; Dennis, E. A. *J. Mol. Evol.* **1990**, *31*, 228.
(38) Dennis, E. A. *J. Biol. Chem.* **1994**, *269*, 13057.
(39) Dennis, E. A. *Trends Biochem. Sci.* **1997**, *22*, 1.
(40) Balsinde, J.; Balboa, M. A.; Insel, P. A.; Dennis, E. A. *Annu. Rev. Pharmacol. Toxicol.* **1999**, *39*, 175.
(41) Tischfield, J. A. *J. Biol. Chem.* **1997**, *272*, 17247−50.
(42) Cupillard, L.; Koumanov, K.; Matteri, M. G.; Lazdunski, M.; Lambeau, G. *J. Biol. Chem.* **1997**, *272*, 15745.
(43) Valentin, E.; Ghomashchi, F.; Gelb, M. H.; Lazdunski, M.; Lambeau, G. *J. Biol. Chem.* **1999**, *274*, 31195.
(44) (a) Valentin E.; Lambeau G. *Biochim. Biophys. Acta* **2000**, *1488*, 59. (b) Lambeau, G.; Lazdunski, M. *Trends Pharmacol. Sci.* **1999**, *20*, 162.
(45) (a) Nicolas, J. P.; Lin, Y.; Lambeau, G.; Ghomashchi, F.; Lazdunski, F.; Gelb, M. H. *J. Biol. Chem.* **1997**, *272*, 7173. (b) Valentin, E.; Ghomashchi, F.; Gelb, M. H.; Lazdunski, M.; Lambeau, G. *J. Biol. Chem.* **2000**, *275*, 7492.
(46) Bezzine, S.; Koduri, R. S.; Valentin, E.; Murakami, M.; Kudo, I.; Ghomashchi, F.; Sadilek, M.; Lambeau, G.; Gelb, M. H. *J. Biol. Chem.* **2000**, *275*, 3179.
(47) McIntosh, J. M.; Ghomashchi, F.; Gelb, M. H.; Dooley, D. J.; Stoehr, S. J.; Giordani, A. B.; Naisbitt, S. R.; Olivera, B. M.; Conodipine, M. *J. Biol. Chem.* **1995**, *270*, 3518.
(48) Jain, M. K. *Curr. Top. Membr. Transp.* **1973**, *4*, 175.
(49) (a) Jain, M. K.; Cordes, E. H. *J. Membr. Biol.* **1973**, *14*, 101. (b) Jain, M. K.; Cordes, E. H. *J. Membr. Biol.* **1973**, *14*, 119.
(50) Dennis, E. A. *Arch. Biochem. Biophys.* **1973**, *158*, 485.
(51) Upreti, G. C.; Jain, M. K. *J. Membr. Biol.* **1980**, *55*, 113.
(52) Jain, M. K.; Gelb, M. H.; Rogers, J.; Berg, O. G. *Methods Enzymol.* **1995**, *249*, 567.
(53) Berg, O. G.; Rogers, J.; Yu, B.-Z.; Yao, J.; Romsted, L. S.; Jain, M. K. *Biochemistry* **1997**, *36*, 14512.
(54) Verheij, H. M.; Volwerk, J. J.; Jensen, E. H. J. M.; Puijk, W. C.; Dijkstra, B. W.; Drenth, J.; de Haas, G. H. *Biochemistry* **1980**, *19*, 743.
(55) Annand, R. R.; Kontoyianni, M.; Penzotti, E.; Dudlen, T.; Lybrand, T. P.; Gelb, M. H. *Biochemistry* **1996**, *35*, 4591.
(56) Yu, B.-Z.; Rogers, J.; Nicol, G. R.; Theopold, K. H.; Seshadri, K.; Vishweshwara, S.; Jain, M. K. *Biochemistry* **1998**, *37*, 12576.
(57) (a) Zographi, G.; Verger, R.; De Haas, G. H. *Chem. Phys. Lipids* **1971**, *7*, 185. (b) Verger, R.; Mieras, M. C. E.; de Haas, G. H. *J. Biol. Chem.* **1973**, *248*, 4023. (c) Verger, R.; Mieras, M. C. E.; de Haas, G. H. *J. Biol. Chem.* **1973**, *251*, 3128.
(58) Jain, M. K.; Ranadive, G. N.; Rogers, J.; Yu, B.-Z.; Berg, O. G. *Biochemistry* **1991**, *30*, 7306.
(59) Jain, M. K.; Tao, W.; Rogers, J.; Arenson, C.; Eibl, H.; Yu, B.-Z. *Biochemistry* **1991**, *30*, 10256.
(60) Jain, M. K.; Yuan, W.; Gelb, M. H. *Biochemistry* **1989**, *28*, 4135.
(61) Gelb, M. H.; Jain, M. K.; Berg, O. G. *FASEB J.* **1994**, *8*, 916.
(62) Gelb, M. H.; Berg, O. G.; Jain, M. K. *Curr. Biol.* **1991**, *1*, 836.
(63) Jain, M. K.; Rogers, J. *Biochim. Biophys. Acta* **1989**, *1003*, 91−97.
(64) Ghomashchi, F.; Yu, B.-Z.; Berg, O. G.; Jain, M. K.; Gelb, M. H. *Biochemistry* **1991**, *30*, 7318.
(65) Dijkstra, B. W.; Drenth, J.; Kalk, K. H.; Vandrmaelen, P. J. *J. Mol. Biol.* **1978**, *124*, 53.
(66) (a) Dijkstra, B. W.; Drenth, J.; Kalk, K. H. *Nature* **1981**, *289*, 604. (b) Steiner, R. A.; Rozeboom, H. L.; De Vries, A.; Kalk, K. H.; Murshudov, G.; Wilson, K. S.; Dijkstra, B. W. *Acta Crystallogr.* **2001**, *D57*, 516.
(67) Dijkstra, B. W.; Kalk, K. H.; Hol, W. G. J.; Drenth, J. *J. Mol. Biol.* **1981**, *147*, 97.
(68) Dijkstra, B. W.; Renetseder, R.; Kalk, K. H.; Hol, W. G. J.; Drenth, J. *J. Mol. Biol.* **1983**, *168*, 163.
(69) Dijkstra, B. W.; Kalk, K. H.; Drenth, J.; de Hass, G. H.; Egmond, M.; Slotboom, A. J. *Biochemistry* **1984**, *23*, 2759.
(70) Scott, D. L.; Sigler, P. B. *Adv. Protein Chem.* **1994**, *45*, 53.
(71) Yuan, C.; Li, Y.; Byeon, I.; Li, Y.; Tsai, M. D. *Biochemistry* **1999**, *38*, 2909.
(72) Yuan, C.; Li, Y.; Byeon, I.; Poi, M.; Tsai, M. D. *Biochemistry* **1999**, *38*, 2919.
(73) Yuan, C.; Tsai, M. D. *Biochim. Biophys. Acta* **1999**, *1441*, 215.
(74) Van den Berg, B.; Tessari, M.; Boelens, R.; Dijkman, R.; Kaptein, R.; de Haas, G. H.; Verheij, H. M. *J. Biomol. NMR* **1995**, *5*, 110.
(75) Van den Berg, B.; Tessari, M.; de Haas, G. H.; Verheij, H. M.; Boelens, R.; Kaptein, R. *EMBO J.* **1995**, *14*, 4123.
(76) van den Berg, B.; Tessari, M.; Boelens, R.; Dijkman, R.; de Haas, G. H.; Kaptein, R.; Verheij, H. M. *Nat. Struct. Biol.* **1995**, *2*, 402.
(77) Ramirez, F.; Jain, M. K. *Proteins* **1991**, *9*, 229.
(78) (a) Zhou, F.; Schulten, K. *Proteins: Struct., Funct., Genet.* **1996**, *25*, 12. (b) Tieleman, D. P.; Marrink, S. J.; Berendsen, H. J. C. *Biochim. Biophys. Acta* **1997**, *1331*, 235.
(79) Lin, Y.; Nielsen, R.; Murray, D.; Hubbell, W. L.; Mailer, C.; Robinson, B. H.; Gelb, M. H. *Science* **1998**, *279*, 1925.
(80) Pan, Y. H.; Epstein, T. M.; Jain, M. K.; Bahnson, B. J. *Biochemistry* **2001**, *40*, 609.
(81) Berg, O. G.; Jain, M. K. *Interfacial Enzyme Kinetics: Trunover, Processivity, and Replenishment*; Wiley: London, **2002**, in press.
(82) Jain, M. K.; Gelb, M. K. *Methods Enzymol.* **1991**, *197*, 112.
(83) Jain, M. K.; Ranadive, G. N.; Yu, B.-Z.; Verheij, H. M. *Biochemistry* **1991**, *30*, 7330.
(84) Jain, M. K.; Rogers, J.; Berg, O.; Gelb, M. H. *Biochemistry* **1991**, *30*, 7340.
(85) Jain, M. K.; Yu, B.-Z.; Rogers, J.; Gelb, M. H.; Tsai, M. D.; Hendrickson, E. K.; Hendrickson, S. *Biochemistry* **1992**, *31*, 7841.
(86) Ghomashchi, F.; O'Hare, T.; Clary, D.; Gelb, M. H. *Biochemistry* **1991**, *30*, 7298−7305. Deng, T.; Noel, J. O.; Tsai, M.-D. *Gene* **1990**, *93*, 229.
(87) Sekar, K.; Eswaramoorthy, S.; Jain, M. K.; Sundaralingam, M. *Biochemistry* **1997**, *36*, 14186.
(88) Thunnissen, M. M. G. M.; Eiso, A. B.; Kalk, K. H.; Drenth, J.; Dijkstra, B. W.; Kuipers, O. P.; Dijkman, R.; de Haas, G. H.; Verheij, H. M. *Nature* **1990**, *347*, 689.
(89) Tomoo, K.; Yamane, Y.; Ishida, T.; Fujii, S.; Ikeda, K.; Iwama, S.; Katsumura, S.; Sumiya, S.; Miyagawa, H.; Kitamura, K. *Biochim. Biophys. Acta* **1997**, *1340*, 178.
(90) Cha, S. S.; Lee, D.; Adams, J.; Kurdyla, J. T.; Jones, C. S.; Marshall, L. A.; Bolognese, B.; Abdel-Meguid, S. S.; Oh, B. H. *J. Med. Chem.* **1996**, *39*, 3878.
(91) White, S. P.; Scott, D. L.; Otwinowski, Z.; Gelb, M. H.; Sigler, P. B. *Science* **1990**, *250*, 1560.
(92) Scott, D. L.; White, S. P.; Otwinowski, Z.; Yuan, W.; Gelb, M. H.; Sigler, P. B. *Science* **1990**, *250*, 1541.
(93) Sekar, K.; Kumar, A.; Liu, X.; Tsai, M. D.; Gelb, M. H.; Sundaralingam, M. *Acta Crystallogr.* **1998**, *D54*, 334.
(94) Scott, D. L.; White, S. P.; Browning, J. L.; Rosa, J. J.; Gelb, M. H.; Sigler, P. B. *Science* **1991**, *254*, 1007.
(95) Seshadri, K.; Vishveshwara, S.; Jain, M. K. *Proc. Indian Acad. Sci.* **1994**, *106*, 1177.
(96) Bonsen, P. P. M.; DeHaas, G. H.; Pieterson, W. A.; Van Deenen, L. L. M. *Biochim. Biophys. Acta* **1972**, *270*, 364.
(97) De Haas, G. H.; Scharrenburg, G. J. M.; Slotboom, A. J. *Biochemistry* **1987**, *26*, 3402.
(98) De Haas, G. H.; Dijkman, R.; Ransac, S.; Verger, R. *Biochim. Biophys. Acta* **1990**, *1046*, 249.
(99) De Haas, G. H.; Dijkman, R.; Lugtigeid,; Dekker: N.; Van den Berg, L.; Egmond, M. R.; Verheij, H. M. *Biochim. Biophys. Acta* **1993**, *1167*, 282.
(100) De Haas, G. H.; Dijkman, R.; Boots, J. W. P.; Verheij, H. M. *Biochim. Biophys. Acta* **1995**, *1257*, 87.
(101) Ransac, S.; Riviere, C.; Soulie, J. M.; Gancet, C.; Verger, R.; de Haas, G. H. *Biochim. Biophys. Acta* **1990**, *1043*, 57.
(102) Yu, L.; Deems, R. A.; Hadju, J.; Dennis, E. A. *J. Biol. Chem.* **1990**, *265*, 2657.
(103) Jain, M. K.; Ghomashchi, G.; Yu, B.-Z.; Bayburt, T.; Murphy, D.; Houck, D.; Brownell, J.; Reid, J. C.; Solowiej, J. E.; Jarrell, R.; Sasser, M.; Gelb, M. H. *J. Med. Chem.* **1992**, *35*, 3584.
(104) Lin, H. K.; Gelb, M. H. *J. Am. Chem. Soc.* **1993**, *115*, 3932−3942.
(105) (a) Schevitz, R. W.; Bach, N. J.; Carlson, D. G.; Chigadze, S. E.; Hartley, L. W.; Jones, N. D.; Mihelich, E. D. *Nat. Struct. Biol.* **1999**, *2*, 458. (b) Beaton, H. G.; Bennion, C.; Connolly, S.; Cook, A. R.; Gensmantel, N. P.; Hallam, C.; Hardy, K.; Hitchin, B.; Jackson, C. G.; Robinson, D. H. *J. Med. Chem.* **1994**, *37*, 557. (c) Bennion, C.; Connolly, S.; Gensmantel, N. P.; Hallam, C.; Jackson, C. G.; Primrose, W. U.; Roberts, G. C. K.; Robinson, D. H.; Slaich, P. K. *J. Med. Chem.* **1992**, *35*, 2939.
(106) Finzel, B. C.; Weber, P. C.; Ohlendorf, D. H.; Salemme, F. R. *Acta Crystallogr.* **1991**, *B47*, 814.
(107) Apitz-Castro, R. J.; Jain, M. K.; de Haas, G. H. *Biochim. Biophys. Acta* **1982**, *688*, 349.
(108) Jain, M. K.; Egmond, M. R.; Verheij, H. M.; Apitz-Castro, R. J.; Dijkman, R.; de Haas, G. H. *Biochim. Biophys. Acta* **1982**, *688*, 341.
(109) Derwenda, Z. S.; Ho, Y. S. *Biochim. Biophys. Acta* **1999**, *1441*, 229.
(110) Ghomashchi, G.; Schuttel, S.; Jain, M. K.; Gelb, M. H. *Biochemistry* **1992**, *31*, 3814.
(111) Kim, T. M.; Dodia, C.; Chen, X.; Hennigan, B. B.; Jain, M. K.; Feinstein, S. I.; Fisher, A. B. *Am. J. Physiol.* **1998**, *274*, L750−761.
(112) Kishino, J.; Kawamoto, K.; Ishizaki, J.; Verheij, H. M.; Ohara, O.; Arita, H. *J. Biochem.* **1995**, *117*, 420.

(113) (a) Ohara, O.; Ishizaki, J.; Arita, H. *Prog. Lipid Res.* **1995**, *34*, 117. (b) Murakami, M.; Nahatani, Y.; Atsumi, G.; Inoue, K.; Kudo, I. *Crit. Rev. Immunol.* **1997**, *17*, 225.
(114) Hanasaki, K.; Ono, T.; Saiga, A.; Morioka, Y.; Ikeda M.; Kawamoto, K.; Higashino, K.; Nakano, K.; Yamada, K.; Ishizaki, J.; Arita, H. *J. Biol. Chem.* **1999**, 274, 34203.
(115) Bayburt, T.; Yu, B.-Z.; Lin, H.; Browning, J.; Jain, M. K.; Gelb, M. H. *Biochemistry* **1993**, *32*, 573.
(116) Qu, X. D.; Lehrer, R. I. *Infect. Immun.* **1998**, *66*, 2791−2797.
(117) Foreman-Wykert, A. K.; Weinrauch, Y.; Elsbach, P.; Weiss, J. *J. Clin. Invest.* **1999**, *103*, 715.
(118) (a) Buckland, A. G.; Heeley, E. L.; Wilton, D. C. *Biochim. Biophys. Acta* **2000**, *1484*, 195. (b) Buckland, A. G.; Wilton, D. C. *Biochim. Biophys. Acta* **2000**, *1488*, 71. (c) Edwards, S. H.; Baker, S. F.; Wilton, D. C. *Biochem. Soc Trans.* **1998**, S239.
(119) Weiss, J.; Wright, G.; Bekkers, A. C. A. P. A.; Van den Bergh, C.; Verheij, H. M. *J. Biol. Chem.* **1991**, *266*, 4162.
(120) Yu, B.-Z.; Rogers, J.; Ranadive, G. N.; Baker, S.; Wilton, D. C.; Apitz-Castro, R.; Jain, M. K. *Biochemistry* **1997**, *36*, 12400.
(121) Yu, B.-Z.; Berg, O. G.; Jain, M. K. *Biochemistry* **1999**, *38*, 10449.
(122) Yu, B.-Z.; Berg, O. G.; Jain, M. K. *Biochemistry* **1993**, *32*, 6485.
(123) Jain, M. K.; Yu, B.-Z.; Berg, O. G. *Biochemistry* **1993**, *32*, 11319.
(124) Upreti, G. C.; Jain, M. K. *Arch. Biochem. Biophys.* **1978**, *188*, 364−375.
(125) (a) Wilschut, J. C.; Regts, J.; Scherphof, G. *FEBS Lett.* **1979**, *98*, 181. (b) Wilshut, J. C.; Regts, J.; Westenberg, H.; Scherphof, G. *Biochim. Biophys. Acta* **1978**, *508*, 185.
(126) Yu, B.-Z.; Ghomashchi, F.; Cajal, Y.; Annand, R. R.; Berg, O. G.; Gelb, M. H.; Jain, M. K. *Biochemistry* **1997**, *36*, 3870.
(127) Cajal, Y.; Berg, O. G.; Jain, M. K. *Biochem. Biophys. Res. Commun.* **1995**, *210*, 746.
(128) Cajal, Y.; Rogers, J.; Berg, O. G.; Jain, M. K. *Biochemistry* **1996**, *35*, 299.
(129) Cajal, Y.; Ghanta, J.; Surolia, A. K.; Easwaran, E.; Jain, M. K. *Biochemistry* **1996**, *35*, 5684.
(130) Cajal, Y.; Jain, M. K. *Biochemistry* **1997**, *36*, 3882.
(131) Cajal, Y.; Boggs, J.; Jain, M. K. *Biochemistry* **1997**, *36*, 2566.
(132) Cajal, Y.; Dodia, C.; Fisher, A. B.; Jain, M. K. *Biochemistry* **1998**, *37*, 12178.
(133) Liechty, A.; Chen, J.; Jain, M. K. *Biochim. Biophys. Acta*. **2000**, *1463*, 55.
(134) (a) Oh, J. T.; Van Dyk, T. J.; Cajal, Y.; Dhurjati, P.; Sasser M.; Jain, M. K. *Biochem. Biophys. Res. Commun.* **1998**, *246*, 619. (b) Oh, J. T.; Van Dyk, T. J.; Cajal, Y.; Sasser M.; Jain, M. K. *Biochim. Biophys. Acta* **1999**, *1415*, 235. (c) Oh, J. T.; Cajal, Y.; Skowronska, E. M.; Belkin, S.; Chen, J.; Van Dyk, T. K.; Sasser, M.; Jain, M. K. *Biochim. Biophys. Acta*. **2000**, *1463*, 43.
(135) Aniansson, E. A. G.; Wall, S. N.; Almgren, M.; Hoffman, H.; Klelman, I.; Ulbricht, W.; Zana, R.; Lang, J.; Tondre, C. *J. Phys. Chem.* **1976**, *80*, 905.
(136) Soltys, C. E.; Roberts, M. F. *Biochemistry* **1994**, *33*, 11608−11617.
(137) Jain, M. K.; Rogers, J.; Hendrickson, H. S.; Berg, O. G. *Biochemistry* **1993**, *32*, 8360.
(138) Hille, J. D. R.; Donne-Op den Kelder, G. M.; de Haas, G. H.; Egmond, M. R. *Biochemistry* **1981**, *20*, 4068.
(139) (a) Van Oort, M. G.; Dijkman, R.; Hille, J. D. R.; De Haas, G. H. *Biochemistry* **1985**, *24*, 7987. (b) Van Oort, M. G.; Dijkman, R.; Hille, J. D. R.; De Haas, G. H. *Biochemistry* **1985**, *24*, 7993.
(140) Deveer, A. M. Th. J.; Dijkman, R.; Leuveling-Tjeenk, M.; Van der Berg, L.; Ransac, S.; Batenberg, M.; Egmond, M.; Verheij, H.; de Haas, G. H. *Biochemistry* **1991**, *30*, 10034.
(141) Van Eijk, J. H.; Verheij, H. M.; Dijkman, R.; de Haas, G. H. *Eur. J. Biochem.* **1983**, *132*, 183.
(142) Van Eijk, J. H.; Verheij, H. M.; de Haas, G. H. *Eur. J. Biochem.* **1984**, *140*, 407.
(143) Yuan, W.; Quinn, D. M.; Sigler, P. B.; Gelb, M. H. *Biochemistry* **1990**, *29*, 6082.
(144) Rogers, J.; Yu, B.-Z.; Jain, M. K. *Biochemistry* **1992**, *31*, 6056.
(145) Kilby, P. M.; Primrose, W. U.; Roberts, G. C. K. *Biochem. J.* **1995**, *305*, 935.
(146) Janssen, M. J. W.; Burghout, P. J.; Verheij, H. M.; Slotboom, A. J.; Egmond, M. R. *Eur. J. Biochem.* **1999**, *263*, 782.
(147) Lefkowitz, L. J.; Deems, R. A.; Dennis, E. A. *Biochemistry* **1999**, *38*, 14174.
(148) Carman, G. M.; Deems, R. A.; Dennis, E. A. *J. Biol. Chem.* **1995**, *270*, 18711.
(149) (a) Hendrickson, H. S.; Dennis, E. A. *J. Biol. Chem.* **1984**, *259*, 5734. (b) Hendrickson, H. S.; Dennis, E. A. *J. Biol. Chem.* **1984**, *259*, 5740.
(150) Gonzalez-Navarro, H.; Bano, M. C.; Abad, C. *Biochemistry* **2001**, *40*, 3174.
(151) Nichols, J. W. *Biochemistry* **1985**, *24*, 6390.
(152) Nichols, J. W.; Pagano, R. E. *Biochemistry* **1982**, *21*, 1720.
(153) Nichols, J. W. *Biochemistry* **1988**, *27*, 879.
(154) Fullington, D. A.; Shoemaker, D. G.; Nichols, J. W. *Biochemistry* **1990**, *29*, 879.
(155) Niewenhuizen, W.; Steenbergh, P.; De Haas, G. H. *Eur. J. Biochem.* **1973**, *40*, 1.
(156) Janssen, M. J. W.; Vermeulen, L.; van der Helm, H. A.; Aarsman, A. J.; Slotboom, A. J.; Egmond, M. R. *Biochim. Biophys. Acta* **1999**, *1440*, 59.
(157) Lugtigheid, R. B.; Otten-Kupers, M. A.; Verheij, H. M.; de Haas, G. H. *Eur. J. Biochem.* **1993**, *213*, 517.
(158) Franken, P. A.; Van den Berg, L.; Huang, J.; Gunyuzlu, P.; Lugtigheid, R. B.; Verheij, H. M.; de Haas, G. H. *Eur. J. Biochem.* **1992**, *203*, 89.
(159) Jain, M. K.; Apitz-Castro, R. C. *J. Biol. Chem.* **1978**, 253, 7005.
(160) (a) Tinker, D. O.; Purdon, A. D.; Wei, J.; Mason, E. *Can. J. Biochem.* **1978**, *56*, 552. (b) Tinker, D. O.; Wei, J. *Can. J. Biochem* **1979**, *57*, 97.
(161) Jain, M. K.; Streb, M.; Rogers, J.; De Haas, G. H. *Biochem. Pharmacol.* **1984**, *33*, 2541.
(162) (a) Fernandez, M. S.; Mejia, R.; Zavala, E.; Pacheco, F. *Biochem. Cell. Biol.* **1991**, *69*, 715. (b). Fernandez, M. S.; Mejia, R.; Zavala, E. *Biochem. Cell. Biol.* **1991**, *69*, 722.
(163) Yu, B.-Z.; Jain, M. K. *Biochim. Biophys. Acta* **1989**, *980*, 15.
(164) Jain, M. K.; Yu, B.-Z.; Kozubek, A. *Biochim. Biophys. Acta* **1989**, *980*, 23.
(165) Kinkaid, A. R.; Wilton, D. C. *Biochem. J.* **1995**, *308*, 507.
(166) Upreti, G. C.; Rainier, S.; Jain, M. K. *J. Membr. Biol.* **1980**, *55*, 97.
(167) (a) Jain, M. K.; De Haas, G. H. *Biochim. Biophys. Acta* **1983**, *736*, 157. (b) Inoue, T.; Yanagihara, S.; Misono, Y.; Suzuki, M. *Chem. Phys. Lipids* **2001**, *109*, 117.
(168) Bell, J. D.; Burnside, M.; Owen, J. A.; Royall, M. L.; Baker, M. L.; *Biochemistry* **1996**, *35*, 4945.
(169) Henshaw, J. B.; Olsen, C. A.; Farnbach, A. R.; Nielson, K. H.; Bell, J. D. *Biochemistry* **1998**, *37*, 10709.
(170) Op den Kamp, J. A. F.; Kaurez, M. Th.; Van Deenen, L. L. M. *Biochim. Biophys. Acta* **1975**, *406*, 169.
(171) Burack, W. R.; Biltonen, R. L. *Chem. Phys. Lipids* **1994**, *73*, 209.
(172) Honger, T.; Jorgensen, K.; Biltonen, R. L.; Mouritsen, O. G. *Biochemistry* **1996**, *35*, 9003.
(173) Grandbois, M.; Clausen-Schaumann, H.; Gaub, H. *Biophys. J.* **1998**, *74*, 2398.
(174) Callisen, T. H.; Talmon, Y. *Biochemistry* **1998**, *37*, 10987.
(175) Jain, M. K.; Jahagirdar, D. V. *Biochim. Biophys. Acta* **1985**, *814*, 313.
(176) Jain, M. K.; Jahagirdar, D. V. *Biochim. Biophys. Acta* **1985**, *814*, 319.
(177) Jain, M. K.; Yu, B.-Z.; Gelb, M. H.; Berg, O. G. *Mediators Inflammation* **1992**, *1*, 85−100.
(178) (a) Cajal, Y.; Berg, O. G.; Jain, M. K. *Langmuir* **2000**, *16*, 252. (b) Berg, O. G.; Cajal, Y.; Jain, M. K. Manuscript in preparation.
(179) Ransac, S.; Iavanova, M.; Verger, R.; Panaiotov, I. *Methods Enzymol.* **1997**, *286*, 263.
(180) Panaiotov, I.; Ivanova, M.; Verger, R. *Curr. Opin. Colloid Interface Sci.* **1997**, *2*, 517.
(181) Pattus, F.; Slotboom, A. J.; De Haas, G. H. *Biochemistry* **1979**, *18*, 1691.
(182) (a) Van der Wiele, F. C.; Atsma, W.; Dijkman, R.; Schreurs, A. M. M.; Slotboom, A. J.; de Haas, G. H. *Biochemistry* **1988**, *27*, 1683. (b) Van der Wiele, F. C.; Atsma, W.; Roelofsen, B.; Linde, M. van; Binsbergen, J.; Radvanyi, F.; Rayova, D.; Slotboom, A. J.; de Haas, G. H. *Biochemistry* **1988**, *27*, 1688.
(183) Radvanyi, F.; Jordon, L.; Russo-Marie, F.; Bon, C. *Anal. Biochem.* **1989**, *177*, 103.
(184) Bayburt, T.; Yu, B.-Z.; Street, I.; Ghomashchi, F.; Laliberte, F.; Perrier, H.; Wang, Z.; Homan, R.; Jain, M. K.; Gelb, M. H. *Anal. Biochem.* **1995**, *232*, 7.
(185) Wu, S. K.; Cho, W. *Anal. Biochem.* **1994**, *221*, 152.
(186) Wu, S. K.; Cho, W. *Biochemistry* **1993**, *32*, 13902.
(187) Lewis, A. A.; Soltys, C. E.; Yu, K.; Roberts, M. F. *Biochemistry* **1994**, *33*, 5000.
(188) Soltys, C. E.; Bian, J.; Roberts, M. F. *Biochemistry* **1993**, *32*, 9545.
(189) Kinkaid, A. R.; Wilton, D. C. *Anal. Biochem.* **1993**, *212*, 65.
(190) Janssen, M. J. W.; van de Wiel, W. A. E. C.; Beiboer, S. H. W.; van Kampen, M. D.; Verheij, H. M.; Slotboom A. J.; Egmond, M. R. *Protein Eng.* **1999**, *12*, 497.
(191) Yu, B.-Z.; Rogers, J.; Tsai, M. D.; Pidgeon, C.; Jain, M. K. *Biochemistry* **1999**, *38*, 4875.
(192) Yu, B. Z.; Janssen, M. J. W.; Verheij, H. M.; Jain, M. K. *Biochemistry* **2000**, *39*, 5702.
(193) Yu, B. Z.; Poi, M. J.; Ramagopal, U. A.; Jain, R.; Ramakumar, S.; Berg, O. G.; Tsai, M. D.; Sekar, K.; Jain, M. K. *Biochemistry* **2000**, *39*, 12312.
(194) Pieterson, W. A.; Vidal, J. C.; Volwerk, J. J.; de Haas, G. H. *Biochemistry* **1974**, *13*, 1455.
(195) Dam-Mieras, M. C. E.; Slotboom, A. J.; Pieterson, W. A.; DeHaas, G. H. *Biochemistry* **1975**, *14*, 5387.
(196) Araujo, P. S.; Rosseneu, M. Y.; Kremer, J. M. H.; van Zolen, E. J. J.; De Haas, G. H. *Biochemistry* **1979**, *18*, 580.
(197) (a) Jain, M. K.; Vaz, V. L. C. *Biochim. Biophys. Acta* **1987**, *905*, 1. (b) Rebecchi, M.; Peterson, A.; McLaughlin, S. *Biochemistry*

1992, *31*, 12742. (c) Jung, L. S.; Shumaker-Parry, J. S.; Campbell, C. T.; Yee, S. S.; Gelb, M. H. *J. Am. Chem. Soc.* **2000**, *122*, 4177.
(198) Jain, M. K.; Rogers, J.; de Haas, G. H. *Biochim. Biophys. Acta* **1988**, *940*, 51.
(199) Lin, G. L.; Noel, J.; Loffredo, W.; Sable, H.; Tsai, M.-D. *J. Biol. Chem.* **1988**, *263*, 13208.
(200) Rogers, J.; Yu, B.-Z.; Serves, S. V.; Tsivgoulis, G. M.; Sotiropoulos, D. N.; Ioannou, P. V.; Jain, M. K. *Biochemistry* **1996**, *35*, 9375.
(201) (a) Cho, W.; Tomasselli, A. G.; Heinrickson, R. L.; Kezdy, F. J. *J. Biol. Chem.* **1988**, *263*, 11237. (b) Cho, W.; Markowitz, M. A.; Kezdy, F. J. *J. Am. Chem. Soc.* **1988**, *110*, 5166. (c) Cho, W.; Shen, Z.; Wu, S. K. *Biochemistry* **1994**, *33*, 11598. (d) Tomasselli, A. G.; Hui, J.; Fisher, J.; Zurcher-Neely, H.; Reardon, I. M.; Oriaku, E.; Kezdy, F. J.; Heinrickson, R. L. *J. Biol. Chem.* **1989**, *264*, 10041.
(202) Lugtigheid, R. B.; Nicolaes, G. A. F.; Veldhuizen, E. J. A.; Slotboom, A. J.; Verheij, H. M.; de Haas, G. H. *Eur. J. Biochem.* **1993**, *216*, 519.
(203) Shen, Z.; Wu, S. K.; Cho, W. *Biochemistry* **1994**, *33*, 11598−11607.
(204) (a) Jain, M. K.; Zakim, D. *Biochim. Biophys. Acta* **1987**, *906*, 33. (b) Maurray, D.; Arbuzova, A.; Honig, B.; McLaughlin, S. In *Current Topics in Membranes: Peptide-Lipid Interactions*; Simin, S., McIntosh, T., Eds.; Academic Press: New York, in press. (c) Goni, F. M.; Ostolaza, H. *Braz. J. Med. Biol. Res.* **1998**, *31*, 1019. (d) Buckland, A. G.; Wilton, D. C. *Biochim. Biophys. Acta* **2000a**, *1483*, 199.
(205) Kuipers, O. P.; Vincent, M.; Brochon, J. C.; Verheij, H. M.; de Haas, G. H.; Gallay, J. *Biochemistry* **1991**, *30*, 8771.
(206) Kuipers, O. P.; Thunnissen, M. M. G. M.; de Geus, P.; Dijkstra, B. W.; Drenth, J.; Verheij, H. M.; de Haas, G. H. *Science* **1989**, *244*, 82.
(207) Jain, M. K.; Maliwal, B. P. *Biochemistry* **1993**, *32*, 11838−11846.
(208) Maliwal, B. P.; Yu, B.-Z.; Szacinski, H.; Squier, T.; van Binsbergen, J.; Slotboom, A. J.; Jain, M. K. *Biochemistry* **1994**, *33*, 4509.
(209) Hjorath, A.; Carrieere, F.; Cudrey, C.; Woldike, H.; Boel, E.; Lawson, D, M.; Ferrato, F.; Cambillau, C.; Dodson, G. G.; Thim, L.; Verger, R. *Biochemistry* **1993**, *32*, 4702.
(210) Brozowski, A. M.; Savage, H.; Verma, C. S.; Turkenburg, J. P.; Lawson, D. M.; Svendsen, A.; Patkar, S. *Biochemistry* **2000**, *39*, 15071.
(211) Tatulian, S. A. *Biochim. Biophys. Acta* **1983**, *736*, 189.
(212) (a) Bapista, M. D. S.; Cuccovia, I.; Chaimovich, H.; Politi, M. J.; Reed, W. F. *J. Phys. Chem.* **1992**, *96*, 6442. (b) Collins, K. D.; Washabaugh, M. W. *Q. Rev. Biophys.* **1985**, *18*, 323. (c) Bunton, C. A.; Nome, F.; Quina, F.; Romsted, L. S. *Acc. Chem. Res.* **1991**, *24*, 357. (d) Bunton, C. A.; Mhala, M. M.; Moffatt, J. R. *J. Org. Chem.* **1987**, *52*, 3832. (e) Bunton, C. A.; Mhala, M. M.; Moffatt, J. R. *J. Phys. Chem.* **1989**, *93*, 854. (f) Correia, V. R.; Cuccovia, I. M.; Stelmo, M.; Chaimovich, H. *J. Am. Chem. Soc.* **1992**, *114*, 2144. (g) Cuccovia, I.; Romsted, L. S.; Chaimovich, H. *J. Colloid Interface Sci* **1999**, *220*, 96. (h) Fendler, J. H. *Membrane Mimetic Chemistry***;** Wiley-Interscience: New York, 1982. (i) Chaudhuri, A.; Loughlin, J. A.; Romsted, L. S.; Yao, J. *J. Am. Chem. Soc.* **1993**, *115*, 8351.
(213) Adam G.; Delbruck, M. In *Structural Chemistry and Molecular Biology*; Rich, A., Davidson, N., Eds.; W. H. Freeman and Co. Publishers: San Francisco, 1968, p 198.
(214) Page, M. I.; Jencks, W. P. *Proc. Natl. Acad. Sci. U.S.A.* **1971**, *68*, 1678.
(215) Ben-Tal, N.; Honig, B.; Bagdassarian, C. K.; Ben-Shaul, A. *Biophys. J.* **2000**, *79*, 1180.
(216) Berg, O. G. *Biophys. J.* **1985**, *47*, 1−14.
(217) Jencks, W. P. *Adv. Enzymol.* **1975**, *43*, 219−410.
(218) Smoluchowski, M. von *Z. Phys. Chem.* **1917**, *92*, 129.
(219) Bala, P.; Grochowski, P.; Nowinski, K.; Lesyng, B.; McCammon, J. A. *Biophys. J.* **2000**, *79*, 1253.
(220) (a) Jones, S. T.; Ahlstrom, P.; Berendsen, H. J. C.; Pickersgill, R. W. *Biochim. Biophys. Acta* **1993**, *1162*, 135. (b) Ohishi, H.; Fuji, S.; Tomoo, K.; Ishida, T.; Ikeda, K.; Tanabe, K.; Kitamure, K. *J. Biochem. (Tokyo)* **1993**, *114*, 210.
(221) Sessions, R. B.; Dauber-Osguthorpe, P.; Campbells, M. M.; Osguthorpe, D. J. *Proteins: Struct., Funct., Genet.* **1992**, *14*, 45.
(222) Beiboer, S. H.; van den Berg; B.; Dekker: N.; Cox, R. C.; Verheij, H. M. *Protein Eng.* **1996**, *9*, 345.
(223) Slaich, P. K.; Primrose, W. U.; Robinson, D. H.; Wharton, C. W.; White, A. J.; Drabble, K.; Roberts, C. K. *Biochem. J.* **1992**, *288*, 167.
(224) Kuipers, O. P.; Franken, P. A.; Hendriks, R.; Verheij, H. M.; de Haas, G. H. *Protein Eng.* **1990**, *4* 199.
(225) Sekar, K.; Yu, B.-Z.; Rogers, J.; Lutton, J.; Liu, X.; Chen, X.; Tsai, M. D.; Jain, M. K.; Sundaralingam, M. *Biochemistry* **1997b**, *36*, 3104.
(226) Hartmann, M.; Merx, K. M.; van Eldik, R.; Clark, T. *J. Mol. Model.* **1998**, *4*, 355.
(227) Schurer, G.; Lanig, H.; Clark, T. *J. Phys. Chem.* **2000**, *B104*, 1349.
(228) Quinn, D. M.; Sutton, L. D. In *Enzyme Mechanism from Isotope Effects*, Cook, P. D., Ed.; CRC Press: Boca Raton, 1991; p 73.
(229) Liu, X.; Zhu, H.; Huang, B.; Rogers, J.; Yu, B.-Z.; Kumar, A.; Jain, M. K.; Sundaralingam, M.; Tsai, M.-D. *Biochemistry* **1995**, *34*, 7322.
(230) (a) Scharrenburg, G. J. M.; Puijk, W.; Egmond, M. R.; DeHaas, G. H.; Slotboom, A. J. *Biochemistry* **1981**, *20*, 1584. (b) Scharrenburg, G. J. M.; Puijk, W.; Egmond, M. R.; van der Schaft, P. H.; DeHaas, G. H.; Slotboom, A. J. *Biochemistry* **1982**, *21*, 1345. (c) Scharrenburg, G. J. M.; Puijk, W.; DeHaas, G. H.; Slotboom, A. J. *Eur. J. Biochem.* **1983**, *133*, 83. (d) Scharrenburg, G. J. M.; Jansen, E. H. J. M.; Egmond, M. R.; van der Schaft, P. H.; DeHaas, G. H.; Slotboom, A. J. *Biochemistry* **1984**, *21*, 6285.
(231) (a) Baker, S. F.; Othman, R.; Wilton, D. C. *Biochemistry* **1998**, *37*, 13203. (b) Othman, R.; Baker, S.; Li, Y.; Worrall, A. F.; Wilton, D. C. *Biochim. Biophys. Acta* **1996**, *1303*, 92.
(232) Volwerk, J. J.; DeHaas, G. H. In *Molecular Biology of Lipid-Protein Interactions*, Jost, P. C., Griffith, O. H., Eds.; Wiley: New York, 1982; pp 69−149.
(233) (a) Snitko, Y.; Koduri, R. S.; Han, S. K.; Molini, B. J.; Wilton, D. C.; Gelb, M. H.; Cho, W. *Biochemistry* **1997**, *36*, 14325. (b) Snitko, Y.; Han, S. K.; Lee, B. I.; Cho, W. *Biochemistry* **1999**, *38*, 7803.
(234) Di Marco, D.; Marki, F.; Hofstetter, H.; Schmitz, A.; Van OOstrum, J.; Grutter, M. G. *J. Biochem.* **1992**, *112*, 350.
(235) Dua, R.; Wu, S. K.; Cho, W. *J. Biol. Chem.* **1995**, *270*, 263.
(236) Weiss, J.; Inada, M.; Elsbach, P.; Crow, R. M.; *J. Biol. Chem.* **1994**, *269*, 26221.
(237) Lee, B. I.; Yoon, E. T.; Cho, W. *Biochemistry* **1996**, *35*, 4231.
(238) Bekkers, A. C. A. P. A.; Franken, P. A.; Toxopeus, E.; Verheij, H. M.; DeHaas, G. H. *Biochim. Biophys. Acta* **1991**, *1076*, 374.
(239) Kuipers, O. P.; Kerver, J.; Van Meersbergen, J.; Vis, R.; Dijkman, R.; Verheij, H. M.; de Haas, G. H. *Protein Eng.* **1990**, *3*, 599.
(240) Han, S. K.; Kim, K. P.; Koduri, R.; Bittova, L.; Monoz, N. M.; Leff, A. R.; Wilton, D. C.; Gelb, M. H.; Cho, W. *J. Biol. Chem.* **1999**, *274*, 11881.
(241) (a) Pickersgill, R. W.; Sumner, I. G.; Collins, M. E.; Warwicker, J.; Perry, B.; Bhat, K. M.; Goodenough, P. W. *FEBS Lett.* **1991**, *281*, 219. (b) Bhat, K. M.; Pickersgill, R. W.; Perry, B. N.; Brown, R. A.; Jones, S. T.; Mueller-Harbey, I.; Sumner, I. G.; Goodenough, P. W. *Biochemistry* **1993**, *32*, 12203.
(242) Li, Y.; Tsai, M.-D. *J. Am. Chem. Soc.* **1993**, *115*, 8523.
(243) Li, Y.; Yu, B.-Z.; Zhu, H.; Jain, M. K.; Tsai, M. D. *Biochemistry* **1994**, *33*, 14714.
(244) Van den Bergh, C. J.; Slotboom, A. J.; Verheij, H. M.; de Haas, G. H. *Eur. J. Biochem.* **1988**, *176*, 353.
(245) Dupureur, C. M.; Yu, B.-Z.; Jain, M. K.; Noel, J. P.; Deng, T.; Li, Y.; Byeon, I. L.; Tsai, M. D. *Biochemistry* **1992**, *31*, 6402.
(246) Thunnissen, M. M.; Franken, P. A.; de Haas, G. H.; Drenth, J.; Kalk, K. H.; Verheij, H. M.; Dijkstra, B. W. *Protein Eng.* **1992**, *5*, 597.
(247) (a) Noel, J. P.; Tsai, M.-D. *J. Cell. Biochem* **1989**, *40*, 309. (b) Noel, J. P.; Deng, T.; Hamilton, K. J.; Tsai, M. D. *J. Am. Chem. Soc.* **1990**, *112*, 3704. (c) Noel, J. P.; Deng, T.; Kelly, K. J.; Tsai, M.-D. *J. Am. Chem. Soc.* **1990**, *112*, 3704.
(248) Noel, J. P.; Bingman, C. A.; Deng, T.; Dupureur, C. M.; Hamilton, K. J.; Jiang, R.; Kwak, J.; Sekharudu, C.; Sundaralingam, M.; Tsai, M. D. *Biochemistry* **1991**, *30*, 11801.
(249) Lugtigheid, R. B.; Otten-Kuipers, M. A.; Verheij, H. M.; De Haas, G. H. *Eur. J. Biochem.* **1993**, *213*, 517.
(250) (a) Kuipers, O. P.; Dijkman, R.; Pals, C. E. M.; Verheij, H. M.; de Haas, G. H. *Protein Eng.* **1989**, *2*, 467. (b) Kuipers, O. P.; Dekker: N.; Verheij, H. M.; de Haas, G. H. *Biochemistry* **1990**, *29*, 6094.
(251) Sumandea, M.; Das, S.; Sumandea, C.; Cho, W. *Biochemistry* **1999**, *38*, 16290.
(252) Thunnissen, M. M.; Franken, P. A.; de Haas, G. H.; Drenth, J.; Kalk, K. H.; Verheij, H. M.; Dijkstra, B. W. *J. Mol. Biol.* **1993**, *232*, 839.
(253) Lin, Y.; Ghomashchi, F.; Nielson, R.; Snitko, Y.; Yu, B. Z.; Han, S. K.; Cho, W.; Wilton, D. C.; Jain, M. K.; Robindosn, B. H.; Gelb, M. H. *Biochem. Soc. Trans.* **1998**, *26*, 341.
(254) Van den Bergh, C. J.; Bekkers, A. C. A.; Verheij, H. M.; de Haas, G. H. *Eur. J. Biochem.* **1989**, *182*, 307.
(255) Zhu, H.-X.; Dupureur, C. M.; Zhang, X.-Y.; Tsai, M. D; *Biochemistry* **1995**, *34*, 15307.
(256) Kumar, A.; Sekharudu, C.; Dupureur, C. M.; Zhu, H.; Tsai, M. D.; Sundaralingam, M. *Protein Sci.* **1994**, *3*, 2073.
(257) Kumar, A.; Sekharudu, C.; Ramakrishnan, B.; Dupureur, C. M.; Zhu, H.-X.; Tsai, M.-D.; Sundaralingam, M. *Protein Sci.* **1994**, *3*, 2082.
(258) Sekar, K.; Biswas, R.; Li, Y.; Tsai, M.-D.; Sundaralingam, M. *Acta Crystallogr.* **1999**, *D55*, 443.
(259) Dupureur, C. M.; Yu, B.-Z.; Mamone, J. A.; Jain, M. K.; Tsai, M. D. *Biochemistry* **1992**, *31*, 10576.
(260) Huang, B.; Yu, B.-Z.; Rogers, J.; Byeon, I. J. L.; Sekar, K.; Chen, X.; Sundaralingam, M.; Tsai, M. D.; Jain, M. K. *Biochemistry* **1996**, *35*, 12164.

(261) Bekkers, A. C. A. P. A.; Vuurst, H.; Willigen, G.; Akkrman, J. W. N.; Verheij, H. M. *Thromb. Hemost.* **1995**, *74*, 1138.
(262) Janssen, M. J. W.; Verheij, H. M.; Slotboom, A. J.; Egmond, M. R. *Eur. J. Biochem*. **1999**, *261*, 197.
(263) Rogers, J.; Yu, B.-Z.; Tsai, M. D.; Berg, O. G.; Jain, M. K. *Biochemistry* **1998**, *37*, 9549.
(264) Koduri, R. S.; Baker, S. F.; Snitko, T.; Han, S. K.; Cho, W.; Wilton, D. C.; Gelb, M. H. *J. Biol. Chem*. **1998**, *273*, 32142.
(265) Verheij, H. M. In *Phospholipase A_2 in Clinical Inflammation, Molecular Approaches to Pathophysiology*; Glaser, K. B., Vadas, P., Eds.; CRC Press: Boca Raton, 1995; pp 3−24.
(266) Pace, C. N. *Methods Enzymol*. **1986**, *131*, 266.
(267) Tsai, M.-D.; Yan, H. *Biochemistry* **1991**, *30*, 6806.
(268) Sekar, K.; Sekharudu, C.; Tsai, M.-D.; Sundaralingam, M. *Acta Crystallogr*. **1998**, *D54*, 342.
(269) Sekharudu, C.; Ramakrishnan, B.; Huang, B.-H.; Jiang, R.-T.; Dupureur, C. M.; Tsai, M.-D.; Sundaralingam, M. *Protein Sci*. **1992**, *1*, 1585.
(270) Rajakannan, V.; Yogavel, M.; Poi, M. J.; Prakash, A. J.; Velmurugan, D.; Tsai, M.-D.; Sekar, K. Manuscript in prepration.
(271) Epstein, T. M.; Yu, B. Z.; Pan, Y. H.; Tuton, S. P.; Maliwal, B. P.; Jain, M. K.; Bahnson, B. J. *Biochemistry* **2001**, in press.
(272) Dupureur, C. M.; Deng, T.; Kwak, J.; Noel, J. P.; Tsai, M. D. *J. Am. Chem. Soc* **1990**, *112*, 7074.
(273) Dupureur, C. M.; Li, Y.; Tsai, M.-D.; *J. Am. Chem. Soc*. **1992**, *114*, 2748.
(274) Fleer, E. A. M.; Verheij, H. M.; De Haas, G. H. *Eur. J. Biochem*. **1981**, *113*, 283.
(275) (a) Bruzik, K.; Gupte, S. M.; Tsai, M.-D. *J. Am. Chem. Soc*. **1982**, *104*, 4682. (b) Bruzik, K.; Tsai, M.-D. *Methods Enzymol*. **1991**, *197*, 258.
(276) Tsai, T.-C.; Hart, J.; Jiang, R.-T.; Bruzik K.; Tsai, M.-D. *Biochemistry* **1985**, *24*, 3180.
(277) Donne-Op den Kelder, G. M.; de Haas, G. H.; Egmond, M. R. *Biochemistry* **1983**, *22*, 2470.
(278) Ptitsyn, O. B. In *Protein Folding*; Creighton, T. E., Ed.; Freeman: New York, 1992; pp 243−300.
(279) Ptitsyn, O. B. *Curr. Opin. Struct. Biol*. **1995**, *5*, 74.
(280) Tzeng, M.; Yen, C.; Hseu, M.; Dupeureur, C. M.; Tsai, M. D. *J. Biol. Chem*. **1995**, *270*, 2120.
(281) Beal, R. E.; Toscana-Cantaffa, D.; Young, P.; Rechsteiner, M.; Pickert, C. M. *Biochemistry* **1998**, *37*, 2925.
(282) Sharp, K. A.; Nicholls, A.; Friedman, R.; Honig, B. *Biochemistry* **1991**, *30*, 9686.
(283) Ortiz, A. R.; Pisabarro, M. T.; Gallego, J.; Gago, F. *Biochemistry* **1992**, *31*, 2887.
(284) Scott, D. L.; Mandel, A. M.; Sigler, P. B.; Honig, B. *Biophys. J*. **1994**, *67*, 493.
(285) Warwicker, J. *FEBS Lett*. **1997**, *404*, 159.
(286) Ghomashchi F.; Lin Y.; Hixon M. S.; Yu B.-Z.; Annand R.; Jain M K.; Gelb M. H. *Biochemistry*. **1998**, *37*, 6697.
(287) Han, S. K.: Yoon, E. T.; Scott, D. L.; Sigler, P. B.: Cho, W. *J. Biol. Chem*. **1997**, *272*, 3573.
(288) Chakrabarti, P. *J. Mol. Biol*. **1993**, *234*, 463.

CR990139W